Aalto university
School of Engineering

Saara Lassila

Soil permeability reduction of a dike by injecting organic matter and aluminum: field data analysis

Diplomityö, joka on jätetty opinnäytteenä tarkastettavaksi diplomi-insinöörin tutkintoa varten.

Espoo 19.11.2018
Supervisor: Professor Leena Korkiala-Tanttu

Aalto-yliopisto
Insinööritieteiden korkeakoulu

Aalto-yliopisto, PL 11000, 00076 AALTO
www.aalto.fi
Diplomityön tiivistelmä

Työntekijä Saara Lassila

Työn nimi Maapadon vedenläpäisevyyden pienentäminen organispohjaisella injektoinilla: kenttämittausten analyysi

Maisteriohjelma Master's programme in Geoengineering **Koodi** ENG23

Työn valvoja Professori Leena Korkiala-Tanttu

Työn ohjaaja(t) TkT Susanne Laumann ja DI Ilona Häkkinen

Päivämäärä 19.11.2018 **Sivumäärä** 78+8 **Kieli** englanti

Tämä diplomityö on osa SoSEAL (Soil Sealing by Enhanced Aluminum and DOM Leaching) tutkimusprojektia, jonka tarkoituksena on kehittää uusi tapa vähentää maan vedenläpäisevyyttä. Maahan injektoidaan alumiinista ja orgaanisesta aineesta koostuvaa seosta, joka muodostaa maan partikkeleiden välit tukkivia hiutaleita. Tekniikkaa kokeiltiin vuotavan maapadon kunnostamiseksi De Gijsterissa. Seosta ruiskutettiin koko pohjavettä johtavan kerroksen paksuudelle tarkoituksena muodostaa metrin levyinen seinämä. Koealueelle asennettiin monitorointikaivoja, joiden vedenpinnan korkeutta mittaamalla seurattiin pohjaveden virtausta. Koealueella tehtiin pumppauskokeita sekä ennen injektointeja että niiden jälkeen. Kenttämittausanalyysin tavoitteena oli osoittaa injektoinnin vaikutus akviferin vedenläpäisevyyteen.

Vedenpinnan vaihtelun muutosta analysoitiin visuaalisin ja analyyttisin keinoin. Visualliset vertailut osoittivat, että pohjaveden virtaus sekä pumppauskokeiden aikana että niiden ulkopuolella, oli muuttunut. Ero pohjavedenpinnan tasossa maapadon päältä katsottuna ylimmän ja alimman kaivon välillä kasvoi. Vedenpinnan taso ei kuitenkaan laskenut odotuksien mukaisesti injektointilinjalla vaan muutama metriä kauempana. Lähtötilanteeseen verrattuna injektointien jälkeen pumpatessa vedenpinnan alenema tapahtui hitaammin injektointilinjan toisella puolella testikaivoon nähden ja nopeammin samalla puolella kuin testikaivo. Vedenjohtavuuden muutoksen suuruuden määrittämiseksi käytettiin Neumanin metodia, joka on kehitetty homogeenisille anisotrooppisille vapaille akvifereille. Pumppauskokeiden aika ja alenema piirretään logaritmiselle asteikoille ja syntynyttä pistekäyrää verrataan tyyppikäyriin. Neumanin metodissa on erilliset käyrät aikaisen vaiheen ja myöhäisen vaiheen alenemille. Tässä tutkimuksessa mittaustulosten ja tyyppikäyrien yhdistämisessä käytiin apuna Fittsin kehittämää Excel-työkalua.

Analyysit viittasivat vedenläpäisevyyden pienentyneen odotuksia vähemmän ja hiutaleiden levittäytyneen odotuksia suuremmalla alueelle injektointilinjan alapuolelle. Hiutaleet ovat liikkuneet pois injektointilinjalta injektointiin käytetyn paineen vaikutuksesta. Tuloksiin liittyvät epävarmuudet ja virhemarginaalit olivat suuria. Neumanin metodin suurin puute on olettamus maan homogeenisuudesta. Jatkotutkimuksissa pumppauskokeiden analyysimetodia tulisi vaihtaa. Vedenläpäisevyyden pitkäaikaisen vähenemisen varmistamiseksi hiutaleiden käyttäytymistä pohjaveden virtauksen vaikutuksen alaisuudessa tulisi tutkia lisää laboratoriossa.

Avainsanat vapaa akviferi, vedenpinnan alenema, pumppauskoe, permeabiliteetti, Neumanin metodi

Aalto University
School of Engineering

Aalto University, P.O. BOX 11000, 00076
AALTO
www.aalto.fi

Abstract of master's thesis

Author Saara Lassila

Title of thesis Soil permeability reduction of a dike by injecting organic matter and aluminum: field data analysis

Master programme Master's programme in Geoengineering **Code** ENG23

Thesis supervisor Pr. Leena Korkiala-Tanttu

Thesis advisor(s) Dr. Susanne Laumann and MSc. Ilona Häkkinen

Date 19.11.2018 **Number of pages** 78+8 **Language** English

This thesis was a part of the SoSEAL (Soil Sealing by Enhanced Aluminum and DOM Leaching) research project, which aims at developing a new technique to reduce soil permeability. The permeability of soil is reduced by mixing aluminum and organic matter which react and start forming flocs that blocks the pores between soil particles. A pilot was conducted in a leaking dike of a freshwater reservoir in De Gijster to achieve efficient maintenance. The mixture was injected into the aquifer with the aim of forming a 1 m-thick flow barrier of reduced permeability. Data from the site were collected from monitoring wells and pumping tests were conducted before and after the injection. The aim of the field data analysis is to study the effect of the treatment to the aquifer permeability.

Changes caused by the barrier were analyzed qualitatively and quantitatively. Comparison of data before and after the implementation showed a change in the behavior of the groundwater flow. According to the water level measurement in the monitoring wells, the hydraulic gradient between the top and the toe of the dike increased after the injection. However, the drop in water level did not occur at the injection line. At the beginning of a pumping test, the drawdown at the other side of the injection line regarding the test well was delayed and at the same side, it was accelerated. To quantify the change in hydraulic conductivity the Neuman method was applied. It is a method developed for homogenous, anisotropic, unconfined aquifers. The time and drawdown were plotted on a logarithmic scale and fitted to type curves. The type curves are divided into early time curves and late time curves. The early time curves provided the specific storage of the aquifer and late time curve gives the specific yield. The Neuman method was applied by curve-fitting with using an Excel sheet provided by Fitts.

Due to uncertainties linked to the measurements and the analysis, the quantitative results failed to confirm the reduced permeability. The Neuman method failed to give reliable results due to the heterogeneity of the soil. The comparison of data and the Neuman method, indicated that he reduced permeability zone was not only on the injection line, but it had expanded few meters downstream. The flocs have moved most likely due to the injection pressure. The analysis method is recommended to be changed and the behavior of the flocs under the injection pressure and natural hydraulic gradient should be studied.

Keywords unconfined aquifer, drawdown, pumping test, permeability, Neuman method

Preface

This master thesis is part of the SoSEAL research project that started in TU Delft in 2014. This thesis focused on the second pilot that was implemented on the test site in June 2018. The aim was to define what kind of reduced permeability barrier was created and how it affected the soil permeability of the dike. This thesis was done in co-operation of TU Delft and Aalto University. The work was funded by A-insinöörit.

I want to thank the SoSEAL research team: Pr. Timo Heimovaara, Susanne Laumann and Jiani Zhou. You were of great help in introducing me to the world of ground water flow and working with you was a pleasure. Then I would like to thank Pr. Leena Korkiala-Tanttu from Aalto university and Ilona Häkkinen from A-insinöörit who came up with this out of the box idea of sending me to the Netherlands and supported me during the process with all the help I needed.

Since this work is the last seal for my life as a student, I want to give a big hug to all the amazing people I have met during my studies. I have learned many important skills but most of all I have had an incredibly fun and versatile journey. Eikä syyttä.

Espoo 19.11.2018

Saara Lassila

Table of content

Notations

A	$[m^2]$	area of the aquifer
F	[m]	shape factor of Hvorslev slug test
K	[m/d]	hydraulic conductivity
K_D	[]	dimensionless parameter capturing the unsaturated flow
K_r	[m/d]	radial hydraulic conductivity
K_x	[m/d]	horizontal hydraulic conductivity
K_z	[m/d]	vertical hydraulic conductivity
L	[m]	length of the uncased extension of the well
N	$[m^3/d]$	aquifer leakage or recharge
Q	$[m^3/d]$	flow rate
R	[m]	radius of the well
S	[]	storativity
S_s	[]	specific storage or elastic storage
S_y	[]	specific yield
T	$[m^2/d]$	transmissivity
P	[Pa]	pressure
W	[]	well function
b	[m]	aquifer thickness
Δh	[m]	change in head
r	[m]	distance from the test well
s	[m]	drawdown
s'	[m]	drawdown of a confined aquifer
t	[s]	time
u	[]	dimensionless variable of the well function
v	[m/s]	velocity
η	[]	dimensionless parameter of the Neuman method

Abbreviations

ANN	Artificial Neural Network
CPTu	Piezocone penetration test
DOM	Dissolved Organic Matter
EC	Electrical conductivity
ISSMGE	International Society of Soil Mechanics and Geotechnical Engineering
MICP	Microbially Induced Carbonate Precipitation
N.A.P.	Normaal Amsterdams Peil or Normal Amsterdam Level
SOM	Soil Organic Matter
SoSEAL	Soil Sealing by Enhanced Aluminum and DOM leaching

1 Introduction

Water is essential for life but often problematic for geotechnical structures. Water is present at the ground surface as well as below the ground surface. In the Netherlands, where one third of the land area is situated below the sea level dikes are often used to control the water level (Van Koningsveld et al., 2008). Dikes are affected by both the surface water and the subsurface water flow. Especially, controlling the subsurface water flow is a challenging task (Heimovaara et al., 2014). Seepage occurs when there is a difference in pressure head. Seepage through the dikes can endanger its stability and reduce its effectiveness as a water barrier (Xu et al., 2013). Water flow can be decreased by adding a physical barrier into soil or the properties of the soil can be improved. Reducing soil permeability is a critical issue also on sites where leaking water is contaminated, seepage can harm the existing structures, or the aim is to store water.

This master thesis is a part of a project called SoSEAL (Soil Sealing by Enhanced Aluminum and DOM Leaching). The project aims to reduce soil permeability by injecting a mixture composed of aluminum and organic matter creating a vertical low permeability barrier. With this technique, the barrier is created in a fast and efficient way. The SoSEAL research project started in TU Delft in 2014 (Heimovaara, 2014). The SoSEAL project is run by TU Delft in cooperation with partners from industry. The first pilot was carried out in 2016 in Veersedijk and the second pilot started in 2018 in a freshwater reservoir called De Gijster, where SoSEAL was injected to remediate a leaking dike. More information about the project can be found on the TU Delft website: (https://www.tudelft.nl/technology-transfer/development-innovation/research-exhibition-projects/soseal/).

The main idea behind the reduction of soil permeability is to stop or slow down the water flow. By reducing permeability, the advection of pollutants can be prevented, or leakage can be reduced (Heimovaara et al. 2014). SoSEAL have been developed to reduce the permeability of porous media. SoSEAL could be used for example in reducing seepage through dikes, in the protection of drinking water, sealing leakage around sewage pipes or to achieve a homogenous permeability. In the Netherlands, there are fields used for agriculture that have old riverbeds passing through causing heterogeneities in permeability. One of the applications of the SoSEAL could be homogenizing the permeability of these fields.

At the water reservoir of De Gijster, the goal is to create a zone of reduced permeability by injecting the mixture starting from the bottom of the aquifer to few meters above the groundwater level. The components of the mixture start to react and form flocs as soon as they are in contact. Once the mixture is injected, the flocs grow bigger and fill the spaces between pores as presented in figure 1.1. The size and form of the flocs depend on the shear. The reaction occurring resembles the podzolization reaction encountered in nature (Heimovaara et al. 2014).

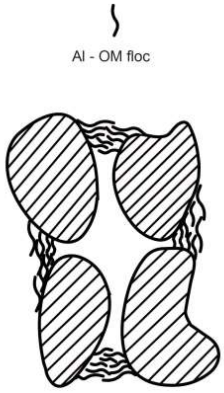

Figure 1.1. The Al-OM interact and clog the voids between soil particles (Bonfiglio, 2016).

The first field test of the SoSEAL was done at a dike stretch in Veersedijk, in the Netherlands, where the dike stability was endangered due to an uplift that could occur if the water surface of the river would increase. The failure mechanism was provoked by the high permeable sand layer underneath the dike. The soil permeability was reduced with SoSEAL to ensure stability. For this first pilot, a circular zone of reduced permeability was designed and implemented to be able to better monitor the changes in flow paths (figure 1.2). (Laumann, 2017).

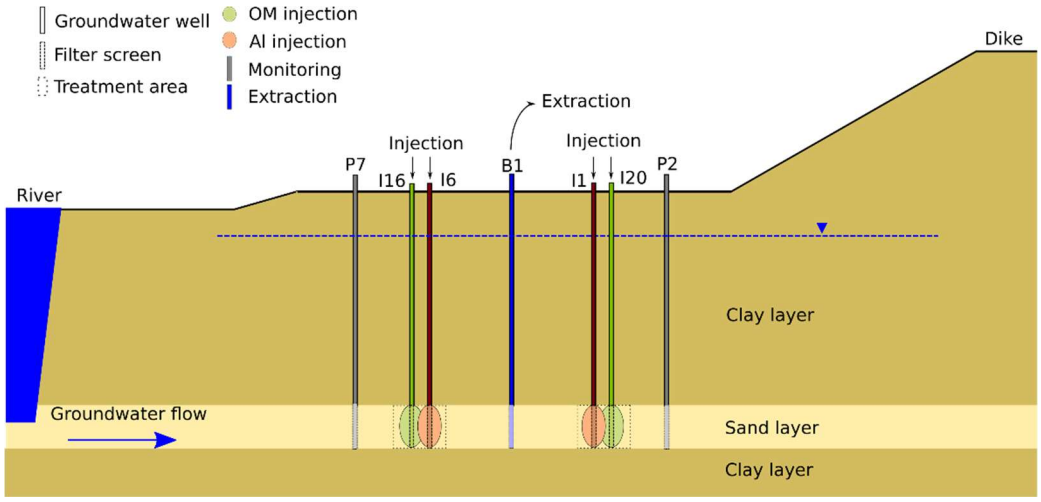

Figure 1.2. A model of the injection in the dike stretch. The diameter of the zone of reduced permeability is 5 m (Laumann, 2017).

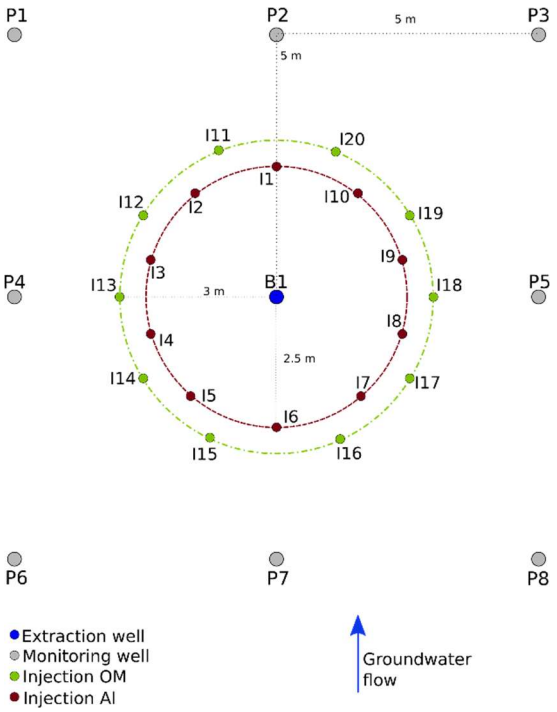

Figure 1.3. The injection pattern of the first pilot. Aluminum and organic matter were injected from separate wells (Laumann, 2017).

In the dike stretch, the reactants were injected from wells situated next to each other and a flow toward the center was created by pumping to ensure the contact between reactants (figure 1.3). The results of the first pilot were promising. The decrease in hydraulic conductivity was estimated to be 40-times. In the first pilot, the organic matter and aluminum were injected separately. However, the results indicated that despite the inward flow, the reactants did not always meet. For this reason, in the second pilot in the water reservoir, the components were mixed in a batch before injecting to ensure that the components get in contact with each other.

This thesis focuses on the process and results obtained from the second pilot. The second pilot aims to reduce the soil permeability to reduce the leakage of the toe of the dike of the freshwater reservoir. The stakeholders of this pilot are Evides, Heijmans and Tauw. Evides owns and operates the freshwater reservoir. Heijmans was the contractor doing the installation of wells and the injection. Tauw provided consulting and was partly responsible for the project management. If the project is successful, the partners are considering treating the entire dike surrounding the freshwater reservoir with the SoSEAL method.

The aim of this master thesis was to test different methods to quantify permeability in the soil before and after the SoSEAL treatment. The hypothesis is that the treatment reduces permeability. To test the hypothesis pumping tests that allow for quantification of permeability reduction were interpreted. Also, other methods, such as observing the change in hydraulic gradient, to detect changes in ground water behavior were studied. Multi-well pumping tests were conducted on-site before and after injection. To demonstrate the effects, a suitable method for pumping test analysis was chosen according to a literature study and preliminary analysis. The method was implemented, and the results were analyzed and discussed. Finally, recommendations for further studies were given.

Due to the complexity and uncertainty linked to the process of defining water permeability of soil, the results are mostly qualitative. Some estimations of the magnitude of the changes in water permeability are given but the focus is on observing a change. The pumping test used for the post-injection analysis were done one month and three months after the injection. The long-term effects were not studied due to time limitations. This thesis concentrates on the effect of the mixture on the permeability of the soil. It is possible that also the soil strength of the injection zone has increased.

2 Theoretical background and definitions

The ground improvement method used on the test site is comparable to several existing grouting methods. Some common grouting methods and classifications of methods are presented. With the injection, the aim is to change the flow path of the water in the aquifer. To affect the course of the water flow, its behavior needs to be understood. Some ground waterflow theory is presented and some definitions linked to aquifers and wells are given.

2.1 Use of grouting in ground improvement

There are several ways to classify different soil improvement methods. The technical committee of the ISSMGE suggested in 2012 that ground improvement methods are divided into 5 main categories: Ground improvement without admixtures in cohesive soils or fill materials, Ground improvement without admixtures in cohesive soils, Ground improvement with admixtures or inclusions, Ground improvement with grouting type admixtures and Earth reinforcement (Lietaert et al., 2012). According to this classification, the SoSEAL method is classified in the group of ground improvement with grouting type admixtures. Its subclass is chemical grouting, which is described as a method where chemicals react in the soil pores by forming a gel or a precipitate to increase the strength or reduce permeability (Lietaert et al., 2012).

Chemical grouting is not yet as commonly used as particulate grouting methods. One of the particulate grouting methods is cement grouting. It is based on filling the cavities and fissures in soil or rock. In jet grouting, columns or panels are formed by injecting grout with high speeds jets. (Lietaert et al., 2012) A controlled amount of cement is injected in a small diameter borehole. With jet grouting, the long-term shear strength can attain values up to 19 MPa in sandy and gravelly soils. (Lunardi, 1997). The disadvantage of most of the cement injection methods is that the grout does not spread wider than where it was injected. Jet grouting is an expensive method and the use of cement is not considered environmentally friendly. (Townsend et al, 2004).

An example of an admixture method is the stabilization with lime. It is often used as a soil stabilization method for clayey soils. When lime is injected to the soil, the clay particles start to form flocs. A cation exchange reaction occurs, when the metallic ions associated with clay particles are in contact with the calcium ions from the lime. (Bell, 1996).

The injection technique of SoSEAL resembles jet grouting. In jet grouting, water is injected to the soil with a high pressure and then the cement mixture is injected to the soil to fill the space that the water has left. Injecting high pressure water allows the cement to flow to a wider radius. In lime grouting, the chemical reaction occurs between injected mass and soil. In SoSEAL, both reacting components are injected to the soil. Instead of binding the soil particles together to a solid mass, the flocs of organic matter and aluminum fill the pore spaces reducing porosity and water content of the soil. The flocs stay attached to the pores due to physical blocking and a chemical bond between the organic matter and iron presents in the sand as impurity. The existing methods are most often implemented to increase the soil strength whereas SoSEAL aims for the reduction of soil permeability.

Another reference technique for SoSEAL is Microbially Induced Carbonate Precipitation (MICP), which is a ground improvement method, where substrates are injected to the soil and under suitable conditions the micro-organisms can catalyze a chemical reaction. In the case of MICP, the reaction occurring is the precipitation of calcium carbonate. MICP aims to improve soil strength. In the MICP method several components need to be injected to the soil: bacteria, calcium carbonate and urea. To induce the precipitation of carbonate, the proportions of component and the conditions need to be optimized. Several injections are required to achieve a cementation. Compared to MICP, the installations needed for SoSEAL are simpler and cheaper. SoSEAL requires only one injection and the soil condition such as pH do not need to be adjusted. (Van Passen, 2009).

2.2 Groundwater flow theory

In the 19th century, Henry Darcy did experiments, where he observed, how water flows through horizontal beds of sand. He deduced that the flow rate through porous media is proportional to the head loss. The flow rate is inversely proportional to the length of the path of water. The path of water depends on the porosity and the thickness of the aquifer. (Todd, 1959).

Darcy did more experiments and based on the results formulated the results in mathematical form. Darcy based his calculation on the Bernoulli equation (Eq. 1). When the proportionality is considered, and the velocity heads are neglected, the equation is simplified to Eq. 2. When Eq 2. is written in general form, it becomes Eq. 3. The parameters are presented in figure 2.1. (Todd, 1959).

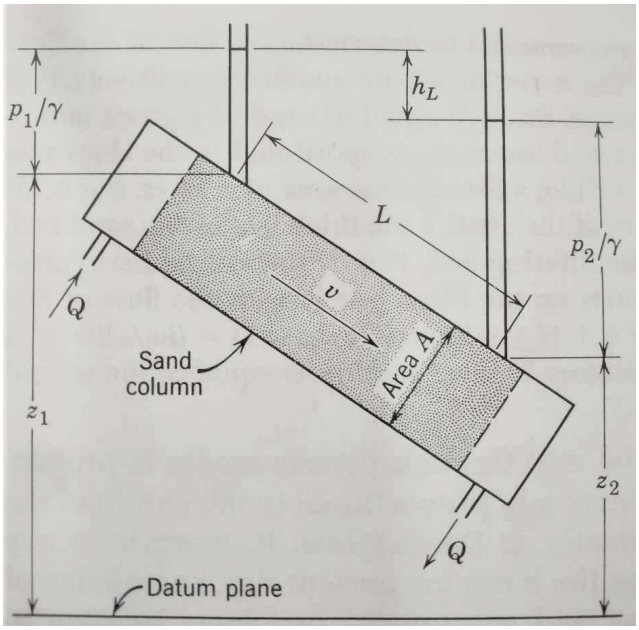

Figure 2.1. The parameters for the Bernoulli equation and Darcy's law (Todd, 1959).

$$\frac{p_1}{\gamma} + \frac{v_1}{2g} + z_1 = \frac{p_2}{\gamma} + \frac{v_2}{2g} + z_2 + h_L \qquad \text{(Eq. 1)}$$

Where p is the pressure, γ is the specific weight of water, v is the velocity of the flow, g is the acceleration of gravity, z is the elevation and h_L is the head loss.

$$Q = -KA\frac{h_L}{L} \quad \text{(Eq. 2)}$$

Where Q is the flow rate, K is the hydraulic conductivity, A is the area of the cross section and L is the length of the between the observation points.

$$Q = -KA\frac{dh}{dl} \quad \text{(Eq. 3)}$$

The use of Darcy's law is limited to laminar flow in porous media. To a flow to be laminar, the Reynolds number N_R should be less than 1 (Eq. 4).

$$N_R = \frac{\rho v D}{\mu} < 1 \quad \text{(Eq. 4)}$$

Where ρ is the fluid density, v the velocity and D the diameter (of a pipe) and μ is the viscosity of the fluid. Most natural underground flows occur with $N_R<1$. Sometimes near the pumped wells, the flow velocity can be so high that Darcy's law may not apply. (Todd, 1959).

2.3 Definitions

2.3.1 Aquifer types

An **aquifer** is a layer with a high hydraulic conductivity that can transfer significant quantities of water under an ordinary hydraulic gradient. An **aquitard** is a layer that has such low permeability that it cannot directly supply water for wells, but it can transfer water between aquifers. Aquifers have properties that help to classify them. In nature, these properties are not unambiguous. Aquifers are typically divided into three main groups: confined aquifers, unconfined aquifers, and leaky aquifers. (Hiscock et al., 2014).

A **confined aquifer** is surrounded by a layer of low permeability from both upper and lower direction (figure 2.2) (Schwartz et al., 2003). The pressure in groundwater is confined by the overlying impermeable layer and therefore it is higher than the atmospheric pressure. A confined aquifer can be also referred to as artesian or pressure aquifers (Todd, 1959).

Unconfined aquifers have the water table as upper boundary and for that reason, they can also be referred to as phreatic aquifers (figure 2.2). Unconfined aquifers can be directly recharged from the ground surface and above the water table there is a capillary fringe that is often neglected in groundwater studies (Bear, 1979).

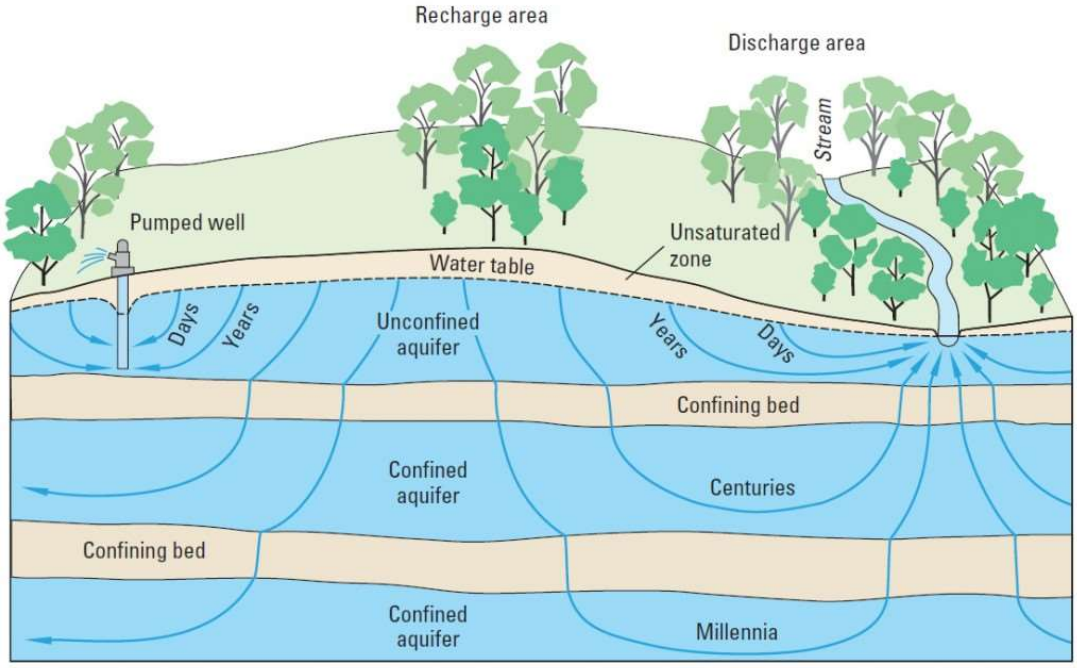

Figure 2.2. A schematic figure of the difference between an unconfined aquifer and a confined aquifer (Otwell, 2016).

Leaky aquifers can be either unconfined or confined aquifers that can be recharged or discharged from the layers above or below (Bear, 1979). Leaky aquifers are formed when a semi-pervious layer or a semi-confining layer is above or below a permeable layer (figure 2.3). A leaky aquifer can be either leaky unconfined aquifers or leaky confined aquifers depending on whether the semi-pervious layer is only at the bottom or also on the top of the aquifer. When a leaky aquifer is pumped, the water is removed by horizontal flow from the aquifer. The aquifer is recharged by vertical flow from the aquitard to the aquifer (Todd, 1959).

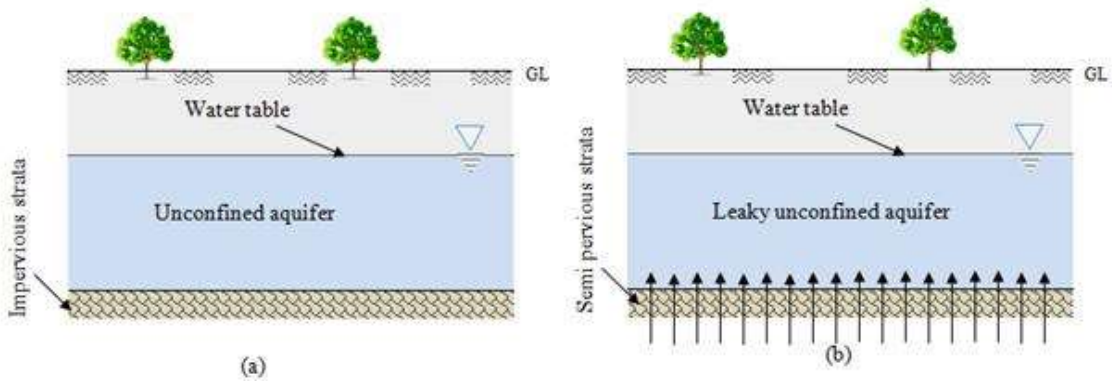

Figure 2.3. The unconfined aquifer has an impervious layer at the bottom whereas the leaky unconfined aquifer has semi-pervious layer at the bottom (NPTEL, 2018).

2.3.2 Aquifer parameters

Intrinsic permeability (k) is a property of the porous material and it is not related to the viscosity of the fluid. Intrinsic permeability is related to the opening sizes of the porous

material. When the term permeability is employed, it refers most of the time to the intrinsic permeability. The SI-unit for permeability is m^2. (Hiscock et al., 2014).

In groundwater studies, the liquid in focus is water so instead of permeability, **hydraulic conductivity** (K) is a more common parameter. In Darcy's law, K is defined, by quoting Schwartz et al. (2003), as "*a constant of proportionality relating the specific discharge and the hydraulic gradient."* In other words, it describes how easily the water flows through a porous media. The SI-unit of hydraulic conductivity is m/s but since the movement is so slow the unit m/d is often applied. Hydraulic conductivities of different soil types vary from $1 \cdot 10^{-8}$ to 1000 (table 2.1) (Bouwer, 1978).

Table 2.1 Hydraulic conductivity of different soil types (Bouwer, 1978).

Materials	Range of K ($m\ day^{-1}$)
Clay soils (surface)	0.2
Deep clay beds	10^{-6}-10^{-2}
Loam soils (surface)	0.1-1
Fine sand	1-5
Medium sand	5-20
Coarse sand	20-100
Gravel	100-1000
Sand and gravel mixes	5-100
Clay, sandand gravel mixes (till)	0.001- 0.1

Schwartz et al. (2003) describe **transmissivity** (T) as the ease of water to flow through the aquifer. As a parameter, it is the rate of water transmitted through a unit width of the aquifer. A common unit for T is m^2/d. The main difference between hydraulic conductivity and transmissivity is that transmissivity is applied for an aquifer with a certain thickness b. The mathematical relation between the parameters is demonstrated in Eq. 5.

$$T = K \cdot b \qquad \text{(Eq. 5)}$$

The transmissivity is not the only aquifer property affecting the groundwater flow. An important parameter is the storativity of the aquifer. Bear (1979) describes **storativity** (S) as "*the volume of water added to a unit horizontal area of the aquifer per unit rise in the water table elevation*" (Eq. 6). The storativity is composed of two components: **specific storage** (S_s) and **specific yield** (S_y) (Eq.7). Both parameters describe the change in the volume of water in the aquifer, but they occur under different circumstances. (Bear,1979).

$$S = \frac{volume\ of\ water}{(uni\ \ area)(unit\ hea\ \ \ change)} \qquad \text{(Eq. 6)}$$

$$S = S_s \cdot b + S_y \qquad \text{(Eq. 7)}$$

The storativity of the unconfined aquifers and confined aquifers differ. When a well in a confined aquifer is pumped the water expands slightly due to the pressuring caused by a declining hydraulic head. This expansion allows a small volume of additional water to flow out. To compensate the water flowing to the well, the aquifer collapses slightly. Specific storage is the amount of water released or stored per unit aquifer thickness by unit of head change. The specific storage is an interesting aquifer property since in geotechnics, water is often considered incompressible. For confined aquifers, the storativity value is composed of only specific storage and it ranges from 10^{-3} to 10^{-5} 1/m.

In an unconfined aquifer, the water drains also from the pores and from the unsaturated zone situated above the water table. For unconfined aquifers, the storage needs to be defined for two stages: early stage and late stage. In the early stage, the water level change occurs, as for the confined aquifers, due to expansion and compression of water and the soil matrix. In the late stage, the head change is caused by the gravity drainage of the pores. The water release or storage of early stage is represented by the specific storage whereas the late stage is represented by the specific yield. Different aquifer materials have different kind of typical specific yield values (table 2.2). The specific yield ranges from 0.1 to 0.3 whereas specific storage ranges from 10^{-3} to 10^{-5} 1/m. Due to the difference of several orders of magnitude, the specific storage can often be neglected for unconfined aquifers. (Schwartz et al., 2003).

Table 2.2. The specific yields of various materials in % (Johnson, 1963).

Material	Number of determinations	Specific yield		
		Maximum	Minimum	Average
Clay	15	5	0	2
Silt	16	19	3	8
Sandy clay	12	12	3	7
Fine sand	17	28	10	21
Medium sand	17	32	15	26
Coarse sand	17	35	20	27
Gravelly sand	15	35	20	25
Fine gravel	17	35	21	25
Medium gravel	14	26	13	23
Coarse gravel	14	26	12	22

2.3.3 Aquifer properties

When the hydraulic conductivity in a given location is independent of direction, the aquifer is said to be **isotropic**. In an **anisotropic** aquifer, the ratio between the horizontal hydraulic conductivity K_x and the vertical hydraulic conductivity K_z differs from 1. This is often the case if the aquifer is composed of several superposed layers. Typically, the horizontal hydraulic conductivity is larger than the vertical hydraulic conductivity. In some layered soils, the K_x/K_z-ratio can be up to 100. (Fitts, 2013).

The definition of **homogeneity** is that the permeability is independent of location. When dealing with groundwater, the flowing material is water, so the definition can be extended to hydraulic conductivity. If in a geological unit in a given direction the hydraulic conductivity is not the same from point to point, the conditions are **heterogeneous**. (Schwartz et al., 2003).

2.3.4 Well parameters

Wells have fixed parameters that are linked to their geometry and physical properties whereas some parameters are linked to the pumping of wells. Fixed parameters of the well are the well length, the filter length, and the inner and outer diameters.

Drawdown (s) is the difference between the static water level and the decreased water level caused by pumping. Water can also be pumped into the well. The term drawdown is also used even though the water level in the well increases. The SI-unit for drawdown is m. (Schwartz et al., 2003).

The drawdown around the pumping well decreases with the distance. When the potentiometric surfaces around the pumped well are measured and drawn, they form an inverted cone that is called the cone of depression (figure 2.4). The radius of influence describes how far away from the pumped well are the edges of the cone of depression. (Schwartz et al., 2003).

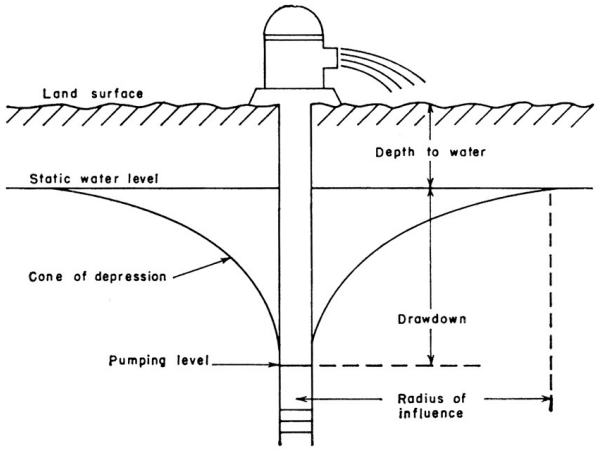

Figure 2.4. A pumped well causes a cone of depression in its surroundings (Kansas Geological Survey, 1965).

Wells can be either partially or fully penetrating. In a partially penetrating well the bottom of the well does not reach the bottom of the aquifer. This creates a vertical flow towards the bottom of the well. For a fully penetrating well, only horizontal flow is assumed. The head loss of a partially penetrated well is bigger due to a higher flow velocity at vicinity of the test well. In some pumping test and slug test analysis methods a fully penetrating well is assumed. A partially penetrating well can be also applied if its effect at the proximity of the test well is considered. (Bear, 1979).

Wellbore storage means that the water stored to the well will flow out of the well causing a quick drawdown. Its effect can be seen from the variation of the derivative of the time-drawdown plot (figure 2.5). Wellbore storage causes the bump in the derivative.

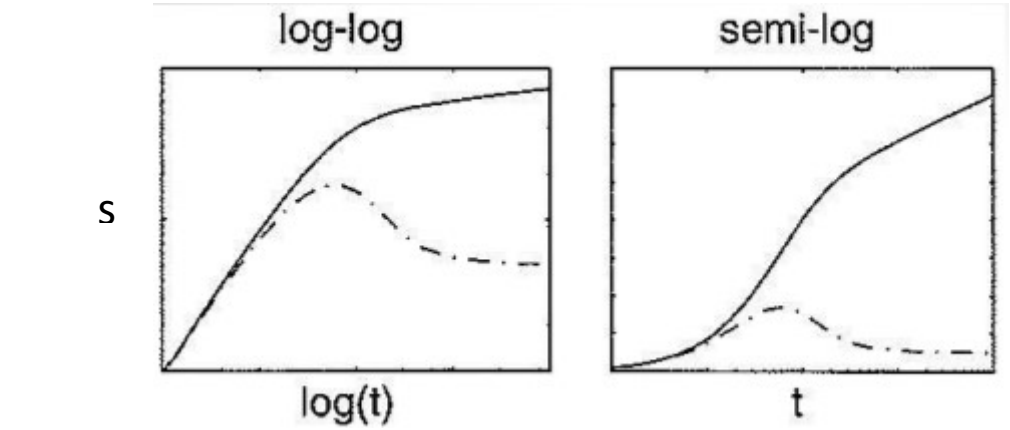

Figure 2.5. The effect of the wellbore storage in the logarithmic derivative drawdown curve (Renard et al. 2009).

The effect of the wellbore storage is easily masked if the start of the pumping test is incorrectly defined. If the interpretation of pumping test data is started too early the effect of the wellbore storage may be falsely interpreted as delayed yield. If the interpretation of data is started too late, the wellbore storage may be completely cut off and the curve resembles a standard Theis (1935) curve (figure 2.6). The Theis curve is explained in section 3.2.1.

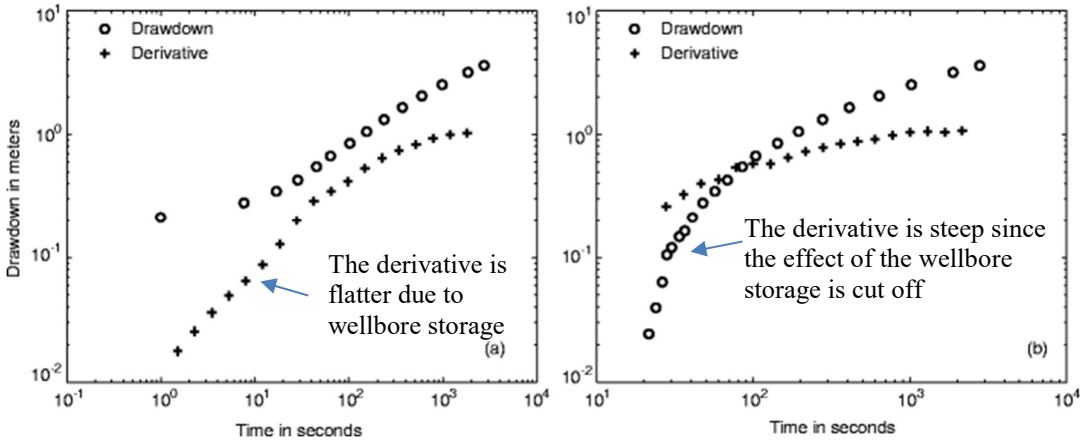

Figure 2.6. Examples of logarithmic drawdown derivatives when the measurements are started too early (left) or too late (right) (Renard et al., 2009).

The water level at the outside of the well does not automatically correspond to the water level observed in the well due to different pressure in the well and in the soil surrounding it. The water surface in the well is not flat but slightly curved (Figure 2.7). The effect of the curvature to the water level is more pronounced in large diameter wells.

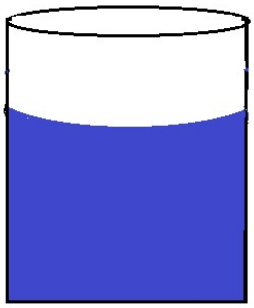

Figure 2.7 The water surface at the walls of wells is slightly higher than in the middle.

Positive skin effect means that there is an increase in pressure drop during the pumping test due to extra flow resistance near the wellbore. Positive skin can occur due to insufficient or plugged perforations, mud invasion or partial penetrations. Negative skin refers to a decrease in pressure drop that is related to a flow enhancement near the wellbore. Some reasons for negative skin friction can be the presence of natural fractures or fissures, well geometry or acidification. (TestWells-website, 2018).

3 Defining soil permeability

Defining permeability is challenging due to the heterogeneity of soil and soil layers. Permeability can be defined from the hydraulic conductivity or transmissivity of the soil. The uncertainty of the estimation of permeability will be partly due to the discrepancies between the mathematical model and the tested system, the error and simplifications of the analysis tool and the uncertainty linked to the data.

The following section presents different techniques, methods and tools to define soil transmissivity and storativity. Then the theory of Neuman (1975) method that was chosen for further analysis is presented in more detail. Finally, some necessary assumptions and sources of errors are presented.

3.1 Measuring techniques

Soil permeability can be defined with either formulas and literature values, laboratory tests, a tracer test, a slug test, or a pumping test (Todd, 1959). Numerical modeling can be used for complex problems if there is enough background information.

The simplest and least reliable way to define the soil permeability is to compare table values of soil. To use this method, the grain size and the degree of compaction need to be known. A slightly more accurate method is to define permeability in the laboratory with a permeameter. The test can be done either as a falling head test or a constant head test. The test is performed by making water flow through the soil sample while flow rate and head loss are measured. Laboratory tests give a reliable value of the permeability of the sample, but it may be a poor representative of the whole aquifer. It is difficult to create the same conditions in the laboratory as in the field and samples get easily disturbed when they are collected from the field. (Todd, 1959).

One approach is to do on-site measurements. A tracer test involves injecting a tracer product such as a salt to a test well and measure the time interval it takes for it to migrate to an observation well. For the tracer test to be successful, the observation wells need to be situated close to each other and the direction of the flow should be known. The transmissivity value obtained from a trace test is a rough estimation. (Todd, 1959).

Slug test is based on the recovery of the water table level after it has been changed rapidly. The test can be a falling head slug test or a rising head test. In a falling head slug test, a slug is dropped to the test well whereas in the rising head test the slug is lifted from the well. The change of water table is monitored with divers situated in the test well. (Fitts, 2013).

In a pumping test, the water is pumped either into or out from a test well. The drawdown induced by the pumping is measured from the test well and monitoring wells. The term drawdown refers to the difference between the initial water level and the water level at time t. A single-well pumping test is a test where pumping and the measurements are from the same well. In a multi-well test pumping test, the drawdown is measured from at least one observation well that is not the test well (Tang et al., 2016). As a difference to slug tests, pumping test is ideally conducted long enough to reach the quasi-steady state. For

groundwater flow problems, on-site measurements are the most reliable method to define transmissivity and therefore they are studied further in the following part.

Richard et al. (2016) studied the effect of the duration to the pumping test values. The conclusion was that the long pumping test gives higher transmissivity values. A reason suggested was that the long duration increases the probability of high-permeability zones to connect. The analysis method should be defined before the start of the pumping test since the methods require different kind of data. The chosen analysis method affects the length of the pumping test required. If the method has a late-time curve, the length of the pumping test should be extended to a minimum of 24 hours.

3.2 Analysis methods and tools

The governing general equations are based on the physical principles of Darcy's law and mass balance. Most groundwater flow theorems are based on the general groundwater flow equation that can be obtained by combining these two principles. Based on these two principles, the transmissivity of an unconfined aquifer with a horizontal base can be estimated by assuming a homogeneous horizontal K. The transmissivity is obtained with the general equations 8 and 9 depending on the conditions. Equation 8 is the linear Poisson equation that assumes steady flow. (Fitts, 2013).

$$\nabla^2(h^2) = -\frac{2N}{K} \quad \text{(Eq. 8)}$$

where N is the net recharge or leakage. If there is no infiltration nor leakage, N=0. The equation 8 is then simplified to equation 9, which is the linear Laplace equation,

$$\nabla^2(h^2) = 0 \quad \text{(Eq. 9)}$$

For the pumping tests and slug tests, a radial flow towards or from the well is assumed. The direction of the flow depends whether water is added to the well or extracted from the well. A radially symmetric solution (Eq. 10) can be used.

$$h^2 = \frac{Q}{\pi K}\ln(r) + C \quad \text{(Eq. 10)}$$

Where Q is the discharge, C is a constant and r is the radial distance from the center of the well to the evaluation point. Equation 10 is a solution for the Laplace equation 9. (Fitts, 2013). Most pumping test and slug test analysis methods are based on the equation 10.

3.2.1 Analyzing of pumping tests

The traditional pumping test analysis methods can be roughly divided into two categories: mathematical methods and graphical methods. Many of the methods are quite old. Thiem developed an equilibrium theory in 1906 and Theis developed his first theory the Theis Nonequilibrium method in 1935. Many of the later theories are updates for the Theis theory. (Fang et al., 1968) All the methods analyzed are multi-well pumping test analysis methods.

Mathematical methods refer to defining the transmissivity and storativity with formulas. The equilibrium theory by **Thiem** (1906) is an example of a rather simple mathematical method. The aquifer transmissivity can be obtained easily when the equilibrium theory is modified (Eq. 11). It is quick to apply but due to several simplifications and assumptions, the reliability of the result needs to be estimated. The Thiem equilibrium theory assumes a confined, homogeneous and isotropic aquifer that has been pumped until it has reached the steady state.

$$T = \frac{Q}{2\pi(h_2 - h_1)} \ln \frac{r_2}{r_1} \quad \text{(Eq. 11)}$$

Where Q is the flow rate, h_1 is the head at the beginning of measurements, h_2 is the head in the observation well at steady state, r_1 is the well radius and r_2 is the distance between the test well and the observation well. (Theis, 1935).

When a graphical method is used, most often the change in head is plotted as a function of time. When plotted on a logarithmic scale, the measured data can be put on top of type curves. Then the data is fitted with the type curves and with the help of matching points, the transmissivity can be calculated.

The different graphical methods to obtain the transmissivity of the soil from pumping tests studied were the Theis method, the Neuman method, and the Cooper-Papadopoulos method. Other methods were also considered but their assumptions did not suit the case studied. All the methods considered assume an aquifer with infinite dimensions, a transient flow and an instant release of water from storage or groundwater surface.

The **Theis** (1935,1941) method is for pumping test analysis of confined, isotropic and homogenous aquifers. The well is assumed to be fully penetrating. Schwartz et al. (2003) formulated the Theis equations in the following way:

$$h_0 - h = \frac{Q}{4\pi T} W(u) \quad \text{(Eq. 12)}$$

$$u = \frac{r^2 S}{4Tt} \quad \text{(Eq. 13)}$$

$$W(u) = \int_u^\infty \frac{e^{-y}}{y} dy \quad \text{(Eq. 14)}$$

Where W(u) is the well function and u (Eq. 13) is a dimensionless variable. Since the well function (Eq. 14) is complicated to solve, tabulated values are used. When the Theis (1935, 1941) method is used for unconfined aquifers, the drawdown should be adjusted with Eq. 15.

$$s = b - (b^2 - 2s'b)^{\frac{1}{2}} \quad \text{(Eq. 15)}$$

where s is the drawdown of the unconfined aquifer, s' is the drawdown of the confined aquifer and b is the original thickness of the aquifer. (Schwartz et al., 2003).

The **Neuman** (1975) method is for an unconfined, anisotropic and homogenous aquifer with a fully or partially penetrating well. It is a combination of two Theis curves; one for the early

time and another for the late time. The theory of Neuman method is explained in detail in section 3.3 and application can be found in section 5.3.3.

The **Papadopulos-Cooper** (1967) method is for confined, isotropic and homogenous aquifers with a fully penetrating well. As a difference to the Theis (1935) method, it considers the wellbore storage. For matching the distance-drawdown method, which is a simplification of the Cooper-Jacob solution, is used. It is based on the Theis late-time curves. The Papadopulos-Cooper method is well suited for pumping tests analysis of large diameter wells. (Papadopulos et al., 1967).

3.2.2 Slug test

One of the hypothesis is that injection could have the same kind of effect than a prolonged slug test. Injecting the mixture to soil would provoke a rise in the water table and the recovery of the water table could be interpreted as a slug test analysis (figure 3.1). The slug tests are single-well tests.

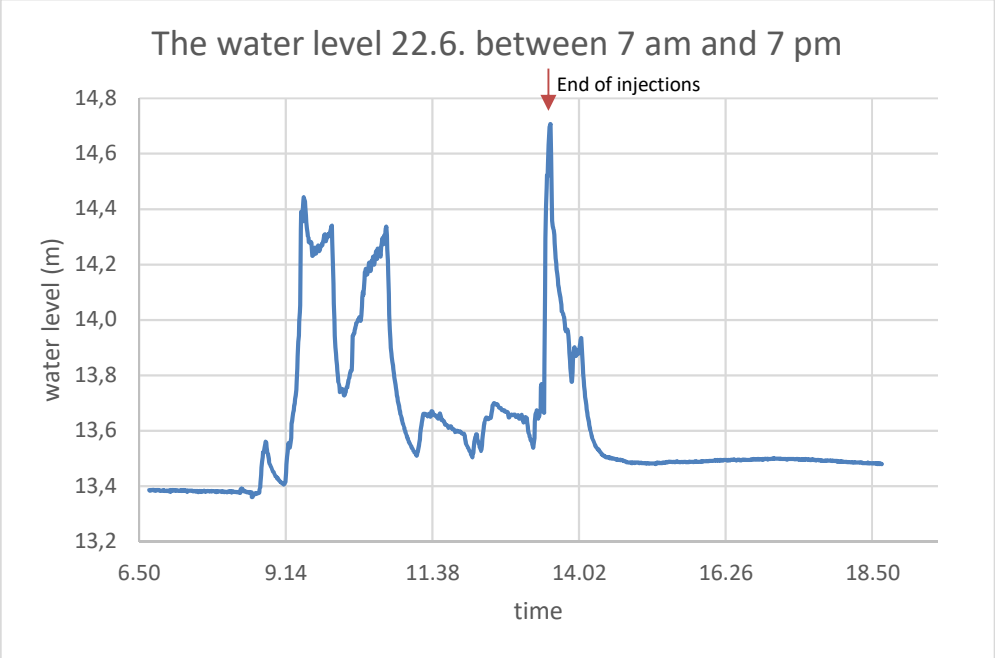

Figure 3.1. The injection stopped at 2 p.m. and the recovery was interpreted as a slug test.

The analysis methods used were the Hvorslev approach and the Cooper-Bredehoeft-Papadopulos (1967) methods. The Hvorslev method (1951) was the first one developed and in the same way as the Theis (1935) in pumping tests, it is the base for the other methods developed afterwards. Hvorslev (1951) and Cooper-Bredehoeft-Papadopulos (1967) both assume a homogenous confined aquifer and the water injected or discharged is released instantaneously from the test well. The test well can be a partially penetrating well for Hvorslev whereas Cooper-Bredehoeft-Papadopulos (1967) assumes a fully penetrating well. Eq. 16 is the Hvorslev equation.

$$K = \frac{A}{F}\frac{1}{t_2 - t_1}\ln\frac{H_1}{H_2} \qquad \text{(Eq. 16)}$$

Where A is the cross-sectional area of the well, F is a shape factor, H_1 and H_2 are the drawdowns at time t_1 and t_2. Schwartz et al. (2003) define different shape factors. The studied case is a cased hole with an uncased extension. The extension must be at least 8-times longer that the radius of the well. The shape factor for this case is (Eq. 17):

$$F = \frac{2\pi}{\ln(\frac{L}{R})} \quad \text{(Eq. 17)}$$

Where L is the length of the uncased extension and R is the radius of the well. When the Eq. 16 and Eq. 17 are combined, the hydraulic conductivity can be calculated (Eq. 18).

$$K = \frac{r^2}{2L(t_2 - t_1)} \ln\frac{L}{r} \ln\frac{H_1}{H_2} \quad \text{(Eq. 18)}$$

The Cooper-Bredehoeft-Papadopulos (1967) method was developed for confined aquifers with a fully penetrating well. Whereas in the Hvorslev approach the data is plotted in the semilog scale and a straight line is fitted to the data points, the Cooper-Bredehoeft-Papadopulos data is fitted to type-curves (figure 3.2). This improves the accuracy of the analysis. (Schwartz et al., 2003).

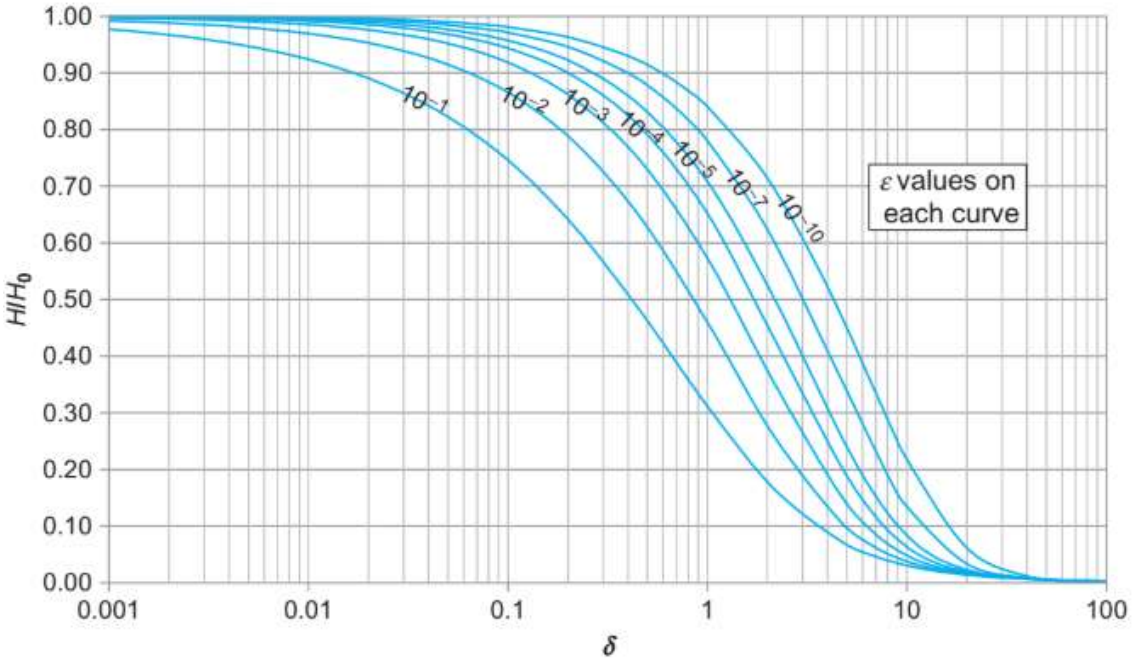

Figure 3.2. The Cooper et al (1967) type curves used in the Cooper-Bredehoeft-Papadopulos slug test analysis (Fitts, 2013).

3.3 The Neuman (1975) method

The method selected to conduct the analysis for all the zones was the Neuman (1975) method. The Neuman (1975) method is the most widely accepted model for pumping test analysis of unconfined aquifers with a radial flow. The measurement data from the water reservoir is fitting well the early time drawdown and the flat part that is the delayed gravity drainage (figure 3.3). (Fitts, 2013).

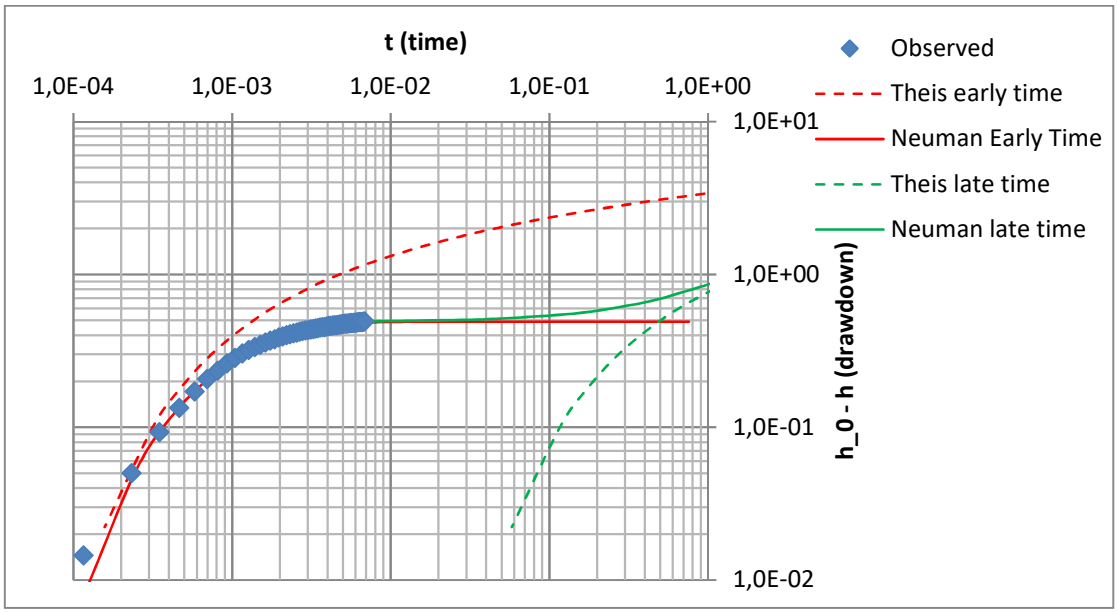

Figure 3.3. The drawdown of the well A5 when a pumping test was conducted in A3 fitted with the Neuman (1975) *method. With this fitting T=3.8 m^2/d and S=3.8·10^{-4}.*

Neuman (1972) developed an analysis to calculate the transmissivity and the storativity for unconfined aquifers. In his publications in 1972,1973 and 1974 he developed his theory and in 1975 he published a new model which is used in this analysis. When the Neuman (1975) method is used to analyze pumping test, the curve-fitting is done for two different curves. The first part is called the early time curve and it has the same shape as the Theis curve. After the early time curve, there is a flat area where the change in drawdown is almost stable. After a while, the curve starts to adopt again the shape of a Theis curve and this part is called the late time curve. Together these three parts form an S-shaped drawdown curve (figure 3.4).

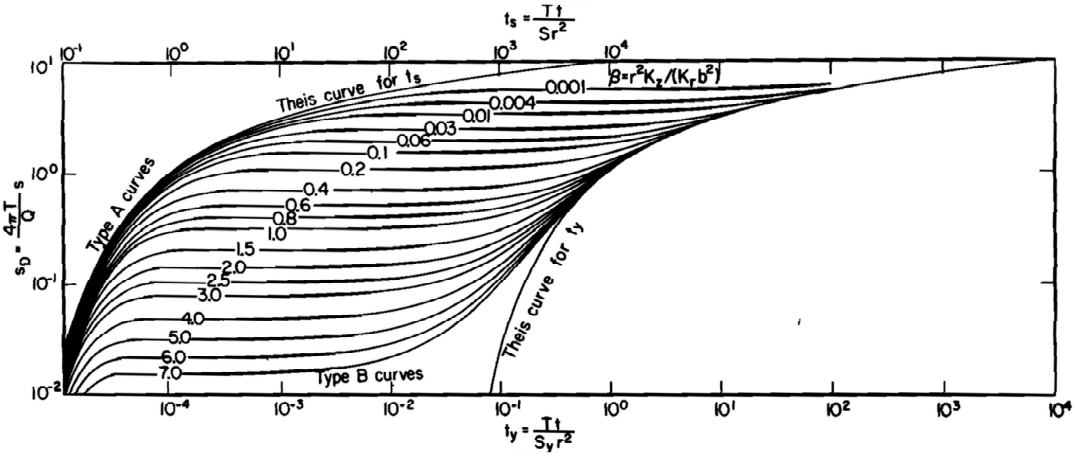

Figure 3.4. The type A and B curves in dimensionless time scales t_s and t_y (Neuman, 1975).

The early time drawdown occurs when water is released from the elastic storage in the saturated zone. The aquifer parameter affecting the early-time storativity is the specific storage which is explained in the section 2.3.3. In the late-time, the drawdown comes from water flowing due to gravity drainage at the water table. It is also called phreatic storage.

The storativity parameter for the late-time curve is the specific yield. Between the early time curve and the late time curve, there is a flat phase called the delayed yield. (Fitts, 2013)

Fitts (2013) presents the formulas for the Neuman (1975) method in the following way

$$h_0 - h = \frac{Q}{4\pi T} W(u_A, u_b, \eta) \quad \text{(Eq. 19)}$$

Where u_A represent the early time response and is defined

$$u_A = \frac{r^2 S}{4T(t-t_0)} \quad \text{(Eq. 20)}$$

And u_B for the water table storage is

$$u_B = \frac{r^2 S_y}{4T(t-t_0)} \quad \text{(Eq. 21)}$$

And the dimensionless parameter η that considers the anisotropy of the aquifer is

$$\eta = \frac{r^2 K_z}{b^2 K_r} \quad \text{(Eq. 22)}$$

The assumptions of the Neuman (1975) method are, as mentioned in section 3.2.1, that the aquifer is unconfined and homogenous. The aquifer is assumed to be of uniform thickness and to have infinite areal extent. The water is assumed to be immediately released from the storage at the beginning of pumping and from the phreatic surface in the later stage. The well is assumed to have a small diameter and it is can be either a fully or partially penetrating well. (Schwartz et al., 2003) The Neuman (1975) method does not require a steady flow nor an isotropic aquifer.

3.4 Uncertainty linked to measurements

3.4.1 Errors due to soil conditions and data collection

The heterogeneity of soil leads to a heterogeneous hydraulic conductivity of the soil which leads to preferential flow. This means that the drawdowns are not distributed according to the cone of depression. The irregularly distributed drawdown reduces the reliability of the drawdown measured from the monitoring well as representative of the drawdown occurring in other places situated at the same distance from the test well. Especially, in the baseline measurement, where there is no zone of reduced permeability, this should be considered. The heterogeneity of the soil can be estimated from the CPT (figure 4.3) and from the soil samples obtained while drilling the monitoring holes (Appendix 1).

When data is measured, measurement errors are always present. According to the diver manufacturer, the maximum error is ± 2 cmH_2O and typical error (67% of the sample fall in the range) is ± 0,5 cmH_2O. The errors are due to linearity, hysteresis, and repeatability. (Van Essen, 2018).

The test dike is surrounded by water by two sides: De Gijster on the top and a tributary of the Amer on the toe. The water level in the river varies according to the tide and the water level of the fresh water reservoir is manually controlled. The water level in the monitoring wells is mostly affected by the tide of the river. The effect can be seen in the diver data (figure 3.5). The head variation can be up to 0.2 m in a day. The tidal effect needs to be considered either by subtracting its effect from the head variations data or by considering it as an additional error. The water level variation in De Gijster and in Amer is presented in Appendix 2.

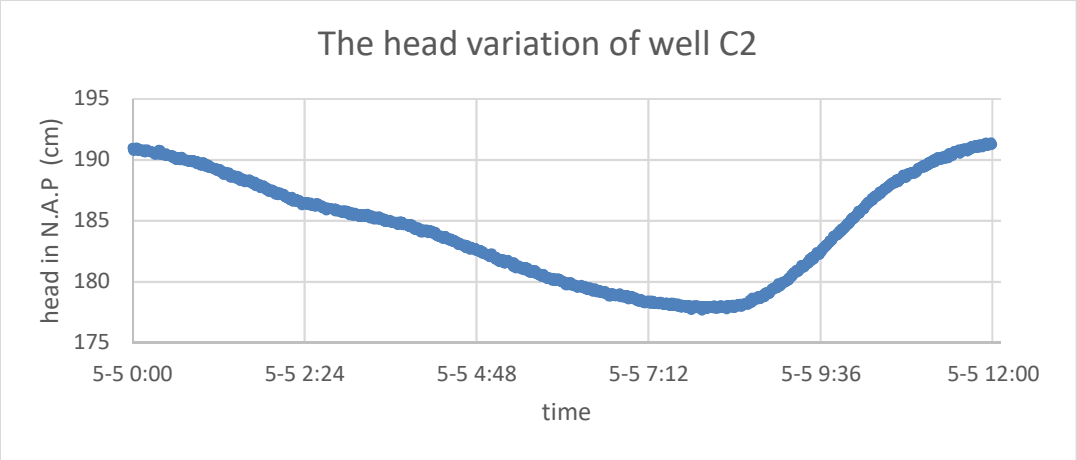

Figure 3.5. The head variation in a 12-hour time span measured before the injection.

3.4.2 Errors due to analysis

To be able to analyze the data, some simplifying assumptions are necessary. When complex reality is fitted into a simplified model, errors are unavoidable. Different models have varying assumptions. Common assumptions are that the aquifer is an isotropic and homogenous aquifer. The water is assumed to be released instantaneously from the storage. The pumping tests are conducted at a constant rate and the quasi-steady state is reached. The analysis is performed in two-dimension with radial flow and the unsaturated zone is not considered.

The studied aquifer is unconfined but for the models that are for confined aquifers, the drawdowns can be adjusted with the Eq. 15. The aquifer is most likely not isotropic; the conductivity is expected to be higher in the horizontal direction. The aquifer is not homogenous nor isotropic, especially not after the injection since the goal of the injection is to create a zone with improved soil properties.

Calvache et al. (2016) showed in a study, where a comparison of pumping test results of a coastal aquifer analyzed with different methods was conducted, that especially the values of storativity were sensitive to variation. The variation is due to soil conditions and analysis method used. The T and S values analyzed with classical methods (Theis and Cooper-Jacob) are reliable if the aquifer does not contain significant vertical heterogeneity. In some cases, the error vertical heterogeneity can cause error up to 100 % for both S and T. However, the tests were conducted on a coastal area where the effect of saline water must be considered.

The aquifer has three-dimensional flow. To bring this three-dimensional problem to two dimensions, the Dupuit-Forchheimer approximation is applied. It restricts the flow to the horizontal plane where h varies only as a function of x and y. This means that the resistance to vertical flow is neglected. According to Fitts (2013), it is reasonable to assume a vertical flow when analyzing long structures like dams. In our case, the studied structure is a dike and its geometry resembles a dam.

Theis (1935) analyzed the drawdown data obtained by L.K. Wenzel and demonstrated that the observed values are smaller than the computed values when the distance from the pumping well increases. However, the curves start to separate after 400 feet (~130 m). In our study, the maximum distance between the test well and the observation well is less than 15 meters. The error due to the distance should be small. (Theis, 1935)

The data is fitted to a curve with a graphical method. The judgment of the person doing the fit plays a role as well as the method used. In the Excel-tools, the choice of the background curve is left to the user. The user also estimates, what is the best fit. The curve-fitting should be conducted in a systematic manner to avoid additional variations in the results.

4 De Gijster – Site description, work plan and implementation

In this section the test site of the second pilot and the implementation of the reduced permeability barrier are presented in detail. The composition and the geometry of the dike is described. All the operations done in the water basin are presented starting from the monitoring system and moving to the injection. Also, the mixture injected, and its behavior is discussed.

4.1 De Gijster water reservoir and its remediation

De Gijster is one of the three freshwater reservoir basins in the national park of Biesbosch (figure 4.1). De Gijster is a storage basin whereas the two other basins are process basins. The capacity of De Gijster is 80 million m^3 of water stored. The seepage amount in De Gijster is approximately 20 000 m^3/d which corresponds to 2 % of the daily production. (Laumann et al., 2017). At the current state, the toe of the dike is in some places too wet and soft for maintenance and to let the cattle pasture in it. After the injection, the area suitable for cattle could be enlarged.

Figure 4.1. The test site is situated at the right end of De Gijster (Photo from Google Maps).

Another remediation project has also been ongoing in De Gijster. Dredging of the bottom of the fresh water reservoir was done to smoothen the step between the bottom of the reservoir and the lowest sand layer (figure 4.2). The dredging work can affect the water surface level of De Gijster and the groundwater flow towards the dike.

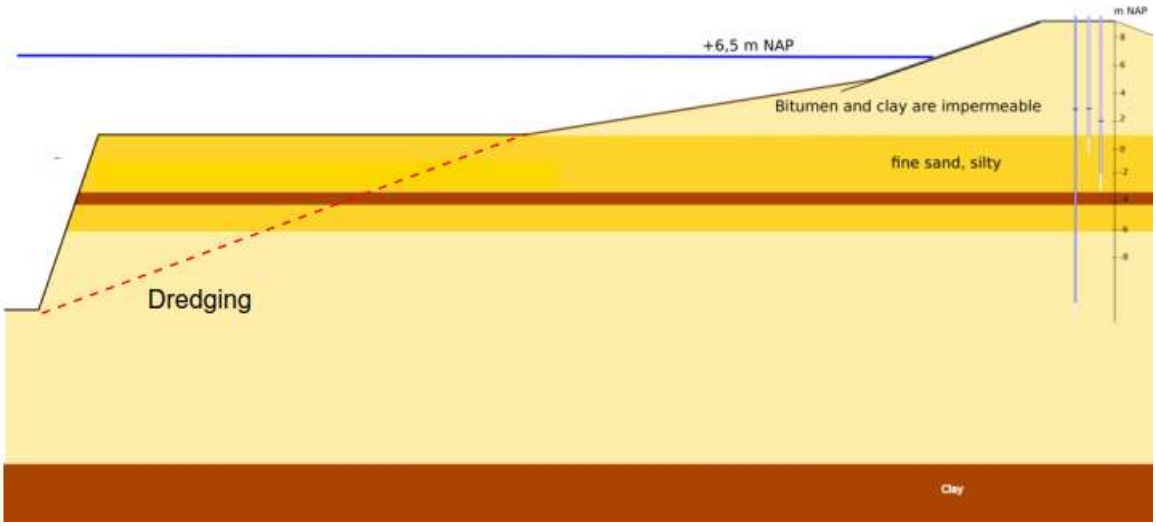

Figure 4.2. The stepping of the bottom of the fresh water reservoir is smoothen by dredging. The dredging line is only an estimation (Modified from Laumann et al., 2017).

4.2 Soil conditions and geometry of the dike

Before the installation of the monitoring system and start of injection, ground investigations were conducted. CPT measurements (figure 4.3) were done in 2011 around the freshwater reservoir and some soil profiles were defined, when installing the monitoring wells in spring 2018. According to the ground investigation and the design drawings, the dike is composed of a 9 m layer of dense medium to coarse sand that is on top of a 3 m layer of finer sand that is partly silty (figure 4.4). The dike has been built on the top of the former soil that was fine sand with silt. For the groundwater level measurement, the N.A.P. (Normal Amsterdam Level) reference plane was used. The groundwater table is at +2,5 m N.A.P. so it is in the top sand layer. Water is estimated to seep through the lower sand layer. To prevent the water flow, a vertical barrier that covers the whole fine sand layer was injected. (Laumann et al., 2017).

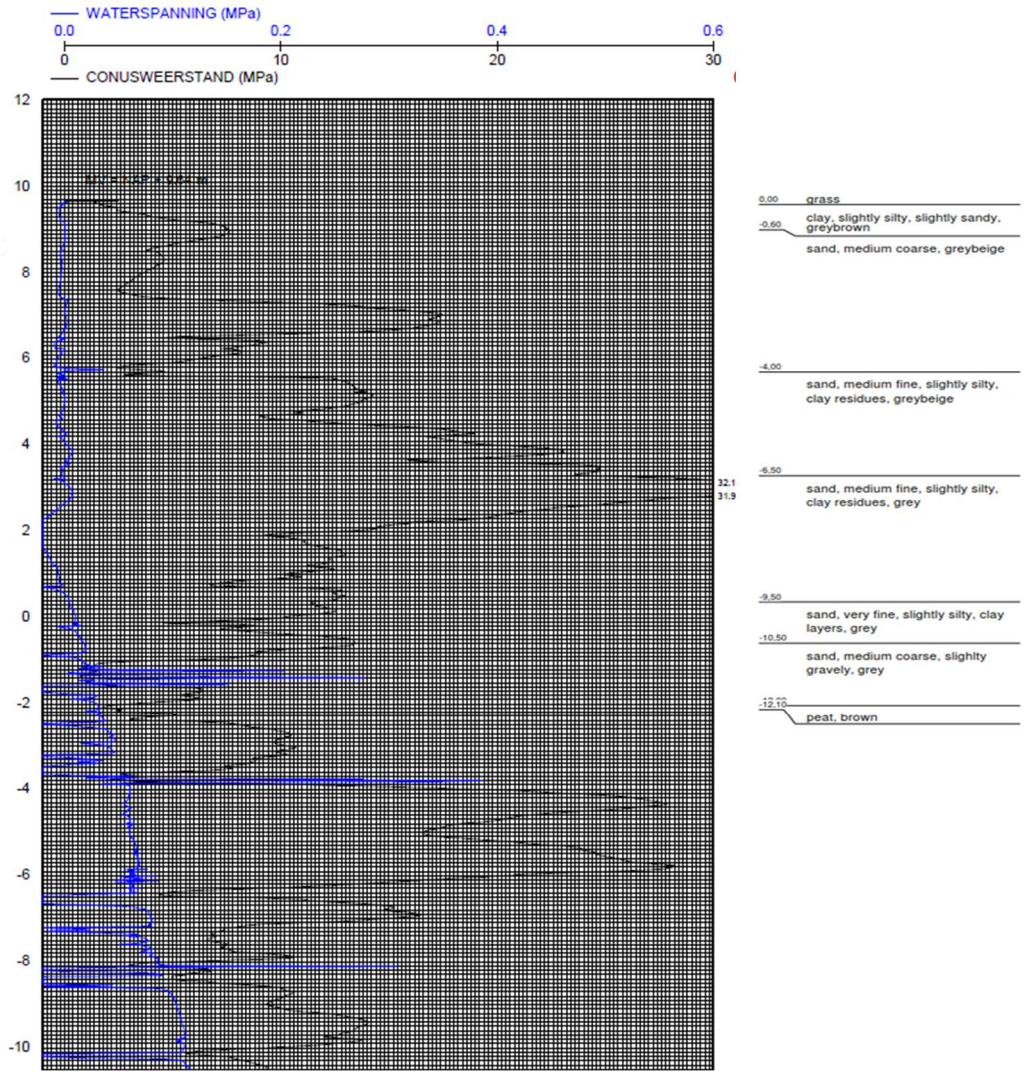

Figure 4.3. A CPT (left) from the injection zone compared to interpretation of the soil profile (right).

When the monitoring wells were installed, soil samples were taken from two wells in each zone. These soil profiles give an indication of the soil layers of the dike. They offer a more detailed estimation of the soil layers and it also shows that there is variation between different parts of the dike. Figure 4.4 is an overview used previously for the illustration of the problem. All the soil profiles are presented in Appendix 1.

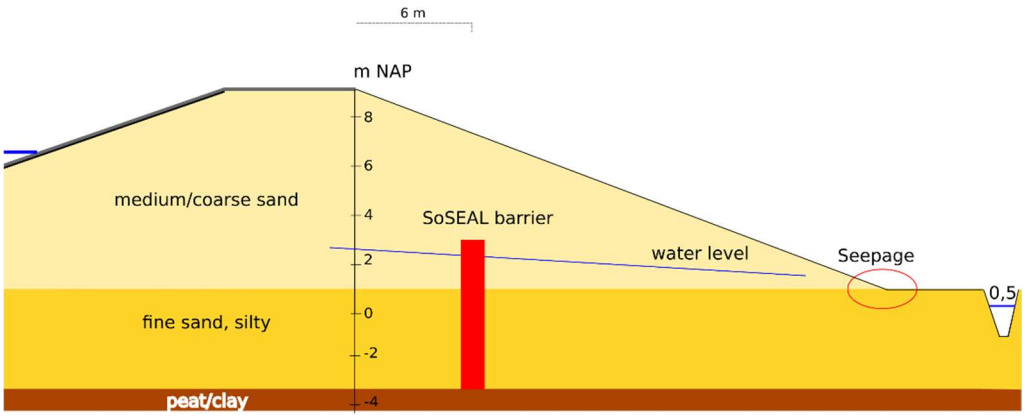

Figure 4.4. The composition of the dike and the planned SoSEAL barrier (Laumann et al., 2018).

4.3 Monitoring system

Before starting the injection, the monitoring system was installed. The system is composed of 30 monitoring wells that were positioned according to figure 4.5. The outer diameter of the wells was 50 mm and they were installed by sonic drilling. The measurements were made with divers that were dropped to the wells with cables that kept them just above the bottom of the well.

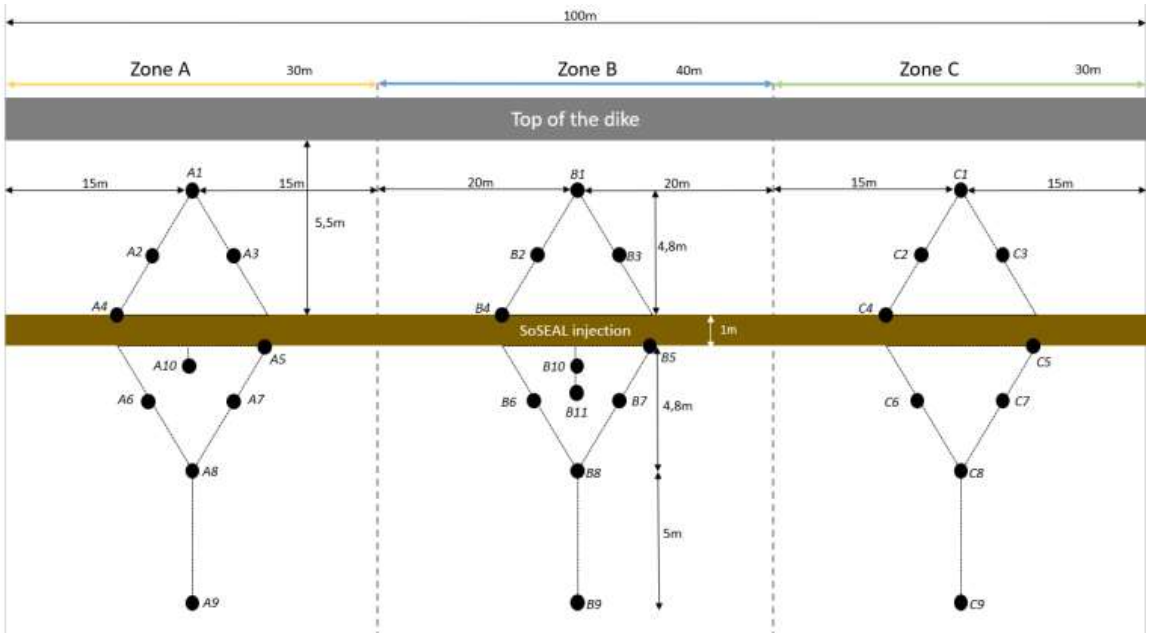

Figure 4.5 The positioning of the monitoring wells.

The well depths vary slightly depending on their positions regarding the slope. The deepest wells are 13 m deep (-3.5 N.A.P.) and they are situated close to the top of the dike. The wells towards the toe of the dike such as B9 are only 10 m deep. The wells were planned to be fully penetrating. However, the depth of the bottom of the aquifer might vary which can lead to a partial penetration. The peat layer is assumed to be a confined layer (figure 4.6) The wells have a 2 m long filter at the bottom. One of the well profiles and the soil profile are presented in figure 4.6. The cable length of the divers is for the most wells is 10.24 m, but

in the shortest wells A9, B9 and C9 the cable length is only 9 m to avoid the divers to touch the bottom of the well.

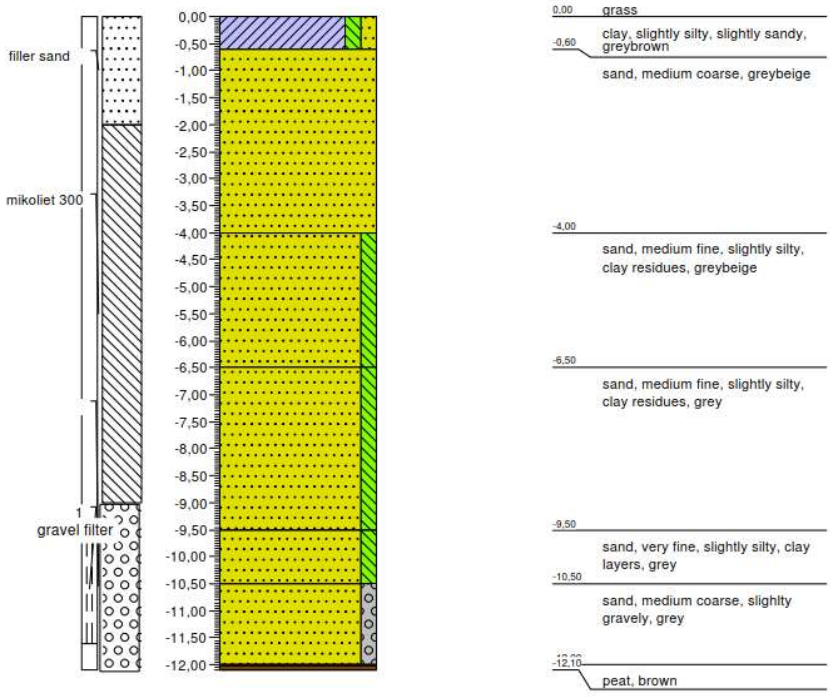

Figure 4.6. The well profile and the soil profile of the monitoring well B6.

The divers used were CTD-divers (DI271) from Van Essen instruments (Figure 4.7). The divers measured the water column on top of them. With that pressure and the cable length the variation of head could be calculated in respect to N.A.P.. Other values measured by the divers were the temperature variation and the electrical conductivity. The measuring frequency of the divers could be set manually. (Van Essen website, 2018).

Figure 4.7. The CTD-divers used for monitoring (Van Essen website, 2018).

4.4 Implementation

4.4.1 The composition of the mixture injected

The mixture consisted of organic matter and aluminum. When these two components are in contact, they form flocs. The organic matter used in de Gijster was HUMIN-P 755 and the aluminum was in a form of the salt aluminum chloride hexahydrate ($AlCl_3 \cdot 6H_2O$) (Bonfiglio, 2016).

HUMIN-P 755 is a humic substance, more precisely a humin. The components of natural organic matter in soil is called humus and it can be divided in humic substances and non-humic substances. According to van Zomeren (2008), humic substances are, "*a series of unidentifiable organic compounds of relatively high-molecular-weight*" (van Zomeren, 2008). The main components of humic substances are carbon, oxygen, hydrogen. (Jones et al. 1998) After all the other components of soil organic matter (SOM) have dissolved to an aqueous base, humin is what is left (Hayes et al, 2017). Regarding the reaction of metal complexation and humic substances, the most relevant groups are carboxyl and phenolic hydroxyl groups. (Csubák, 2017) The product used in this project was produced in Germany by HUMIN-TECH (Bonfiglio, 2016).

The aluminum chloride hexahydrate ($AlCl_3 \cdot 6H_2O$) was in form of a crystal powder that was added to water together with the organic matter. The components and their combination are presented in figure 4.8. The reaction occurring between aluminum and organic matter is a chemical-physical interaction resulting from anion and ligand exchange between organic matter and hydrous aluminum oxide surfaces (Greenland, 1971). In an anion exchange organic anion is attached to oxide surface by coulombic attraction. Ligand exchange is the adsorption of anion by hydrous aluminum oxide that gets incorporated with the surface hydroxyl layer. (Deb et al., 2011) In a solution, the complexation between aluminum and organic matter takes place in minutes (Vis, 2015). The flocs are hydroscopic particles bound by electrostatic attraction and they form aggregates that clog the voids between soil (Bonfiglio, 2016). The reaction between the organic matter and aluminum releases Cl^- and K^+-ions to the water.

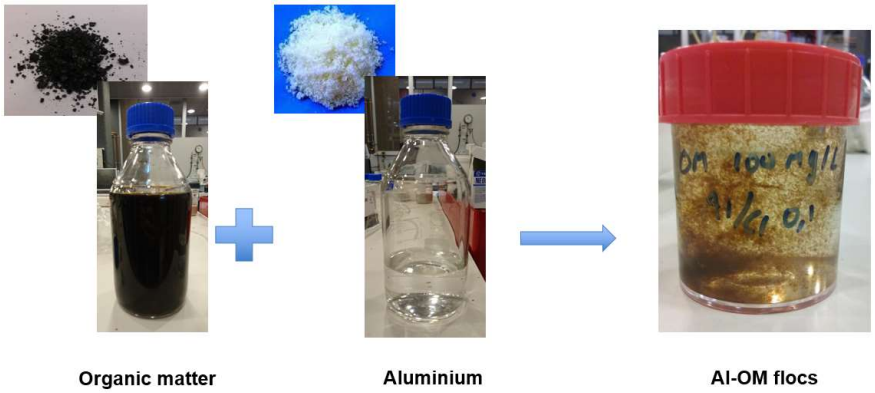

Figure 4.8. Before mixing OM and Al are in a dry form that is soluble in water. When the solutions are combined, flocs start forming (Laumann et al., 2017).

4.4.2 Injection equipment and technique

Aluminum and organic matter where added through the cone pointed in the figure 4.8. Water was flowing in the tube connected to the cone. After combining the components, the mix travels to a mixer, where total blending of the components is guaranteed (figure 4.9). The flocs start to form as soon as the stirring is stopped. The floc size is 100-800 micrometers depending on the stirring rate (Laumann et al., 2018).

Figure 4.9. The stirring batch and on its right side the cone to add Al and OM to the system (Lassila, 2018).

The injection was performed with the equipment of Heijmans (figure 4.10). The machine used is usually utilized to detect metal parts such as mines from the ground. For this experiment, the machine was modified by installing a piping system for the injection and changing the tip to suit the injection.

Figure 4.10. The injection machine on the De Gijster test site (Lassila,2018).

First, the tip of the injection machine was pushed down to the lowest injection level to roughly 13 meters down from the top of the dike. The mixture was injected at one level for three minutes before lifting the tip up by 0.5 m. At each level 130 l of mixture was injected. This took approximately 3 minutes. The highest injection level was at 5.7 meters from the ground surface. One injection contained 130 liters of the mixture so a total of 1.8 m^3 of mixture was injected in each injection point. The injection process was automated.

The plan was to have 100 injection points with a 1 m spacing between them. The goal was to form a barrier with a 1-meter diameter. To ensure a barrier without gaps, an injection pattern with overlapping affected zones was used. (Zhou et al., 2017). The used pattern is presented in figure 4.11. The injection holes were sealed with bentonite pellets (Mikolit 300) to prevent surface water flowing into the hole.

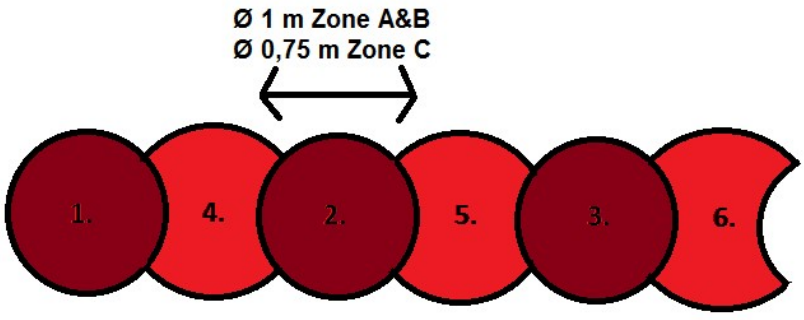

Figure 4.11. The overlapping injection pattern.

4.4.3 Zones

The length of the injected line was 100 m. It was divided into three zones: A, B and C (figure 4.12). The injection started from zone A, then moved to zone B and ended with the zone C. In zone A, the organic matter concentration of the injected mixture was 3 g/l and the spacing of the injection points was 1 meter. In zone B, the injection interval was the same, but the organic matter concentration was 5 g/l. The organic matter concentration and spacing of injection of zone C were defined based on the preliminary results of the two preceding zones. In zone C, the organic matter concentration was kept at 5 g/l but the injection spacing was reduced to 0.75 m. The volume of the mixture injected per injection point was reduced to 1.02 m^3 and the injection time per level was reduced to 2 minutes (Zhou et al, 2017). All the zones were injected in a period of three weeks from the end of June to mid-July 2018 (figure 4.13).

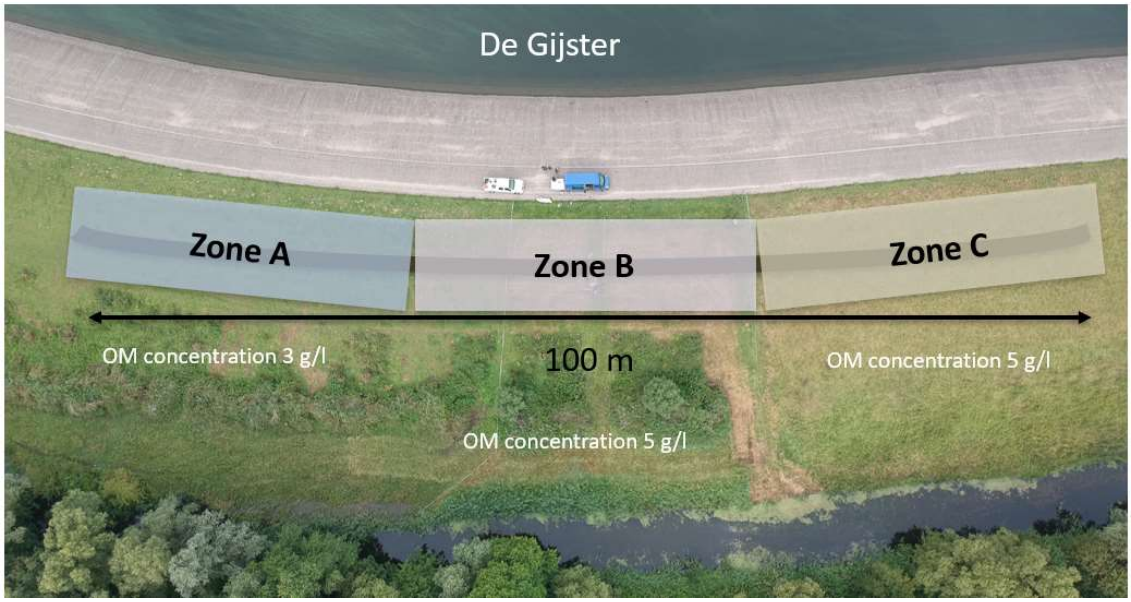

Figure 4.12. The three zones of the De Gijster test site (Laumann, 2017).

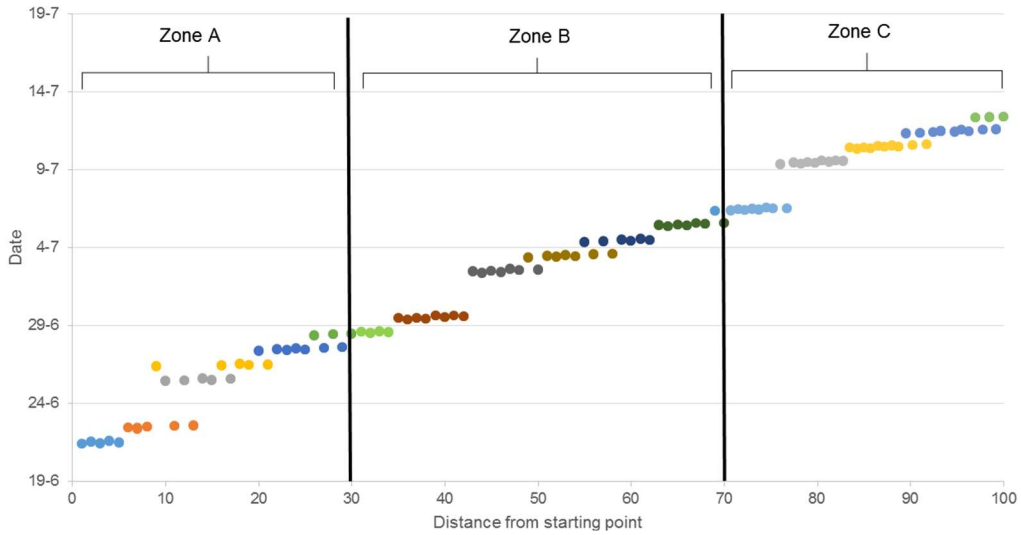

Figure 4.13. The progress of the injection. The colors represent the injection dates (Laumann et al. 2018).

4.4.4 The behavior of the mixture

Bonfiglio (2016) studied the behavior of the components used in SoSEAL project in her master thesis. In the laboratory, columns of different grain size sands were treated with the mixture and their hydraulic conductivity was measured before and after. The results of her experiments were promising and reproducible. The hydraulic conductivity was reduced by 87 % for the finer sands and 61-74 % for coarser sands. (Bonfiglio, 2016) The sands were not from the test site, so they are not directly comparable to the sand of de Gijster. Also, the injection technique in her experiments was different from the one used in the reservoir dike since the components were not mixed beforehand.

The mechanism behind the reduction of soil permeability is based on the reduced pore space by the flocculating mixture (figure 1.1). In laboratory tests, the precipitation band was visually detectable after 30 min. In the injection strategy used on the site of De Gijster, the components already meet so the migration time in the soil before the encountering of the reactants can be subtracted. The laboratory tests did not give an indication about the longevity of the flocs.

5 Data collection and analysis methods

The aim of the data analysis is to study the effect of the SoSEAL injection in the soil permeability in the dike of a water reservoir. This section presents the data obtained from the divers, its treatment and application to the methods described in the previous section. As an outcome, the analysis should show changes in two soil properties influenced by the SoSEAL barrier: the soil permeability k and the storativity S. One of the objectives is to localize the zone of reduced permeability and if possible quantify it.

5.1 Data

5.1.1 Data obtained from the site

The data was collected from divers situated in the monitoring wells. The data collection started in May 2018. Pumping test were conducted on the site in May, June, July and October 2018. The dates of the pumping test are presented in Appendix 3. The tests will continue after October 2018, but the results of later tests are not considered in this thesis.

For the early preliminary measurements, the measurement frequency of the divers was set to 1 hour. Later when performing a pumping test, the frequency was set to 10 seconds. From the start of the injection until a week from the injection, the measurement rate was kept at 10 seconds. From the divers, the data could be downloaded as a DAT-file and transformed into Excel. The water level was corrected with the cable length of the diver. Table 5.1. represents a sample from the corrected data.

Table 5.1. Diver data from the well C3.

Date & Time	Water level N.A.P. (cmH2O)	Pressure (cmH2O)	Temperature (Celsius)	Spec.cond. (mS/cm)
15-6-2018 10:10:00	208.300	1318.925	11.920	0.448
15-6-2018 10:10:10	208.299	1318.925	11.910	0.449
15-6-2018 10:10:20	208.357	1318.983	11.900	0.449
15-6-2018 10:10:30	208.473	1319.100	11.887	0.448
15-6-2018 10:10:40	208.472	1319.100	11.877	0.448
15-6-2018 10:10:50	208.647	1319.275	11.863	0.448
15-6-2018 10:11:00	208.587	1319.217	11.853	0.449
15-6-2018 10:11:10	208.587	1319.217	11.843	0.449
15-6-2018 10:11:20	208.586	1319.217	11.833	0.448
15-6-2018 10:11:30	208.585	1319.217	11.823	0.448
15-6-2018 10:11:40	208.468	1319.100	11.810	0.448
15-6-2018 10:11:50	208.467	1319.100	11.800	0.449
15-6-2018 10:12:00	208.467	1319.100	11.790	0.449
15-6-2018 10:12:10	208.466	1319.100	11.783	0.449
15-6-2018 10:12:20	208.465	1319.100	11.773	0.448
15-6-2018 10:12:30	208.465	1319.100	11.763	0.448
15-6-2018 10:12:40	208.464	1319.100	11.757	0.448
15-6-2018 10:12:50	208.638	1319.275	11.750	0.449
15-6-2018 10:13:00	208.638	1319.275	11.740	0.449
15-6-2018 10:13:10	208.695	1319.333	11.733	0.449

Pumping tests were conducted on-site before and after the injection. Two types of test were used: pumping water to the well and pumping water out of the well. The choice of the test type was decided according to the location of the well. Only in the well situated all the way down the dike (A9, B9 and C9), the pump was powerful enough to keep a steady pumping rate. When water was pumped to the well, a hose was immersed to the water reservoir to obtain the water needed for the test.

An ideal pumping rate was calculated before the pumping tests. On site the pumps were set to approximately that calculated rate. However, due to the lack of accuracy of the pumps, the flow rate was verified by measurement. It was defined as the time needed to pump or infiltrate 5 L of water. The measured flow rate was used for the analysis. The pumping rate should be set as high as possible still maintaining it steady. When water was pumped out of the well, a too high pumping rate could not be maintained since the water could not drain quickly enough. When infiltrating water to the well, a too high rate lead to overflow.

The data contains also the electrical conductivity (EC) measured from the monitoring wells. After the reaction between aluminum and organic matter ions were released to the groundwater: chloride-ions from aluminum chloride and potassium-ions from organic matter. Chloride does not react with the environment and can be considered as conservative tracer. Potassium-ion is a single valent ion with a high tendency of ion exchange. The amount of Cl^--ion is also three times higher than the amount of K^+-ions due to the chemical composition of aluminum chloride and organic matter. Due to the conservativity and higher amount of chloride ions, the increased electrical conductivity is mainly caused by chloride-ions. Observing the EC-values of the monitoring wells can give indication of the groundwater movements.

5.1.2 Test zone and wells

The preliminary analysis was done for all the zones. For the analysis, a well that had a pumping test done both before the injection and after the injection was chosen. To have representative results, the pumping test conducted in the well had to be successful with no overflow. Also, wells that were clogged were avoided. For zone A, the chosen test well was A3, for zone B, B10, and for zone C, C2 (figure 5.1). The natural gradient of the water flow is from the top of the dike towards the injection line. The test well of zone B is below the injection line to estimate the effect of the natural gradient of the water flow. The observation well for drawdown measurements was chosen so that it was situated at the opposite side of the injection line from the test well (figure 5.1). This was done to give an insight into the effects of the injection.

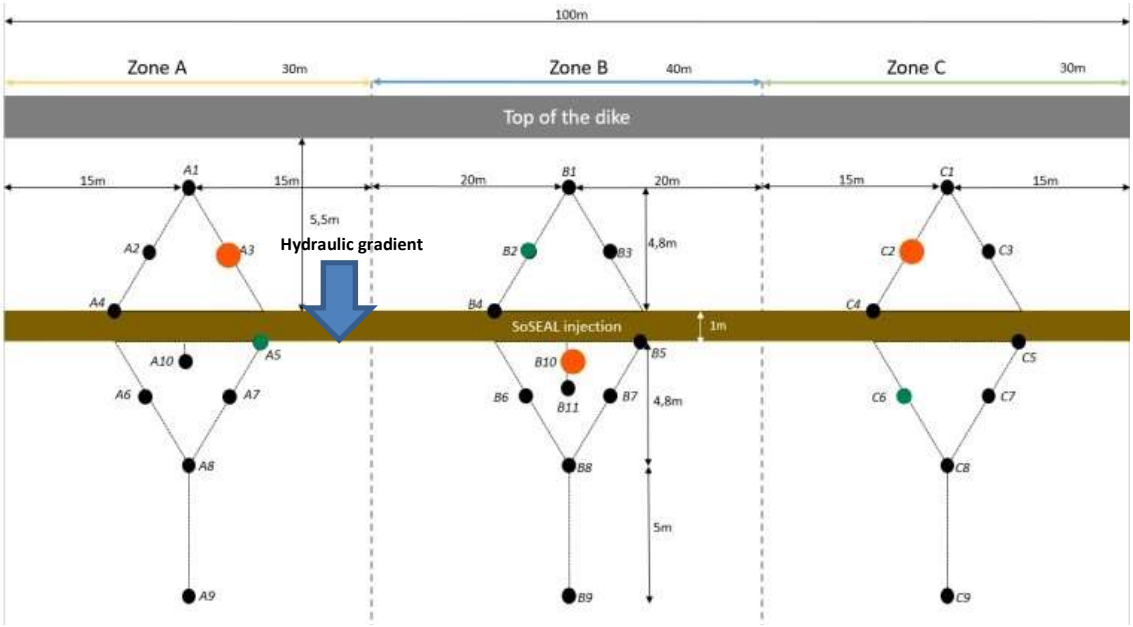

Figure 5.1. The wells chosen for analysis are marked with orange spots and the observation wells are marked with green spots.

To have a better estimation of the reliability of the calculated transmissivity values, the calculations in zone A were repeated but in the other direction so from the well A5 to well A3. Theoretically, the results should be the same than the ones obtained from pumping tests from the A3 to A5 since the distance and the soil in between are the same. The test dates and flow rates are presented in table 5.2.

Table 5.2. The tests used in the analysis.

date	starting time	test well	Flow rate (m3/d)
16.5.	12:40	A3	21.63
19.7.	8:40	A3	28.35
15.5.	13:46	B10	20.85
20.7.	8:45	B10	25.88
4.5.	10:55	C2	25.79
27.7.	9:31	C2	23.57
1.10.	14:20	C9	27

5.2 The shape of the reduced permeability barrier

After observing the change occurring in the soil, the next step was to try to explain the reactions happening in the dike. Different scenarios were created to better understand and visualize the alternatives. The different scenarios are gathered in table 5.3 and some causes for the scenario are suggested. The injected barrier can also be not covered by the different scenarios below or it can be a combination of several scenarios.

Table 5.3. Different scenarios for the shape of the injected reduced permeability barrier.

Scenario	possible causes	Scenario	possible causes
Scenario 1: There is a uniform 1 m thick and 7 m deep barrier at the whole injection length. 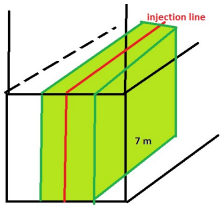	Everything works as expected	**Scenario 2:** There is a uniform thinner than 1 m and 7 m deep barrier at the whole injection length 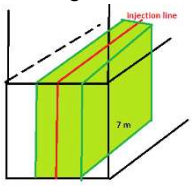	The mixture is not as mobile as expected. The mixture does not flocculate The mixture flows away from the barrier
Scenario 3: There is a uniform thicker than 1 m and 7 m deep barrier at the whole injection length 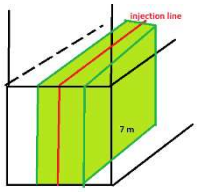	The mixture is more mobile than expected	**Scenario 4:** The barrier contains small holes 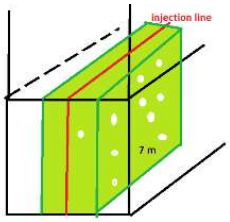	The mixture floccuates unevenly Heterogenuities of the soil affect the floccuation
Scenario 5: The barrier contains large holes 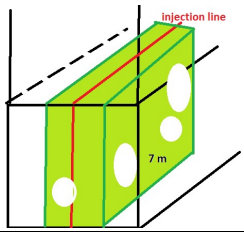	There are high K areas that transport the mixture away The hose of the injection machine is blocked	**Scenario 6:** The barrier depth is less than 7 m 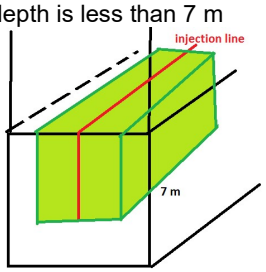	Higher K layer at the top or bottom Upward flow The properties of the soil in the lower level are different. No barrier formation
Scenario 7: The barrier depth is more than 7 m 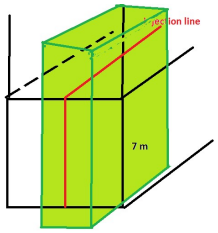	Downward/upward flow Soil layer below the different from expected	**Scenario 8:** The barrier is not on the injection line 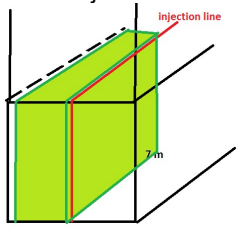	A strong horizontal flow that transports the mixture away before flocculation Delayed flocculation
Scenario 9: The barrier is not of uniform thickness. It is larger from the toe. 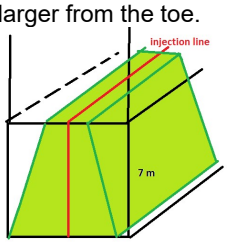	The mixture flows to the injection hole when hose lifted upwards Downward flow Mixture heavier than water	**Scenario 10**: The barrier is not of uniform thickness. It is larger from the top 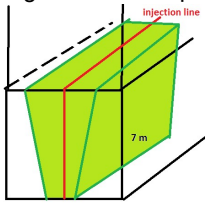	Upward flow Higher K in the upper layers

Scenario 11: The barrier is not uniform. It is thicker from the middle 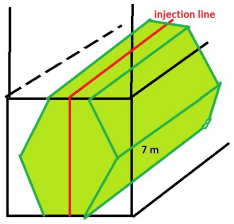	A high K in the middle Flow out in the top and bottom. Dispersion	**Scenario 12:** The barrier is horizontal 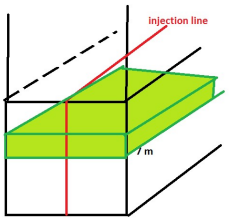	Significantly higher K at some depth Delayed flocculation
Scenario 13: There is no barrier 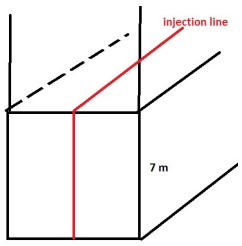	No flocculation Total advection of the mixture		

The electrical conductivity was controlled by the movement of the chloride in the aquifer. With the EC values, the movement of the groundwater could be estimated. When the aluminum and the organic matter flocculated, the chloride stayed inactive and functioned as a tracer. The objective was that the flocs stay immobile and only the chloride is moving. With the variation of the EC in the monitoring wells, information about the groundwater movements in the aquifer was obtained. It can give indications on the possible movements of the flocs and help defining the shape of the reduced permeability barrier. The results of the EC analysis is presented in the section 6.4.

5.3 Choosing suitable analysis methods

5.3.1 Methods for qualitative analysis

With the qualitative analysis, the goal is to see how the injections affect the hydraulic gradient of the dike and the drawdowns at different sides of the injection line. Several types of plots were tested to best illustrate the change between the situation before the SoSEAL injection and the situation after. The hydraulic gradient before and after the injection was plotted as a function of distance. The behavior of the drawdowns was also compared before and after the injection. The analysis methods are discussed in detail in section 5.4 and the results are analyzed in section 6.1.

5.3.2 Different methods and tools for a quantitative analysis

For the quantitative analysis, two different test set ups were presented: the pumping test and the slug test. When it comes to the use of slug test or a pumping test the consensus is that pumping tests give a more reliable result. A study done by Butler et al. (1998) showed that the slug test underestimates the K values. If the slug test values are used, 30 % should be added to de obtained K values. Due to the uncertainty of interpreting the injection as a slug

test and the less accurate results obtained from slug tests, the further studies are conducted only with pumping test analysis methods.

The transmissivity T and the storativity S are the parameters that indicate the change in soil permeability. Parameters needed for the pumping test analysis are the flow rate, the distance between the monitoring well and the test well, the drawdown and the time.

Fitting of the data to the type curves can be done with different techniques: log-log curve matching, semilog drawdown vs. time and pseudo-steady drawdown vs. time. According to Fitts (2013), the log-log curve fitting gives the most accurate results when u >0.01 (Eq 20 and 21). u depends on the transmissivity, storativity, distance from the test well and time. u was calculated for few wells at the end of the pumping test and it was always bigger than 0.01. The logarithmic curve-fitting was selected as the fitting technique.

The fitting can be done by either drawing the measurement points to a log-log graph paper and match it with the type curves or the drawing can be done with the help of computer tools. The first tool presented is a Excel sheets for curve-fitting and the second one is a MATLAB toolbox called Hytool that also aims for the best possible graphical match between the measured data and the type curves.

The Groundwater science book by Fitts (2013) provides an Excel sheet to calculate the transmissivity and storativity from the time and drawdown data. Time and drawdown are plotted in logarithmic scale The T and S are defined by matching the formed curve with a theoretical curve by adjusting the T and S values until the measured values and the theoretical curves match as well as possible (figure 5.3). (Fitts, 2013).

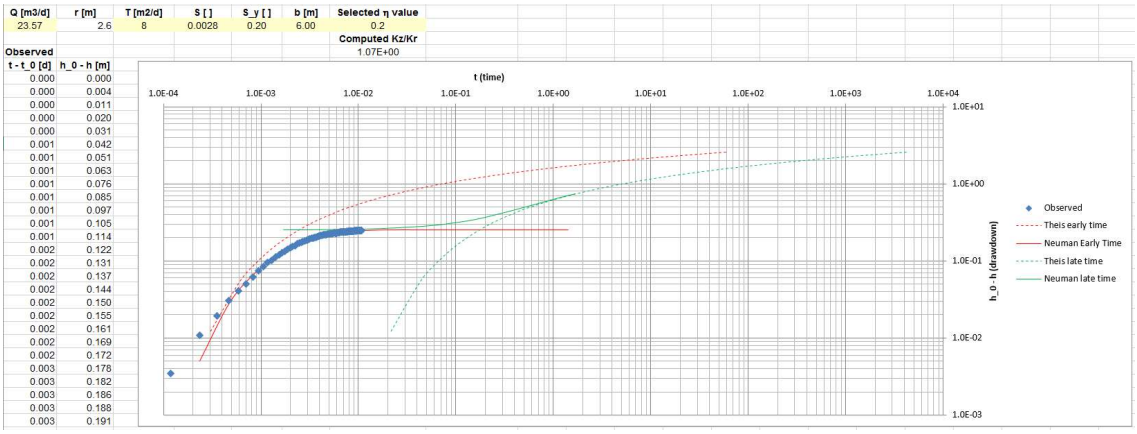

Figure 5.3. The Excel-sheet by Fitts for pumping test analysis is based on curve-fitting. In this example, the observed time is in days and the drawdown is in meters.

A similar spreadsheet is provided by Molano (2011) (figure 5.4). Instead of changing the T and S values, in this spreadsheet, the data is shifted so that it would match one of the type curves. With the shifted values and the choice of type curve, the transmissivity and storativity are calculated.

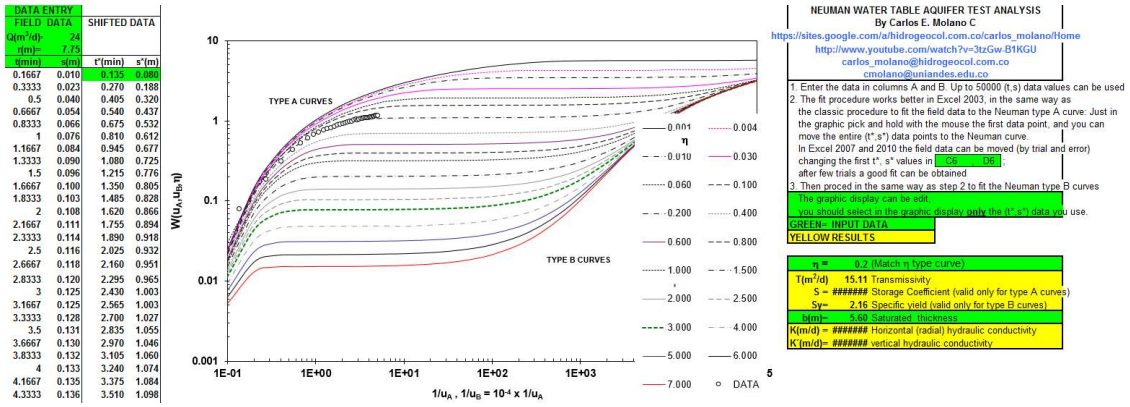

Figure 5.4. The curve fitting method by Molano.

The MATLAB toolbox Hytool contains classical analytical solutions for pumping test and slug test interpretation. Hytool has analytical solutions for confined, unconfined and leaky aquifers. The solutions are often in Laplace-domain and the parameters are obtained by the least-square procedure. (Renard, 2017).

For pumping test, the analytical solutions chosen for further study were the Theis (1935), the Theis (1941) and the Distance-drawdown method (figure 5.5). Theis developed two methods, one in 1935 which is a residual-drawdown solution and then in 1941 he did a new model that assumes a constant head boundary. (Schwartz et al., 2003). The Distance-drawdown method is based on the Papadopulos-Cooper method. Hytool contains two different Distance-drawdown analyses; with one and with two storativity values. The one storativity analysis gave more reasonable wellbore storage values.

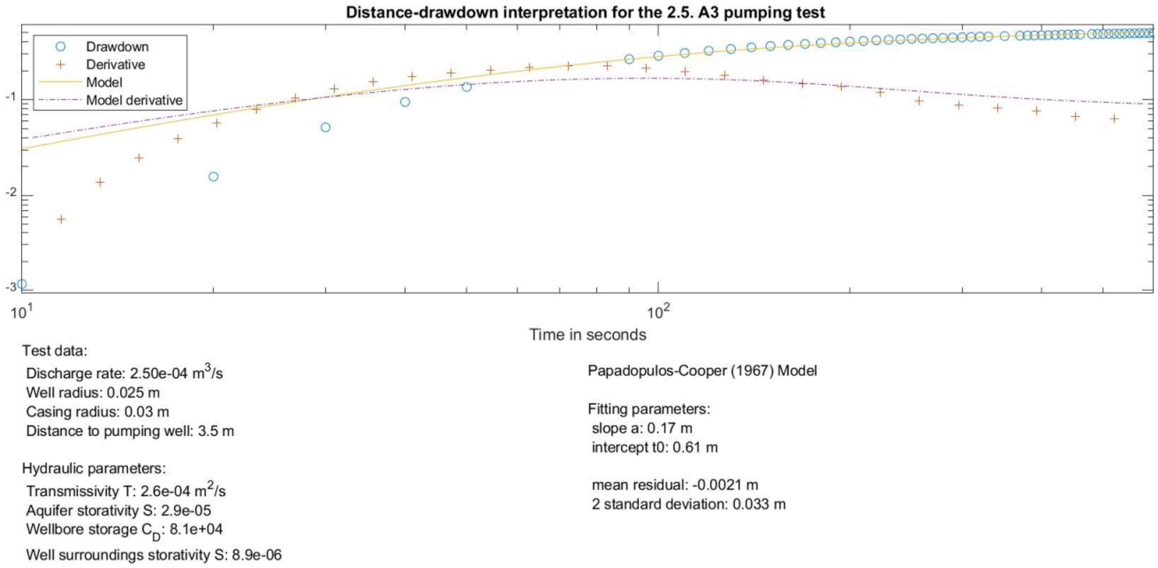

Figure 5.5. A graph obtained from Hytool with distance drawdown method.

The results from the Excel sheet, where the adjustment was done manually, differed from the results obtained from MATLAB. In MATLAB the curve is fitted with a code based on the least square methods. The Theis (1935) method was used both in the Excel sheet and in MATLAB. For zone A before injection, the transmissivities from the Excel were around 9 m^2/d whereas the results from MATLAB were most of the time over 15 m^2/d sometimes up

to 22 m^2/d. The storativity values were smaller from the MATLAB toolbox. The comparison of results obtained with different methods in zone A is presented in table 5.4. The pumping test conducted before July represents baseline measurements. The baseline measurement values from A3 to A5 should be equal to the values from A5 to A3. The results of zones B and C are presented in table 5.5. and the slug test analysis from zone A in table 5.6.

Table 5.4 The transmissivity and storativity values in zone A obtained with different pumping test analysis methods and tools.

		Zone A					
		Before injections				after injections	
		2.5. A5->A3		16.5. A3->A5		19.7. A3->A5	
		T(m2/d)	S	T(m2/d)	S	T(m2/d)	S
Pumping tests	Theis (excel)	9.0	5.0E-04	5.0	6.0E-04	7.0	4.0E-04
	Neuman (Excel)	4.0	3.5E-04	3.8	3.8E-04	3.0	3.0E-04
	Theis (1935) Hytool	16.4	1.8E-04	16.4	1.8E-04	21.9	2.4E-04
	Theis (1941) Hytool	16.4	1.8E-04	12.1	4.0E-04	17.3	9.0E-05
	Papadopulos-Cooper Hytool	19.9	9.2E-05	13.8	2.5E-04	19.9	4.4E-05

Table 5.5 The transmissivity and storativity values in zone B and C obtained with different pumping test analysis methods and tools.

		Zone B				Zone C			
		Before injections		after injections		Before injections		after injections	
		15.5. B10->B2		20.7. B10->B2		4.5. C2->C6		27.7. C2->C6	
		T(m2/d)	S	T(m2/d)	S	T(m2/d)	S	T(m2/d)	S
Pumping tests	Theis (excel)	17.0	3.2E-04	16.0	3.2E-04	15.0	4.5E-04	19.0	4.5E-04
	Neuman (Excel)	9.0	2.2E-04	9.0	2.8E-04	10.0	4.2E-04	9.0	1.0E-03
	Theis (1935) (Hytool)	15.9	6.0E-05	19.9	7.0E-05	37.1	3.4E-04	26.6	1.0E-03
	Theis (1941) (Hytool)	39.7	1.1E-04	40.6	1.3E-04	37.2	3.7E-04	26.8	1.2E-03
	Papadopulos-Cooper (Hytool)	43.2	7.4E-05	44.1	1.0E-04	39.7	2.7E-04	27.6	1.0E-03

Table 5.6 The transmissivity and storativity values in zone A obtained with different slug test analysis methods and tools.

	ZONE A A3->A5	Before (22.6)		After (27.6.)	
		T(m2/d)	S	T(m2/d)	S
Slug tests	Cooper-Bredefort (Hytool)	0.04		0.14	
	Cooper(excel)			0.24	5.0E-05
	Hvorslev (Hand calculation)	0.5		0.13	

Due to the big variance between methods and tools, an average value from all the method cannot be used. The big variation in values also shows the uncertainty of the analysis. To avoid additional uncertainty, the method having generally the best fit and being the most

suitable one when assumption and theory were considered was chosen. The quantitative values are used to estimate the magnitude of the change instead of trying to estimate the absolute value of the aquifer transmissivity.

The Theis (1935,1941) methods are classical methods used in pumping test analysis. The other methods chosen for further analysis, the Neuman (1975) method and the Papadopulos-Cooper, are based on Theis (1935,1941) methods. Theoretically, the early time response should fit the Theis curve well (Schwartz et al., 2003). However, the curve-fitting of the MATLAB code matched the measured curve with the later part of the type curve which leads to bigger transmissivities than expected. When the Theis method was used with the manual fit, the results were different since the start could be weighted more. If the later time was given more weight, the result corresponded to the values obtained from MATLAB. The bad fit with the first measurement points is presented in the figure 5.6. Due to the wrong kind of weighting of the MATLAB code, the hand fitting with the Excel sheet was chosen as the analysis tool.

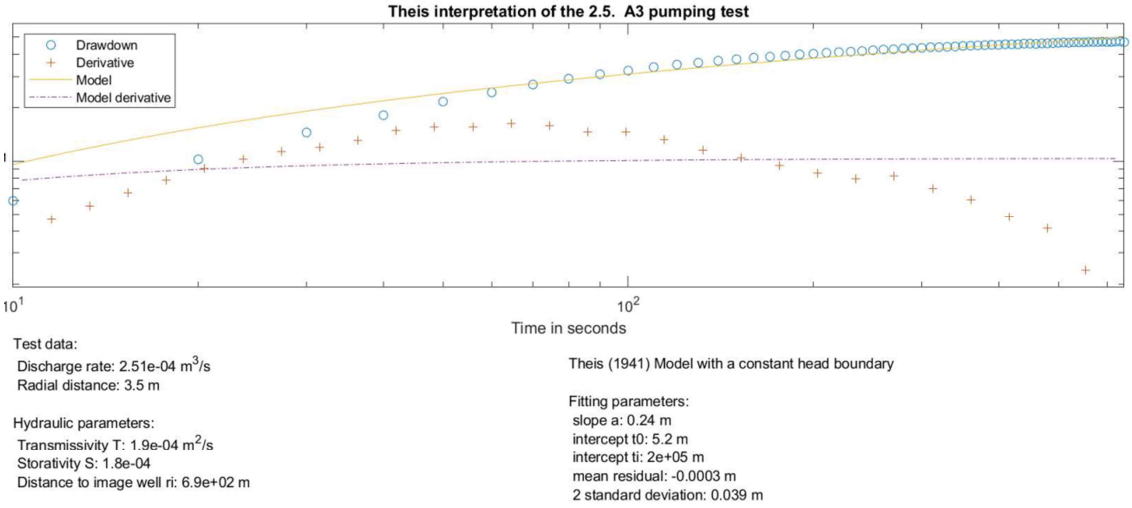

Figure 5.6. A graph obtained from Hytool with Theis (1941) method.

The Theis method was developed to analyze pumping test results of confined aquifers. Even though there is a formula (eq. 15) to match the drawdown of an unconfined aquifer to the drawdown of a confined aquifer, the measurement points started to separate from the theoretical curve after the drawdown started to reach a steadier state (figure 5.7).

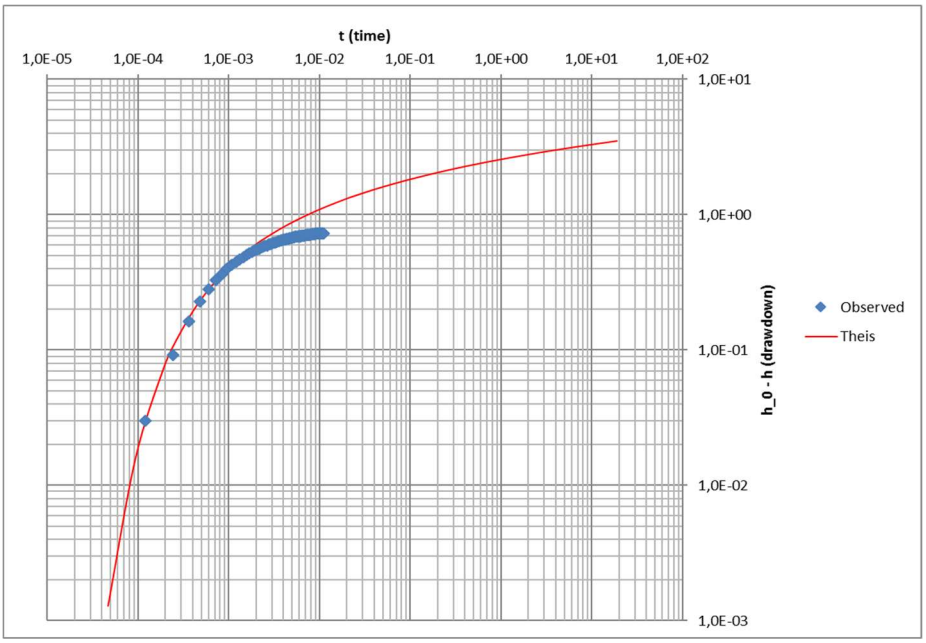

Figure 5.7. The drawdown of the well A5 when a pumping test was conducted in A3 fitted with Theis method. Time in days and drawdown in meters. With this fitting T= 6 m^2/d and S=3.2· 10^{-4}.

The Cooper-Jacob method considers the wellbore storage, which would be advantageous. However, for the Cooper-Jacob method, there is no Excel tool and the curve-fitting of Hytool gave too high values due to the weighting of the later data points.

The Neuman (1975) method was chosen, since the preliminary calculations of the K and S values seemed reasonable (Table 5.4 and 5.5) and the fit of the measurement points to the type curves was good for most wells. In addition to calculating the K- and S-values for different wells, the hydraulic conductivity and storativity before and after the injection were compared. The direction of the change was illustrated with colors and connected to the location of the well. The goal was to see whether a pattern occurred between the change in K and S and the location of different wells (figure 6.7 and 6.8)

Before the slug test was disregarded as analysis method, an analysis was done by using the Hvorslev method and the Cooper-Bredehoeft-Papadopulos method. The hydraulic conductivity was estimated with hand calculations. The variation of the water level was plotted as a function of time to estimate the H_1, H_2, t_1 and t_2. The Cooper-Bredehoeft-Papadopulos method was included in the Hytool-toolbox so analysis could be done with giving the water level variation and time as inputs to the program.

5.3.3 Applying the Neuman Method

The needed steps to conduct an analysis with the Neuman method with hand-fitting are described below. For these analyses, the length was given in meters and the time in days.

1. Insert the flow rate, the radius between the observation well and the test well, and the aquifer thickness to the sheet provided by Fitts (2013).
2. Insert the drawdown and the time to the data columns. The observation points are plotted in logarithmic scale.

3. Adjust the shape of the background curve by changing the η-value.
4. First, the late time curve fitting is done. Change the S_{y}- and T-values to make the curves match the data points. The specific yield value affects the horizontal position of the curve whereas the transmissivity affects the vertical position.
5. Note down the T- and S_{y}- values when the match between the Neuman curve and early time curve is the best possible.
6. For the early time curve matching, change the S-value until the observed values after the steady state match to early time Neuman curve. The T-value from the late time should be suitable also for the early time curve. However, if needed, adjust the T-value.

In figure 5.8. the values inserted in the first two steps are in green. They should not be changed when fitting. The yellow boxes are parameters that can be changed to make a better fit.

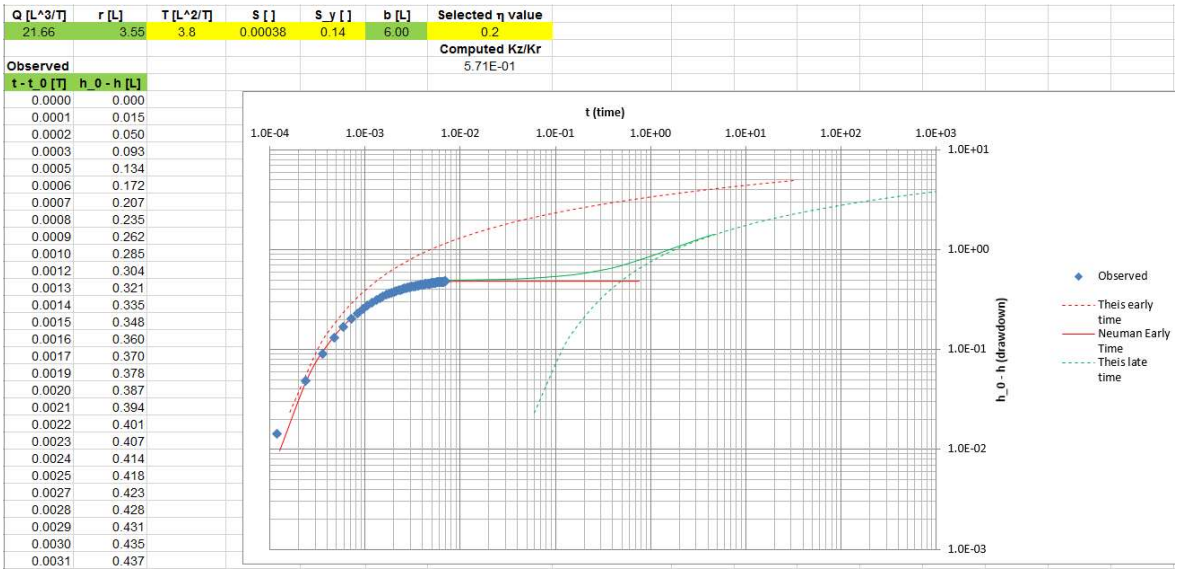

Figure 5.8. The Excel sheet by Fitts (2013) to fit observed data to Neuman (1975) method.

Most of the pumping tests were carried out only relatively short times, from 10 minutes to 1 hour. The measurements are assumed to correspond to the early time response and never reach the late time. In some tests, the flow rate was increased after 10 minutes of testing. The measurements taken after an increase of Q were ignored since the method used allows only one flow rate. Since all the other pumping test, expect the one conducted in October, were only short pumping tests, only the early time curve was fitted.
To have a better picture of the change in permeability, the transmissivity values are transformed to hydraulic conductivities by multiplying the T-value with aquifer thickness. We assume that the bottom of the aquifer is situated at -3.5 m (N.A.P.). The groundwater table varies according to the location of the well. The aquifer thickness was calculated with the water level present the moment the pumping test started. The aquifer thickness varied between 5 and 5.80 m.

Due to the problems with overflowing in zones A and B, the data of zone C was chosen to further analysis and K- and S- values were estimated for each monitoring well with several pumping tests. Test analyzed were selected both from the upper part and the lower part of

the dike so that the natural hydraulic gradient would not affect the results. The pumping test used for the Neuman method analysis and the well distances are presented in Appendix 4.

5.4 Comparison of data before and after the implementation

Before starting the injection in De Gijster, the effect of the SoSEAL barrier was estimated with a COMSOL model. The simulation run by Zhou (2017) lead to results presented in figure 5.9. The model predicted that the low permeability barrier increased the water table on the top part of the dike and lower it at the toe. The head difference created by the barrier was more than 1 m.

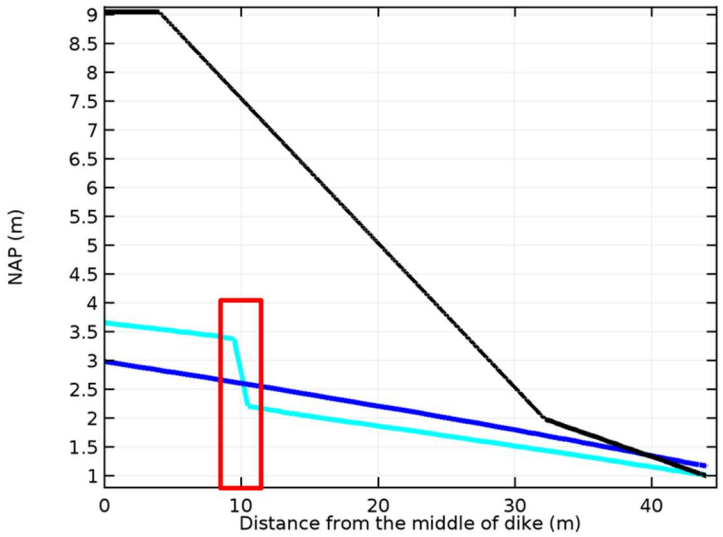

Figure 5.9. Model simulation of the water table in the dike body before (dark blue) and after (light blue) implementation of the flow barrier (red) (Zhou, 2017).

Some comparisons were done with the drawdown data during the pumping tests. The same test wells were used throughout the analysis: A3, B10 and C2. The tests dates and flow rates are presented in table 5.2 of section 5.1.2. The drawdowns of all the wells were plotted as a function of time for all the wells. To make the results more comparable, the drawdowns were normalized by dividing with the flow rate. The pattern of the drawdowns of different wells had changed after the injection. To better visualize the change a new plot was created. The normalized drawdown after the injection (s_{after}/Q_{after}) was subtracted from the normalized drawdown before the injection (s_{before}/Q_{before}) that occurred at the same moment after the start of the test. The remainder (R) was plotted as a function of time. If the R was positive, the drawdown has decreased and if it was negative, the drawdown has increased. The figures are presented in section 6.

The mixture was injected into the soil in liquid state. The flocs were not assumed to be completely immobile since they could be moving around the injection line depending on the hydraulic conductivity and the hydraulic gradient of the aquifer. In an ideal case, the mixture spreads in a circular form with a 0,5 m radius and the injection line as the center line. To estimate the shape of the created barrier, the electrical conductivity of the monitoring well was studied. The chloride functions as a tracer and from the increase of the EC value can indicate a mobilization of the flocs. The results of the electrical conductivity analysis are presented in section 6.4.

6 Results and discussion

The results from the comparison of data are presented first. The changes visible in the qualitative analysis are then given values with the results obtained from the Neuman (1975) method pumping test analysis. The results are discussed together with the errors present. The treatment of the error sources will be started from the beginning of the process, passing through the pumping test and ending up in the analysis. Finally, the reliability of the results is estimated, and the results are compared to literature values.

6.1 Preliminary results

The first plots revealed that there had been a change in the behavior of the drawdowns in the monitoring wells during pumping. The drawdown was plotted as a function of distance from the test well A3 (figure 6.1). The drawdown values were measured 5 minutes after the start of pumping and 5 minutes after pumping had stopped to observe the recovery. When the pumping test drawdowns were plotted as a function of distance, a cone of depression was expected. The overall impression was that there had not been a reduction in drawdown at every monitoring well, instead some monitoring wells were showing a slower recovery after the injection. The flow path appeared to have changed.

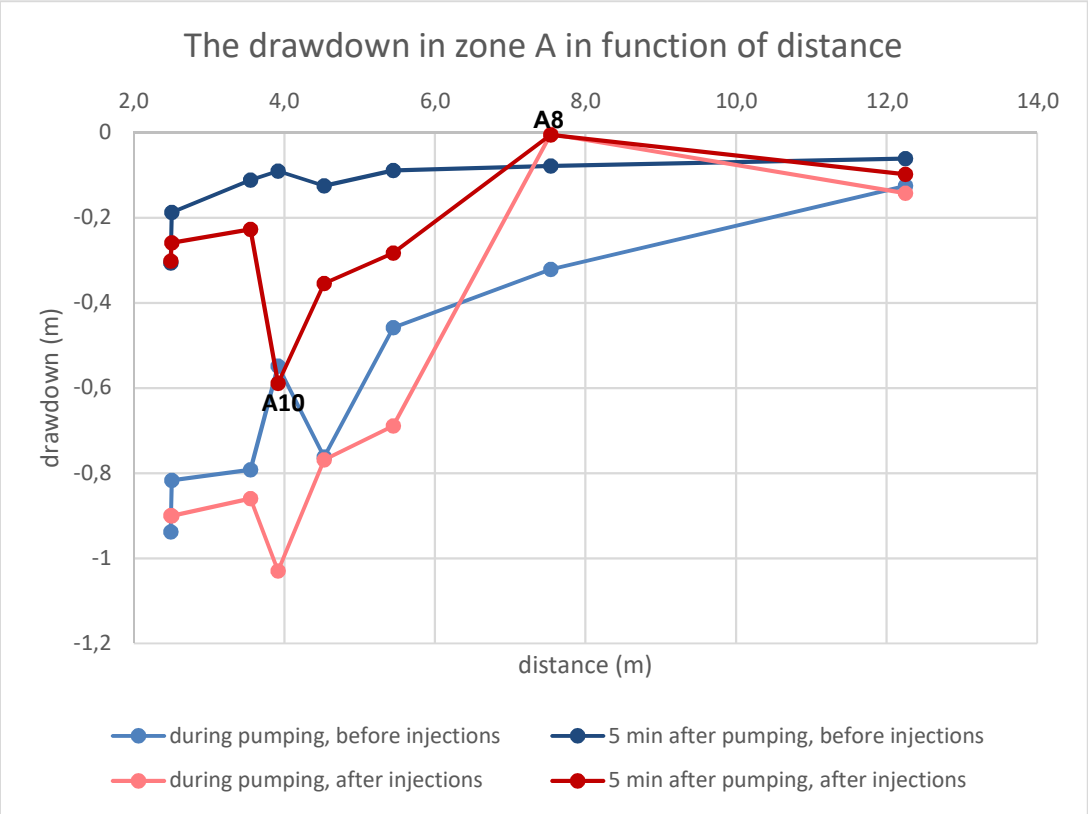

Figure 6.1. The drawdown as a function of distance before and after the injection from well A3 in zone A.

From the figure 6.1, it can be observed that the drawdown was greater near the pumping well and the effect was reduced when the distance increased. The results from the test well A10 (at the distance of 4 m) were not in line with rest of results and they did not follow the form

of a cone of depression. Since the abnormalities were present both before and after injection the data from the well A10 should be neglected. The well A8 (at the distance of 7.5 m) was clogged due to injection which could explain the lack of drawdown after the injection. The numerical values of drawdowns and the abnormalities are presented in table 6.1. In general, figure 6.1 shows that during the pumping the drawdowns were a bit bigger and after the pumping was stopped, the speed of recovery was slower. The difference in drawdowns was biggest in the area situated 4 to 6 m from the test well. The before and after SoSEAL injection results differed but the effect of the zone of reduced permeability could not yet be shown.

Table 6.1. The drawdown values from the pumping tests in A3. The highlighted values are abnormalities.

		during pumping		5 min after pumping	
	Distance from the test well (m)	before injection (cm)	after injection (cm)	before injection (cm)	after injection (cm)
A1	2.5	-93.8	-90.0	-30.6	-30.2
A2	2.5	-81.7	-90.0	-18.7	-25.9
A5	3.6	-79.2	-86.0	-11.1	-22.7
A10	3.9	-54.8	-103.0	-9.0	-58.9
A4	4.5	-76.2	-76.8	-12.5	-35.4
A7	5.5	-45.8	-68.9	-8.9	-28.3
A8	7.5	-32.1	-0.5	-7.8	-0.4
A9	12.3	-12.5	-9.8	-6.0	-14.2

6.2 Comparison of data

The natural hydraulic gradient was plotted to estimate the effect of the injection to the water level of the dike (figure 6.2 and 6.3). Before the injection, the measured data decreased linearly in zone A but the decrease in zone C was less linear. The pre-injection measurements showed a decrease in water level between the wells C4 and C5 situated next to the injection line. The last day of injection was the 14th of July so the data from the 21st July was a week from that. The water level in zone A on the 19th July was similar to the water levels observed before the injection. The data from August and October showed that there was a steeper decrease on the water table 12 m from the top of the dike so between wells A7 and A8.

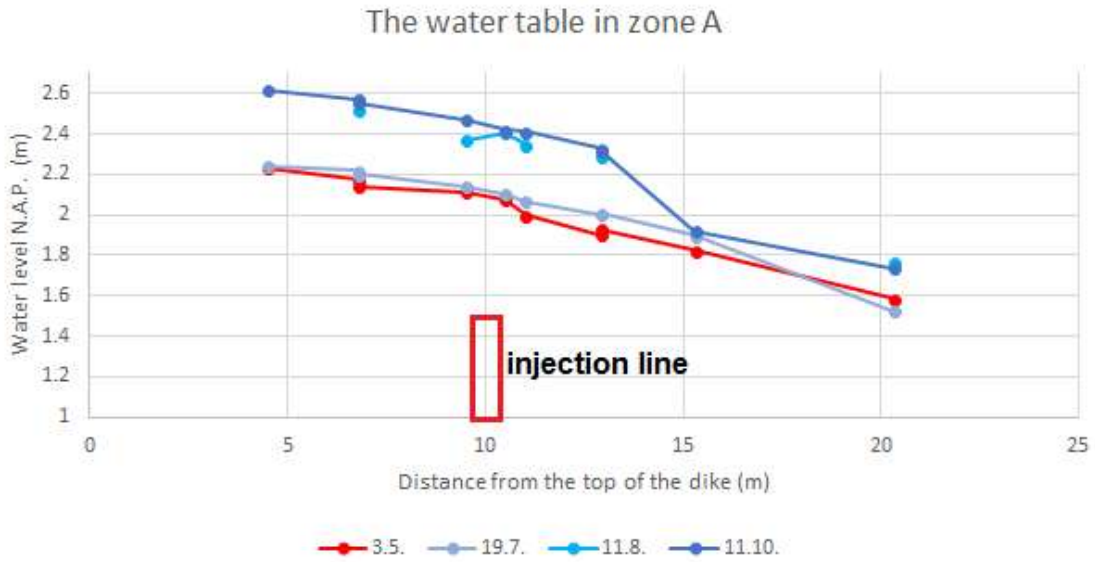

Figure 6.2. The water level in zone A as a function of distance from the top of the dike before (red) and after (blue) the injection.

In zone C, the water levels a week after the injection in the wells C4 and C5 were over 0.1 m higher than in the wells C1, C2 and C3. At the other side of the injection line in C6 and C7 the water level was 0.3 m lower. This can indicate that the water flow through the injection line was decreased. The water followed the path of the least resistance. Since the injection line added flow resistance, the water started to flow around it. The rerouting took time so one week after the injection the water level at in well C4 and C5 were still high. In October the water had already found its preferential flow path and the water level at well C4 and C5 had decreased. In October, the biggest decrease was between the wells C8 and C9, where the water level dropped 0.4 m in 5 m.

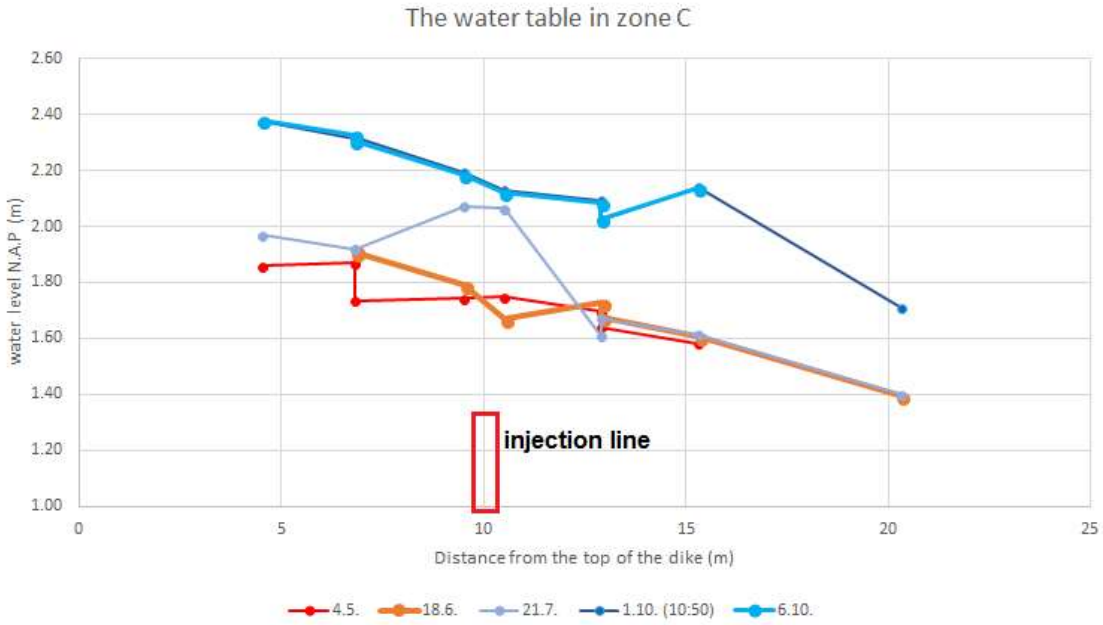

Figure 6.3. The water level in zone C as a function of distance from the top of the dike before (red) and after (blue) the injection.

Before the injection, the Zhou's model (figure 5.9) predicted a natural hydraulic gradient of 0.5 m between the top monitoring well situated 5 m from the top and the lowest monitoring well situated 20 m from the top of the dike. The measurements gave the same magnitude of decrease. After the injection, the model predicted a drop in the water level at the injection line (figure 5.9). The measured data did not show a significant drop at the injection line (fig 6.2 and 6.3). There was a water table level drop in both zones, but 3 to 5 m away from the injection line. After the injection, the model predicted a water table difference of 1.5 m between 5 m and 20 m from the top of the dike. The measured difference was 0.8 m in both zones. In the model, the water table decreased faster after the injection line. If the model (figure 5.9) is accurate, the dislocation of the barrier could explain the smaller change in water table since the decrease of the water table starts later. The water table at the top of dike was 0.4 m higher in August and October. This might have been due to the dredging work done in De Gijster. In the dredging a low permeability sludge layer was removed which is most likely the cause for the increased water table in the dike.

The change in hydraulic gradient is bigger and the water level drop after the injection line is more pronounced in zone A than in zone C. Few weeks after the injection the difference between the zones is small but with time the difference grows. The results from the zone A indicates that the zone of reduced permeability is more efficient in zone A than in the zone C.

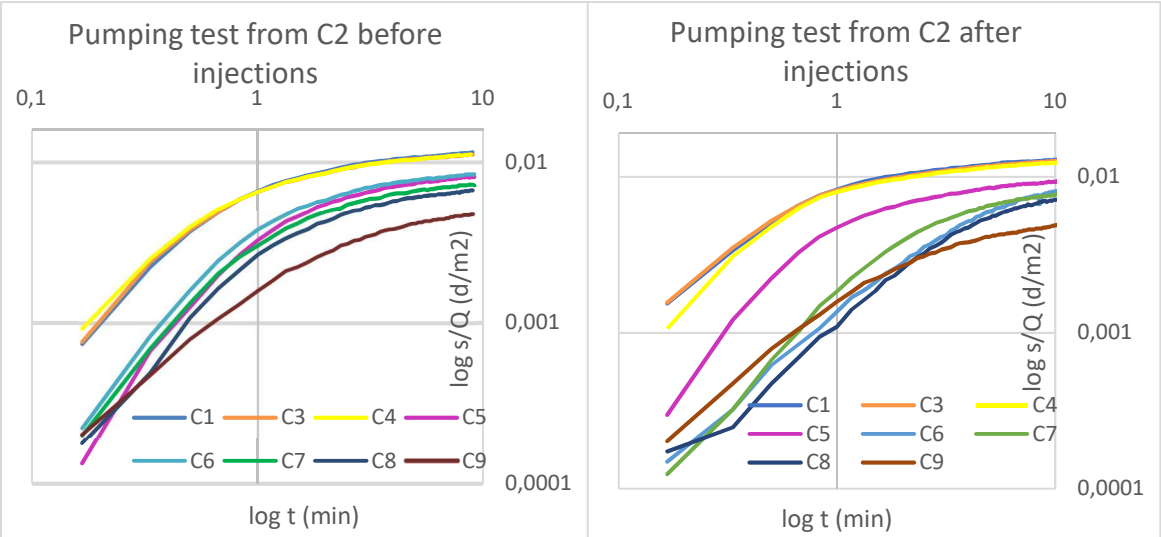

Figure 6.4. The comparison of drawdowns in zone C before and after the injection.

The drawdowns during pumping tests were also compared. When normalized drawdowns were plotted as a function of time, it can be observed that the injection has changed the drawdown (figure 6.4). Before the injection, the wells situated near the test wells had a bigger drawdown and it occurred sooner than in the monitoring wells situated further from the test well. After the injection, the drawdowns of the wells C1, C3 and C4 situated at the same side of the injection line as the test well showed very similar results. However, the wells situated on the other side of the injection line C6, C7 and C8 showed a slower response to pumping. The well C5 was situated close to the injection line which might affect the drawdown and C9 was so far away from the test well that the effect of the pumping test to the drawdown was small. To better visualize the effect of the wall, the difference of normalized drawdowns

was plotted as a function of time (figure 6.5). In the figure a new parameter for the difference of normalized drawdown R is introduced and it is $\frac{s_{before}}{Q_{before}} - \frac{s_{after}}{Q_{after}}$.

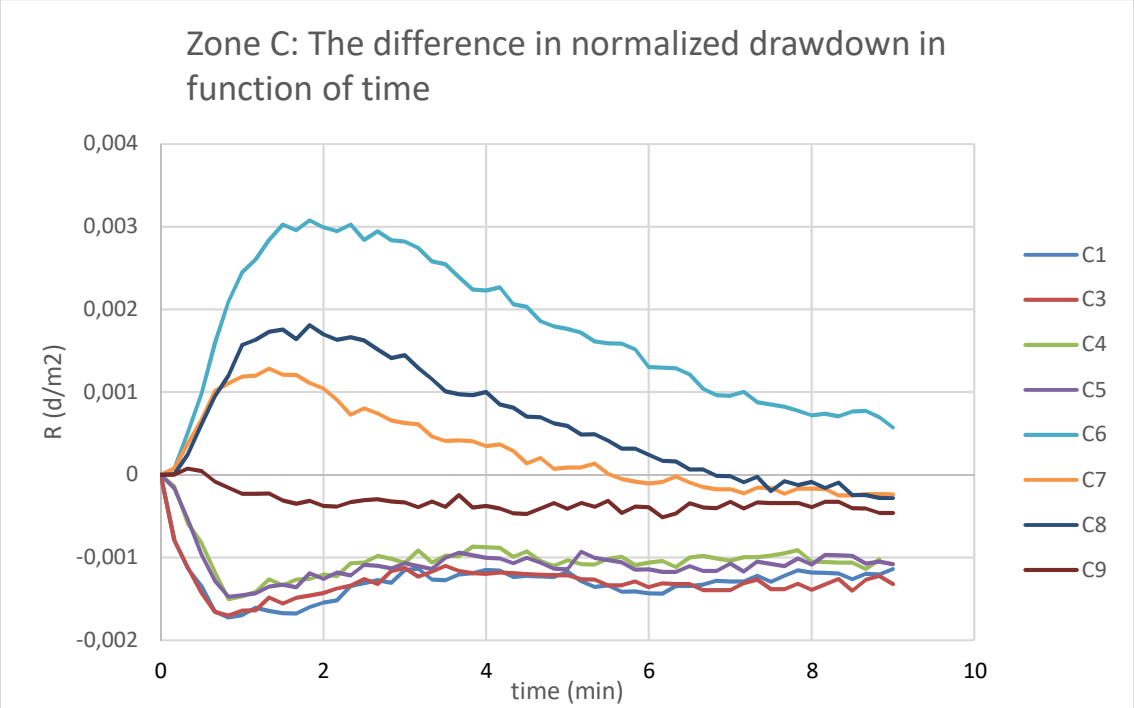

Figure 6.5. The difference in drawdown in zone C when C2 is pumped.

When the R value was positive the drawdown at that moment of pumping was bigger before the injection than after the injection. Wells C6, C7 and C8 had a longer reaction time after the injection which means that they experienced a delayed drawdown (figure 6.5). Wells C1, C3, C4 and C5 experience a faster drawdown after the injection. Also, the drawdown after 9 minutes, stayed a bit higher after the injection. To illustrate the magnitude of values represented by R, an example of the values is given. The difference in drawdowns in well C6 2 minutes after the start of pumping was 80 mm. In R-value, it corresponds to 0,003 d/m^2.

The slower drawdown at the beginning of the test for the wells situated on the other side of the injection line is interesting. What can be noticed is that the drawdown occurred faster than before the injection in the monitoring wells situated at the same side of the injection line. If the barrier had a reduced permeability, it did not allow the water to pass through as easily as earlier. When water was added to the test well, the surface of the water table started first to rise. When the test was continued, the water passed through the barrier and the drawdown was close to the drawdown that occurred before the injection. When water was pumped, the presence of the lower permeability zone partly prevented the flow of water from the other side of the injection line to the test well. After few minutes of pumping, the water flowed also from an extended area from the surroundings and drawdown values were quite close to the values occurring before the injection. If the barrier would be impermeable, no water would flow through. In conclusion, the results indicated that the barrier let some flow through, but it slowed down the water flow and rerouting took time.

The hypothesis of accelerated drawdowns on the same side of the injection line and delayed drawdowns at the opposite side of the barrier would apply for the drawdown of most of the wells in zone C. When water was pumped to well C2, the only wells that were not following

the expected pattern were the wells C5 and C9. The well C9 was situated far away from the test well and after the injection, the drawdown occurring in the well was smaller (0.13 m in C9, 0.21 m in C6 and 0.31 m in C3). With smaller drawdowns, the influence of tidal effect is stronger since proportionally the variations due to the tide are bigger. The well C5 was reacting the same manner than the wells situated at the other side of the injection line. This could indicate that the barrier was not formed under the injection line but lower down the dike (figure 6.6).

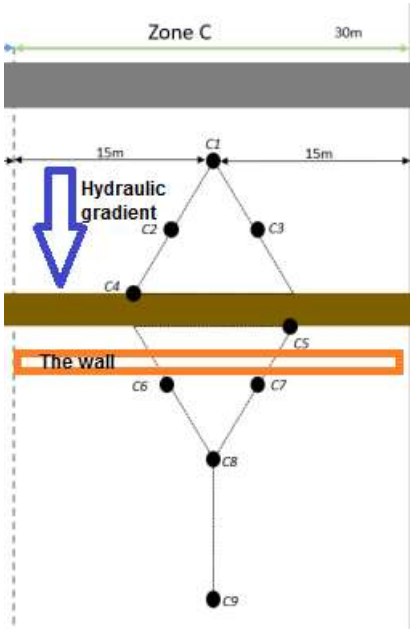

Figure 6.6. A scenario for the location of the barrier.

A possible reason for the scenario represented by the figure 6.6 is that the injection pressure pushed the flocs away from the injection line. The flocs seemed to have moved down the dike. There could have been a preferential flow path that affected the advection of the flocs. There was also a natural hydraulic gradient from the top of the dike towards the toe of the dike. Even though the effect of the natural hydraulic gradient is minor compared to the injection pressure, it could have been partly responsible for the dislocation of the flocs towards the toe of the dike. The well C5 can also be otherwise influenced by the mixture. It can be clogged or there can be a hole next to the observation well.

In zone A, the drawdown is delayed and decreased in wells A4 and A6. In all the other wells, the drawdown occurred sooner and is bigger. The drawdown of wells A7 and A10 was first delayed but after few minutes it increased. In zone B, the drawdowns after the injection was either same as before or smaller. The decrease of drawdown was significant in wells B5, B8 and B7. They are situated on the same side of the injection line as the test well. The graphs are presented in Appendix 5.

6.3 The Neuman method

To quantify the change, the K and S values of all the zones were gathered in Tables 6.2, 6.6 and 6.7. Most attention is paid to the zone C. The results of zone A and B are presented after the analysis of the zone C as a comparison.

Table 6.2. The change in hydraulic conductivity and storativity in zone C. Test well C2.

Well	K_{before} [m/d]	K_{after} [m/d]	K_{after}/K_{before}	S_{before}	S_{after}	S_{after}/S_{before}
C1	1.38	1.16	**0.84**	$7.0 \cdot 10^{-3}$	$1.1 \cdot 10^{-3}$	**0.16**
C3	1.51	2.13	**1.41**	$1.0 \cdot 10^{-3}$	$8.0 \cdot 10^{-4}$	**0.80**
C4	2.4	1.27	**0.53**	$8.9 \cdot 10^{-4}$	$6.0 \cdot 10^{-4}$	**0.67**
C5	1.97	1.68	**0.85**	$5.0 \cdot 10^{-4}$	$3.4 \cdot 10^{-4}$	**0.68**
C6	1.89	1.71	**0.90**	$4.2 \cdot 10^{-4}$	$1.0 \cdot 10^{-3}$	**2.83**
C7	2.27	1.99	**0.87**	$4.0 \cdot 10^{-4}$	$6.2 \cdot 10^{-4}$	**1.55**
C8	2.32	2.11	**0.91**	$3.0 \cdot 10^{-4}$	$5.7 \cdot 10^{-4}$	**1.90**
C9	5.27	3.21	**0.61**	$2.2 \cdot 10^{-4}$	$1.7 \cdot 10^{-4}$	**0.77**

The change in hydraulic conductivity analyzed with the Neuman method was not significant. In zone C, the well C3 had the biggest increase in hydraulic conductivity with an increase of less than 1 m/d. The biggest decrease of hydraulic conductivity was in C9 where the K dropped by 2 m/d from 5.3 m/d to 3.3 m/d. The wells having a substantial change in storativity were not the same ones that had a substantial change in hydraulic conductivity. The hydraulic conductivity and storativity values obtained with the Neuman (1975) method do not have a clear dependency. The storativity represents the drawdown of the first minutes and then it is the hydraulic conductivity that affects the magnitude of the drawdown.

Even before the injection, the K values seemed to increase when moving further away from the test well. The K values after injection followed this pattern but the increase was not as directly proportional to the distance. To study more the effect of the distance, a comparison of the aquifer parameters of zone C was done (table 6.3). The K values were compared from several different tests. Often the longer distance also indicated that the well was situated at the opposite side of the injection line from the test well. For the K values before the injection, the values should have been quite the same since there was no zone of reduced permeability yet.

Table 6.3. The effect of distance to the hydraulic conductivity [m/d] in zone C.

Effect of		Before the injection n=6 average	After the injection n=3 average
all the wells		3	2.6
injection line	wells on the same side of the injection line	2.4	2.2
	wells on the other side of the injection line	3.4	3
distance	Distance from the test well less than 6 m	2	1.7
	Distance from the test well more than 6 m	3.2	3.4

In the K values after the injection the increase of distance seemed to play a bigger role than just passing through the injected zone. To do a valid statistical analysis the number of samples was too low, and the standard variation was from 0.5 to 1.5 m/d. Based on these results, it is hard to demonstrate that the injection is reducing the permeability.

The changes in storativity were more remarkable than with the hydraulic conductivities. The storativity of the well C1 decreased with almost an order of magnitude whereas in the well C6 the storativity was almost 3-times higher (table 6.2).

Table 6.4. The effect of distance to the storativity in zone C.

Effect of		Before the injection n=6 average	After the injection n=3 average
	all the wells	$5.8 \cdot 10^{-4}$	$7.3 \cdot 10^{-4}$
injection line	wells on the same side of the injection line	$8.8 \cdot 10^{-4}$	$1.1 \cdot 10^{-3}$
	wells on the other side of the injection line	$3.4 \cdot 10^{-4}$	$4.0 \cdot 10^{-4}$
distance	Distance from the test well less than 6 m	$9.0 \cdot 10^{-4}$	$1.1 \cdot 10^{-3}$
	Distance from the test well more than 6 m	$6.8 \cdot 10^{-4}$	$4.2 \cdot 10^{-4}$

The increase of distance decreased the storativity value (table 6.4). Before the injection, the value of the wells on the other side of the injection line was bigger than the average of the wells situated at least 6 m from the test well. After the injection, the averages were the same. This signifies that the zone of reduced permeability had an equally big effect on the K-value as the distance. In average, the storativity of all the wells increased. The standard deviation of the storativity was from $1.4 \cdot 10^{-4}$ to $1.4 \cdot 10^{-3}$.

The distance was included in the calculations performed in the Neuman method. The hydraulic conductivities obtained from the curve fitting was normalized by dividing with the distance. Despite the normalization, the wells situated further away from the test well were subjected to a higher hydraulic conductivity even before the injection (table 6.5). The results were studied from the test wells C2 and C6 to observe the effect of the natural hydraulic gradient. The injection did not have significant effect on the difference of the normalized hydraulic conductivity values situated at different sides of the injection line.

Table 6.5. A comparison of the normalized hydraulic conductivities [1/d] and their location regarding the test well.

	Pumping to C2 before		Pumping to C2 after		Pumping to C6 after	
C1	0.58		0.49		0.31	
C2	-	**avg**	-	**avg**	0.37	**avg**
C3	0.60	**0.68**	0.85	**0.60**	0.58	**0.43**
C4	0.86		0.45		0.47	
C5	0.36		0.30		0.40	
C6	0.34	**avg**	0.31	**avg**	-	**avg**
C7	0.37	**0.36**	0.32	**0.29**	0.63	**0.51**
C8	0.30		0.27		0.59	
C9	0.43		0.26		0.41	

same side of the injection line

other side of the injection line

The location of the test well also played a role. When the pumping was done against the natural hydraulic gradient from the lower part of the dike towards the upper part of the dike, the hydraulic conductivities at the side of the test well seemed to be bigger. At the other side of the injection line, the hydraulic conductivities were smaller than when pumped from the upper part of the dike. (table 6.6). The natural hydraulic gradient should be insignificant compared to the gradient caused by the pumping. However, it seemed that it increased the hydraulic conductivity when pumped in the same direction and it decreased the hydraulic conductivity when pumped against it.

The values obtained from the zone A showed in average same kind of minor changes in both hydraulic conductivity and storativity (table 6.6). In zone A, the most notable change occurred in well A6 situated close to injection line at the opposite side from the test well. In zone B the changes in storativity were higher than in the other zones (table 6.7). The high hydraulic conductivity and storativity values of well B8 could be due to some floc migration since from the data it was concluded that the well B7 situated at the vicinity was clogged. Overall, the increase in storativity was bigger than the decrease. The well A9 had the biggest decrease in S with a decrease of 23 %. The well A6 had the biggest increase with an increase of 86 %. In zone B all the values either stayed unchanged or increased.

Table 6.6. The change in hydraulic conductivity and storativity in zone A. Test well A3.

Well	K_{before} [m/d]	K_{after} [m/d]	K_{after}/K_{before}	S_{before}	S_{after}	S_{after}/S_{before}
A1	0.52	0.63	**1.20**	$1.9 \cdot 10^{-3}$	$1.8 \cdot 10^{-3}$	**0.95**
A2	0.62	0.56	**0.9**	$7.5 \cdot 10^{-4}$	$6.0 \cdot 10^{-4}$	**0.80**
A4	0.76	0.62	**0.81**	$3.3 \cdot 10^{-4}$	$5.5 \cdot 10^{-4}$	**1.67**
A5	0.68	0.59	**0.87**	$3.8 \cdot 10^{-4}$	$3.0 \cdot 10^{-4}$	**0.79**
A6	1.05	0.73	**0.69**	$3.5 \cdot 10^{-4}$	$6.5 \cdot 10^{-4}$	**1.86**
A7	1.10	1.14	**1.04**	$3.4 \cdot 10^{-4}$	$4.5 \cdot 10^{-4}$	**1.32**
A8	1.59	-	**-**	$3.0 \cdot 10^{-4}$	-	**-**
A9	7.85	9.56	**1.22**	$6.5 \cdot 10^{-4}$	$5.0 \cdot 10^{-4}$	**0.77**
A10	1.45	0.68	**0.47**	$5.9 \cdot 10^{-4}$	$5.0 \cdot 10^{-4}$	**0.85**

Table 6.7. The change in hydraulic conductivity and storativity in zone B. Test well B10.

Well	K_{before} [m/d]	K_{after} [m/d]	K_{after}/K_{before}	S_{before}	S_{after}	S_{after}/S_{before}
B1	1.98	2.01	**1.02**	$6.5 \cdot 10^{-4}$	$2.5 \cdot 10^{-3}$	**3.85**
B2	1.63	1.62	**0.99**	$2.2 \cdot 10^{-4}$	$2.8 \cdot 10^{-4}$	**1.27**
B3	1.64	1.72	**1.05**	$7.0 \cdot 10^{-4}$	$8.0 \cdot 10^{-4}$	**1.14**
B4	1.66	1.55	**0.94**	$5.5 \cdot 10^{-4}$	$8.5 \cdot 10^{-4}$	**1.55**
B5	1.55	3.66	**2.36**	$1.7 \cdot 10^{-3}$	$1.2 \cdot 10^{-2}$	**7.06**
B6	1.47	1.43	**0.98**	$1.1 \cdot 10^{-3}$	$1.6 \cdot 10^{-3}$	**1.45**
B7	2.33	-	**-**	$1.6 \cdot 10^{-3}$	-	**-**
B8	2.69	9.85	**3.66**	$6.0 \cdot 10^{-4}$	$5.0 \cdot 10^{-3}$	**8.33**
B9	2.52	2.54	**1.01**	$1.6 \cdot 10^{-4}$	$1.9 \cdot 10^{-4}$	**1.19**
B11	1.21	1.13	**0.93**	$9.5 \cdot 10^{-3}$	$1.9 \cdot 10^{-2}$	**2.0**

A visual comparison was done to study the significance of the location of the well. It was based on the direction of changes in hydraulic conductivity and storativity values. The results of the analysis are presented in the figures 6.7 and 6.8.

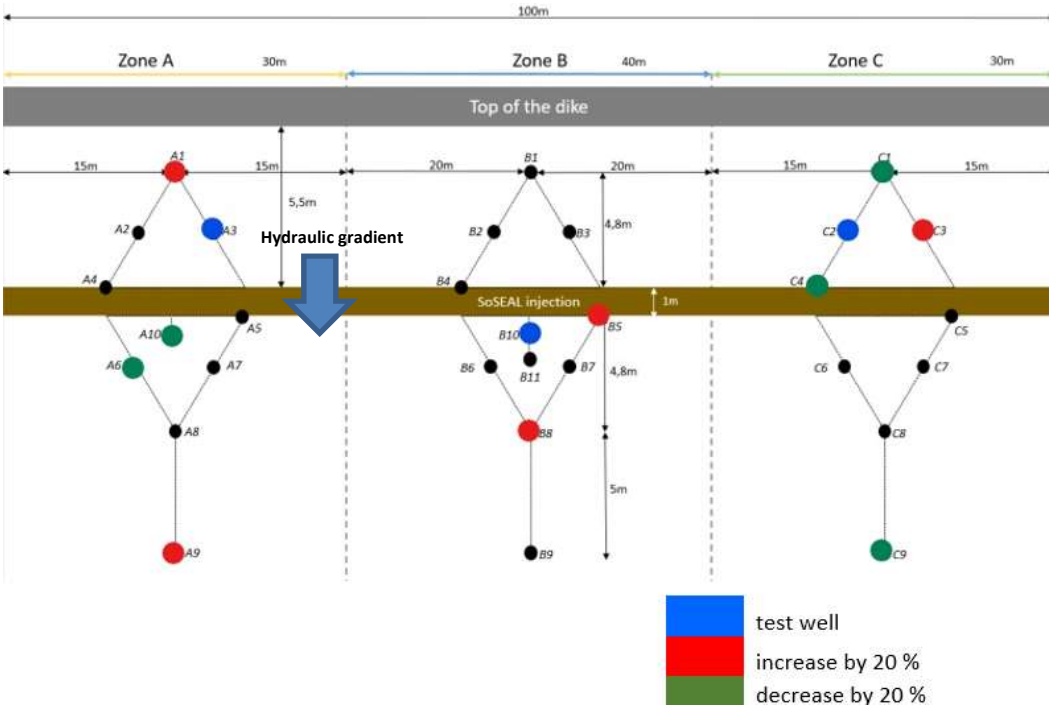

Figure 6.7. The change in hydraulic conductivity before and after the injection.

The visual inspection of the change in hydraulic conductivity did not show any clear patterns. It can be claimed that K increased at the same side of the injection line as the test well. From zones A and C, it can be deducted that K decreased at the opposite side from the test well. However, for both claims, there are also contradictory examples. Wells A8 and B7 were clogged so their results were excluded.

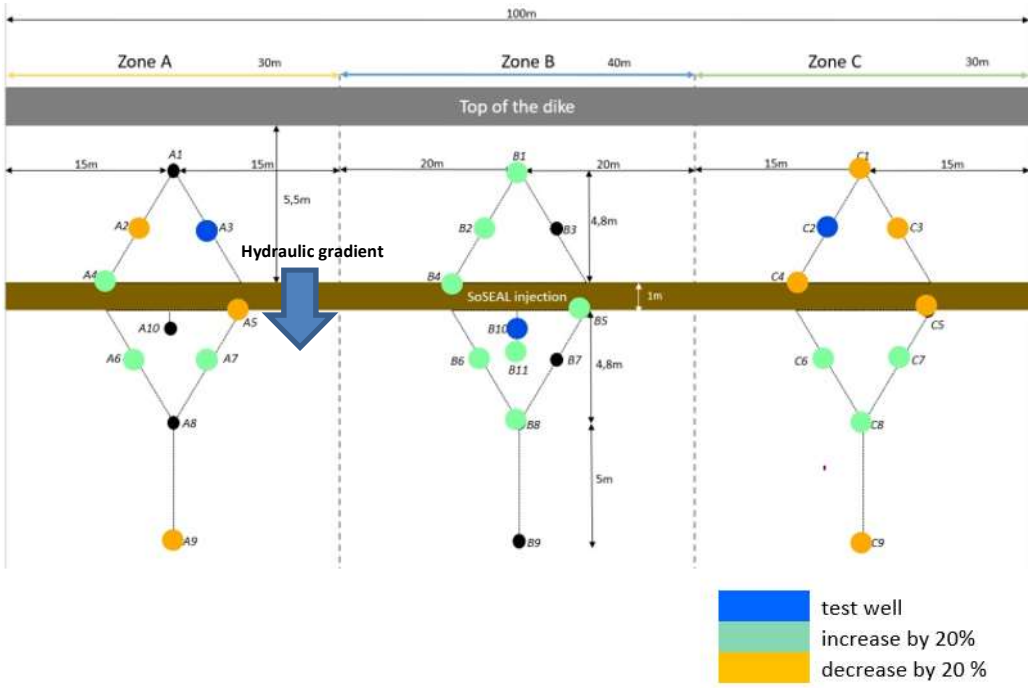

Figure 6.8. The change in storativity before and after injection.

In zone C, the storativity values on the other side of the injection line increased whereas on the same side of the injection line they mainly decreased. The well C5 was an exception but its location just next to the injection line can have an effect. Zone B had a decrease in S at both sides of the injection line. The results of zone A were indecisive. Also, the connections in the change of hydraulic conductivity with the change in storativity were not straightforward.

From the few long pumping tests done in zone C, the specific yield was estimated. Since no long pumping test were conducted during the baseline measurements no comparison could be done. Figure 6.9 shows an example of long pumping test curve fitting and table 6.8 gathers the specific yield values of zone C.

Q [m³/d]	r [m]	T [m²/d]	S [ ]	S_y [ ]	b [m]	Selected η value
27	4.51	12	0.00075	0.23	6.00	0.2
						Computed Kz/Kr
						3.54E-01

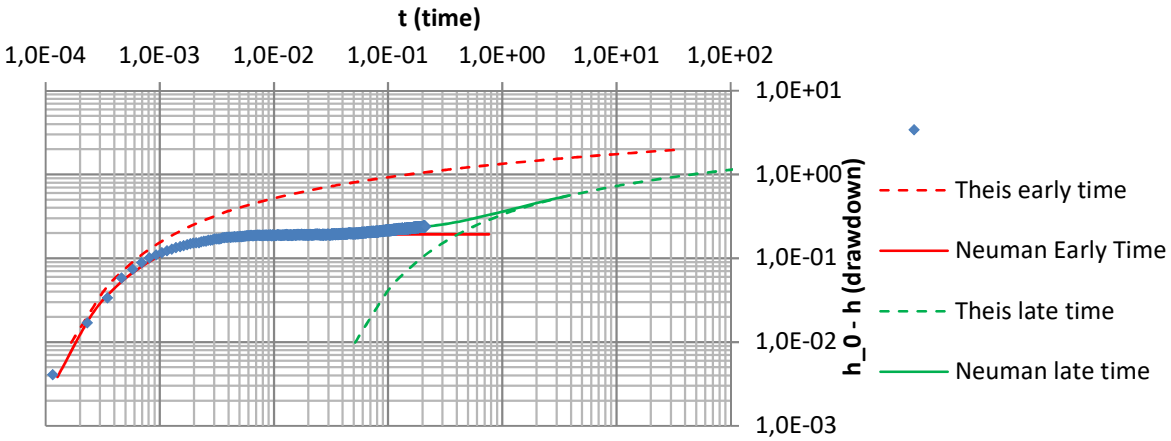

Figure 6.9. The long pumping test from C9 observed from the well C8.

Table 6.8. The specific yield in zone C.

Well ID	S_y	Well ID	S_y
C1	0.04	C5	0.08
C2	-	C6	0.07
C3	0.025	C7	0.08
C4	0.035	C8	0.23

The distance from the test well seemed to have an importance to the specific yield values. The wells C1, C3 and C4 had S_y values close to each other. In the same ways wells C5, C6 and C7 can be grouped. The well C8, situated closest to the test well, had the highest S_y value. There had been a disturbance in the well C2 during the test, so the data could not be fitted.

The transmissivity and storativity obtained from the long pumping test (6 hours) in October were compared with the values from the short pumping test (1 hour) from July. The shorter pumping test reached the flat part of the Neuman curve (delayed yield). The differences in the results are presented in table 6.9.

Table 6.9. The T and S values from the pumping tests of the well C9.

test well	Short pumping test T(m^2/d)	S	Long pumping test T (m^2/d)	S
C1	34	$1.9 \cdot 10^{-4}$	29	$2.5 \cdot 10^{-4}$
C5	15	$4.0 \cdot 10^{-4}$	18.5	$3.2 \cdot 10^{-4}$
C8	11	$1.7 \cdot 10^{-3}$	12	$7.5 \cdot 10^{-4}$

6.4 The reduced permeability barrier

It is complicated to estimate how the ground water moves in the subsurface and even more complicated to try to estimate the flow when the regular flow is perturbed by injecting a flow barrier to the aquifer. The results of the section 6.2 and 6.3 showed that the water flow had changed after the injections. However, the results failed to show where the change low permeability zone was located and why the magnitude of change was lower than expected from the first pilot. Defining the area where the flocs are blocking the pore spaces is important in estimation the behavior of the mixture and the effectiveness of the barrier.

To observe how the mixture moves from the injection line, the electrical conductivity was plotted as a function of time (figure 6.10, 6.11 and 6.12). The change of EC was measured during the injection of the zone in question. The EC levels of the monitoring wells did not change significantly at other moments than the moments plotted in figure 6.10, 6.11 and 6.12.

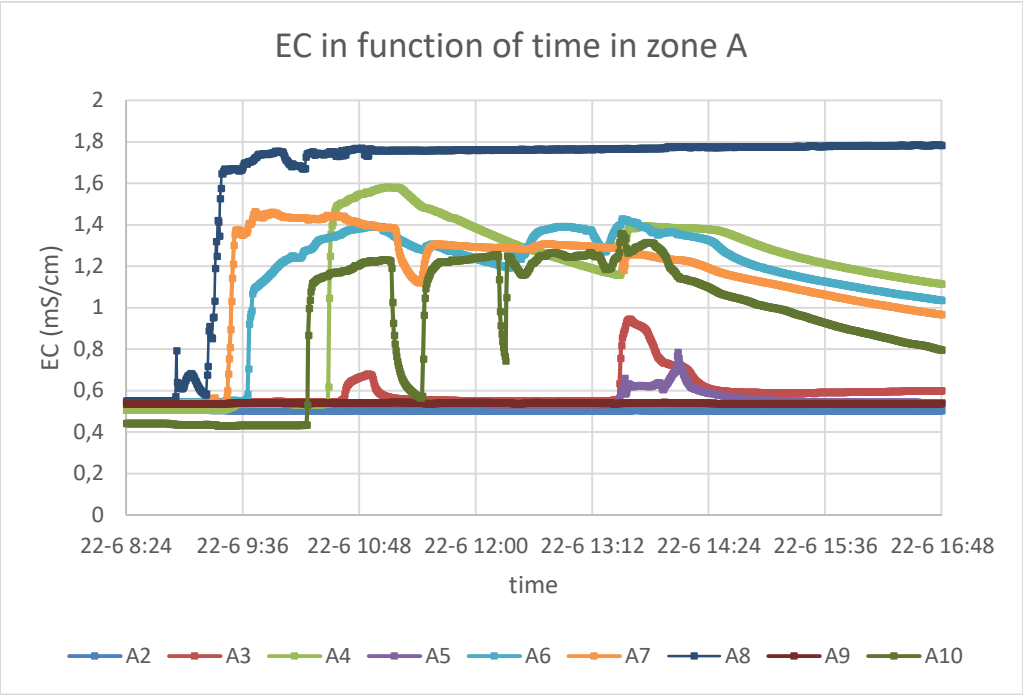

Figure 6.10. The variation of electrical conductivity as a function of time in zone A

The EC increased in the wells situated in the lower part of the dike. As an exception, the well A4 experienced an increase of EC whereas the EC in well A5 remained low the entire time. The constantly high electrical conductivity of the well A8 indicates that it was clogged.

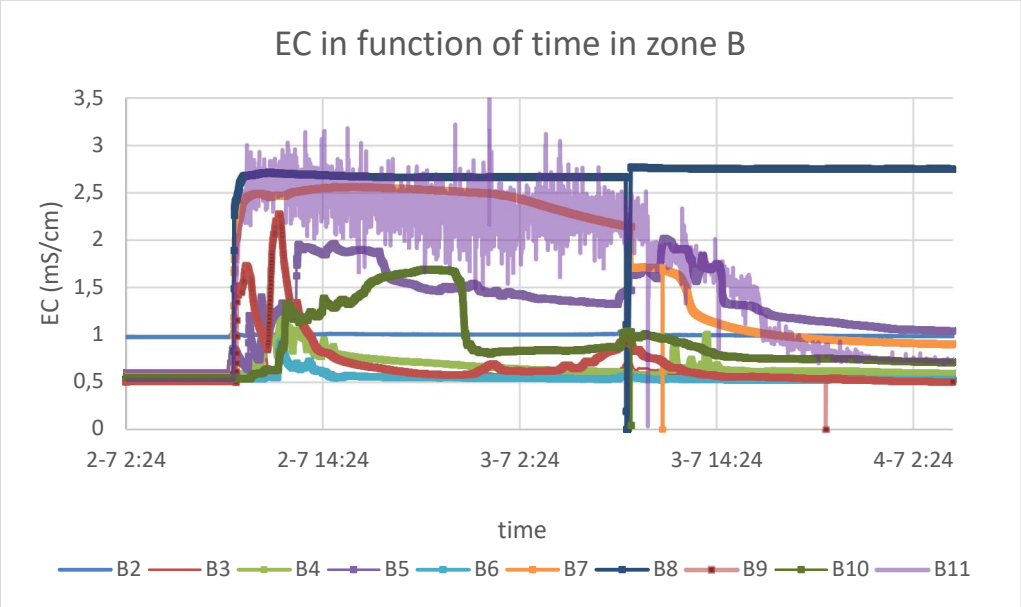

Figure 6.11. The variation of electrical conductivity as a function of time in zone B

In zone B, the electrical conductivity on the top of the dike remained unchanged except of the well B4, which EC value increased by 1 mS/cm. The transport of the chloride reached also the well B9. The well B6 did not experience an increase in electrical conductivity.

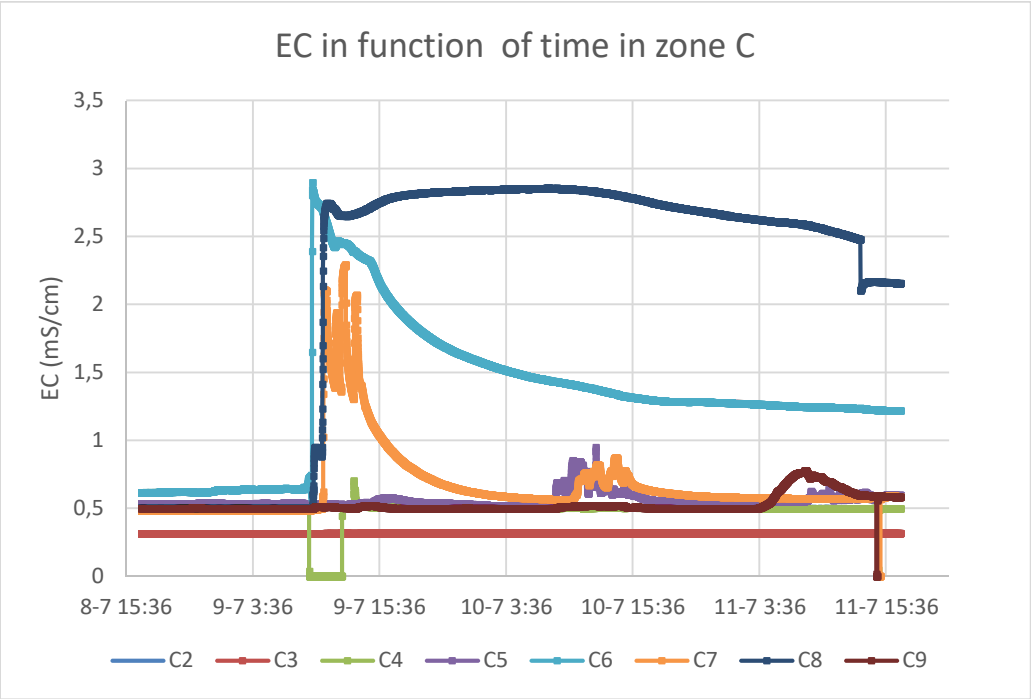

Figure 6.12. The variation of electrical conductivity as a function of time in zone C.

In zone C, the electrical conductivity increased significantly only in wells C6, C7 and C8. They were all situated close to each other and in the lower part of the dike. A slight increase in EC occurred in the well C5 when the injection took place in front of it.

The moment of occurrence of the EC peak had common factors. For zones B and C, the EC peaks happened during the first injection after a weekend. For zone A, the peak took place during the first injection of the second injection day. It seems that water with chloride ions were getting accumulated near the injection line. When the injection was started again, the water containing Cl^--ions moved due to the injection pressure. The filters situated 5 m from the injection line (A8, B8 and C8) reacted fastest and had the biggest increase. The Cl^--ions reached also the wells situated closer to the injection line but a bit later and with lower Cl^--ions concentrations. It is difficult to estimate the flow path of a heterogenous flow. Factors affecting the order and magnitude of the EC increase could be that the filters were only covering the last 2 m of the monitoring well and the injection were done from the bottom up.

During the injection, the well A8 was clogged and some flocs were visible at the bottom of the well. The measurements show that the flocs have been more mobile than expected (fig 6.5.). The electrical conductivity values were used to have an indication of the movements of the flocs. An increase in EC can indicate the migration of the flocs towards the monitoring well. Based on the results of figure 6.12, an estimation of the movements of the flocs was drawn (figure 6.13). The flocs might have migrated all the way to the well C8 that was situated almost 5 m from the injection line. This would mean that the well C5 would be indeed situated at the top part of the injection line. This would correspond to the scenario 8 of the table 5.4. The slight increase of the electrical conductivity in C5 would be due to the injection happening in front of it. It did not indicate a preferential flow towards the well C5 since the increase occurred 4 days after the increase in EC of the other wells.

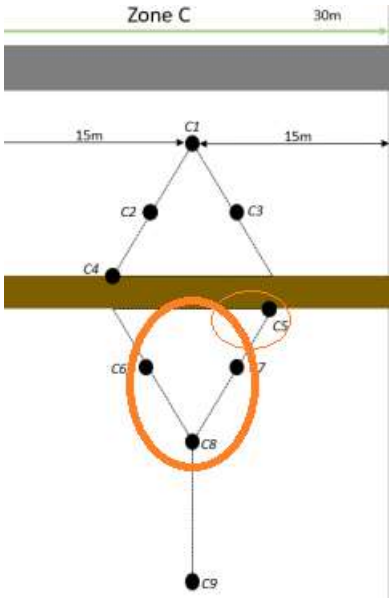

Figure 6.13. The transport area of the Cl^- in zone C.

The measured specific yield values (table 6.8) also indicated that there had been a displacement of the flocs. The S_y value of the well C8 was significantly higher than the value of the well C6 that was situated only 2 m apart. The specific yield is the water released from the storage divided by the aquifer surface per unit decline of the water table. A small specific yield indicates a low permeability material that does not release water from storage. Between the well C9 and the wells situated behind the well C8 the specific yield was lower which can indicate that the flocs were distributed to the whole lower part of the dike. The values at the upper part of the dike (C1, C3 and C4) did not change with the distance since for all of them the possible lower permeability area was situated in front of them.

Instead of having a total displacement of the barrier, it is more likely that some of the flocs are still situated close to the injection line and some started migrating downstream. This would mean that the reduced permeability zone would be thicker than 1 m. It would be a combination of scenarios 3 and 8 presented in table 5.4. In zone C, it could be up to 5 m thick if some flocs are estimated to be at the level of well C7. If the flocs are distributed in a larger area their concentration is smaller which can reduce the effectiveness of the reduced hydraulic conductivity barrier.

One of the possibilities is that the low permeability barrier would contain holes (scenario 4 and 5 in table 5.4). The results of the figure 6.12 indicate towards this direction. The holes could create preferential flow paths and increase the measured hydraulic conductivity of the wells situated in the proximity or in the trajectory of these holes. For example, in the case of pumping C6, the higher K of C3 compared to C2 could indicate that there were holes in the barrier in the proximity of the well C3. If the flocs are moving due to the flow, they can decrease the hydraulic conductivity temporarily.

6.5 Sources of errors

6.5.1 The heterogeneity of the soil

The first factor causing uncertainty to the results was the heterogeneity of the soil. Gravel layers have a higher hydraulic conductivity and therefore the water flows faster in the lower part of the dike. According to the soil profiles (Appendix 1) both zones A and C have layers with a presence of gravel beneath the groundwater table. In zone A the gravel was present in well A3 and A9. This can indicate that the layer of high conductivity reaches throughout the whole zone. The layers of heterogeneity could explain the clogging of the well A8. In zone C the gravel was present in the well C8 situated on the lower part of the dike but not in C4 situated closer to the top of the dike.

The high pressure used in the injections caused a flow of the water in the aquifer. The flocs may have migrated away from the injection line along with the water flow (figure 6.13). In addition to the injection pressure, the natural hydraulic conductivity of the dike might be partly responsible for the migration of the flocs in a longer period of time. The different transportation areas of the zones can explain why the drawdown pattern after the injection of the zone C was closer to the expectation than the other zones.

The behavior of the water flow in test zones can give indication on the extent of different high hydraulic conductivity layers. The EC values measured during the injections reveal the direction and velocity of the flowing water under the effect of the injection pressure. In zone B, according to soil profiles, no gravel layer is present. However, most of the monitoring wells of the lower part of the dike experienced a simultaneous increase in electrical conductivity (figure 6.11). The hypothetical transport areas of figure 6.13 are not based on the gravel layers but on the EC measurement that indicate the migration of Cl^--ions.

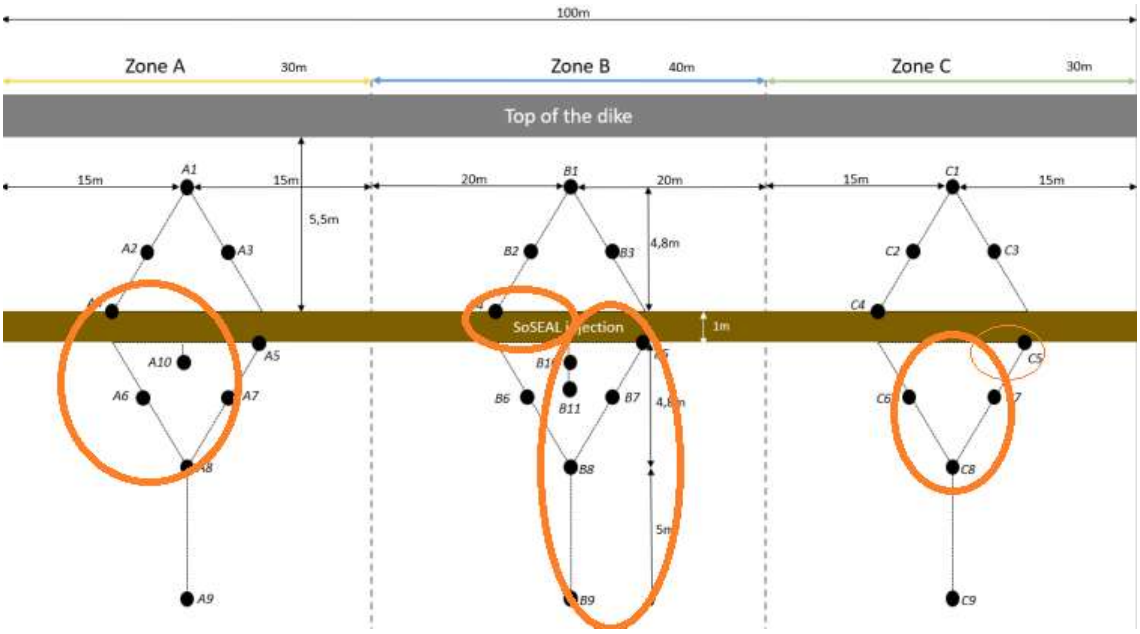

Figure 6.13. The hypothetical transport area of the mixture based on Cl^- ion transport.

6.5.2 The tidal effect

When the pressure is measured from the divers, the factors affecting the measured pressure are the measurement error of the divers, the infiltration of water through the ground surface, and the variation of the ground water level due to the tide. The tide had the biggest influence in the measured data. The longer the pumping test were, the bigger the effect was. As seen from the figure 3.5, the tidal effect could be up to 0.2 m and the amplitude of the tide was about 12 hours. When the pumping test lasts only 10 minutes, the tidal effect will be 3 mm but with a one hour test the effect is almost 20 mm. If the monitoring well is situated far away from the test well and has 80 mm as the total drawdown, an increase or decrease of 20 mm represents a big part of the change noticed. The Neuman method compensates the distance. The effect of the tide leads to under- or overestimation of the transmissivities obtained from the wells further away.

The tidal effect for the long pumping test were tried to be removed, but it turned out to be more complicated than expected. The water level in De Gijster is controlled manually and most of the time it is kept on a steady level. The tide of the river Amer is documented and its relation to the water level variation of the monitoring wells could be estimated. Due to the irregularities in the variations of the water level surface of the Amer, the change in water level in the well A4 was used in the elimination of the tidal effect, when conducting a pumping test in C9. However, regardless of the long distance, the well A4 is also slightly affected by the pumping of C9 so the effect of pumping was exaggerated (figure 6.14). The pumping test started the 1st October at 14:21 and ended at 19:25. The tide decreased the whole period of pumping. Probably, the water level decreased 10 mm lower and a bit faster than it would have only due to the tide. In total, the difference was small, so this method of compensation is accurate enough to be used in the analysis of the long pumping tests.

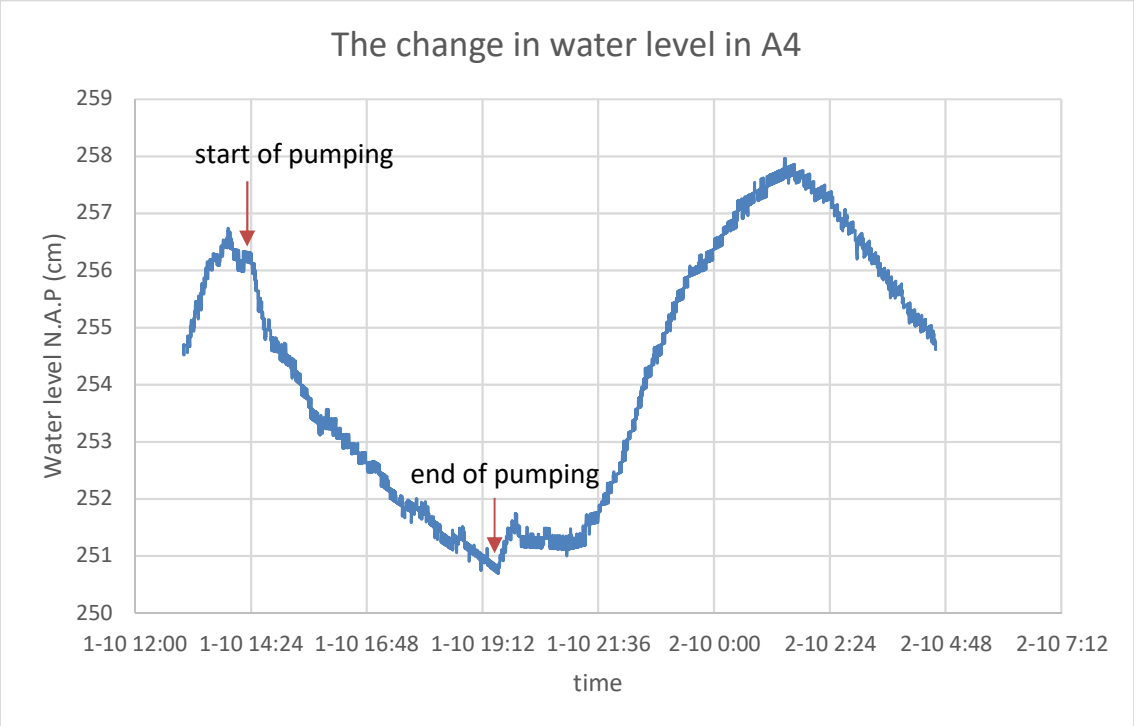

Figure 6.14. The water level variation of the well A4 during the pumping test from C.

The tide had a significant effect on the water level of the monitoring wells in the dike of the water reservoir. For further studies, to eliminate the tidal effect during the pumping tests, it is easier to choose a moment when the tide is throughout the test period going either up or down. If possible, data from monitoring well, that is outside of the cone of depression of the pumping test, should be used, so that its water level change could be used to estimate and eliminate the effect of the tide.

6.5.3 The pumping tests

The tests were conducted with a pump placed on the ground surface just above the test well. A suitable submersible pump was not available for this part of testing, since the outer diameter of the well was only 50 mm. With the vacuum created by the above-ground pump, water could be lifted up to about 7 m. The water table was high enough only in the monitoring wells situated at the lower part of the dike so from the wells A9, B9 and C9. For all the other wells, the water was pumped to the well. For the pumping test, a high pumping rate is recommended. However, an overflow occurred as soon as the water was infiltrated to the test well with a rate higher than 25 m^3/d. Sometimes the overflow happened 10 min after the start of the test but at times it took more than one hour to happen.

The pumping rate of the pump was set by adjusting the amount of water that flowed through the valve. The pumping rate was estimated by measuring the time needed to fill 5 L of water to a canister. Due to the uncertainty of the measurement technique, the flow rate may contain some error. The flow rate was measured several times during the pumping test and the value seemed to stay relatively constant. The water for infiltrating was taken from the freshwater reservoir. Some variation in the flow rate occurred, when the weather was particularly windy, and the hose moved along the waves. The effect of the waves could be spotted from the drawdown data as a wavy impulse. The variation made the curve fitting more challenging.

To reach the late time curve of the Neuman method, the pumping test should be maintained for a day instead of an hour. Due to the limited amount of time on the test field and the lack of electricity on site, at first, only short pumping test were done. It was only after applying the Neuman method to the data, that the importance of longer pumping test was recognized. Two longer pumping test were done in October but no long pumping tests are available before the injection.

6.5.4 The method and tool used for analysis

The Neuman (1975) method is for fully or partially penetrating wells but the effect of the partial penetration needs to be estimated. The monitoring wells were not certain to penetrate the last 0.5 m of the aquifer and the filter covered only 2 m of the 5.5 m thick aquifer. In his paper in 1975 Neuman presents a solution for a partially penetrating well. However, in his publication in 1974 Neuman showed that the effects of the partial penetration of the late-time drawdown can be neglected at distances greater than (Eq 23, 24):

$$\mathrm{r} = \frac{\mathrm{b}}{\mathrm{K_D^{0,5}}} \quad \text{(Eq. 23)}$$

$$K_D = \frac{K_z}{K_r} \quad \text{(Eq. 24)}$$

From the pumping test in C9 in October, the obtained K_D is 0.093. With an aquifer thickness of 5.5 m, the distance where the effect of the partial penetration disappears is 1.8 m. In case where pumping was done from the well C9, all the wells were situated further away than 1.8 m. The effect of the partial penetration can be neglected for that particular pumping test. Due to the lack of long pumping test data, K_D cannot be estimated for other pumping tests. In this analysis, the effect of the partial penetration to the early-time drawdown was not estimated. If the aquifer dimensions correspond to ground investigations, the non-penetrating fraction is small. In case the aquifer continues deeper than estimated, the effect can be more important. The effect of the filter not covering the entire aquifer thickness is not considered at this point.

Another factor that the Neuman method does not consider is the wellbore storage. In De Gijster the outer diameter of the well was 50 mm. It is not considered a large well but since the pumping rate of the tests was relatively low, the effect of the wellbore storage might be pronounced. Ignoring the wellbore storage leads to an underestimation of transmissivity. The wellbore storage affects the specific storage values since the wellbore storage is important at the beginning of the pumping test. What has been interpreted as specific storage might be due to wellbore storage. In some fits, the wellbore storage might be even eliminated due to a bad choice of starting moment.

In this study, the three-dimensional flow was not considered. Two-dimensional flow was assumed with the Dupuit-Forchheimer assumption. According to Zech et al. (2016), the effects of three-dimensional flow should be investigated, when the distance between the observation well and the pumping well correspond to the aquifer thickness (Zech et al. 2016). In this study the radial distance was sometimes equal to the aquifer thickness.

In hand-fitting, the person doing the fit decides, when the fit is the best possible. Since it is not an automated process some variation in the results can occur. In the Excel tool, the first decision to be done is to select the background curve. Sometimes, the ideal curve could be between two curves. Depending on the value selected, the T and S values can vary significantly. Figure 6.15 illustrates the effect of the choice of the background curve (η-value). In the analysis, the background curve that always stayed at the same side of the measurement point was preferred. From the examples below, the first one with η=0.2 was chosen. When the change of transmissivity measured was in average less than 5 m^2/d, the variation due to the choice of background curve is significant (12 m^2/d vs. 21 m^2/d). The storativity values were on average more consistent

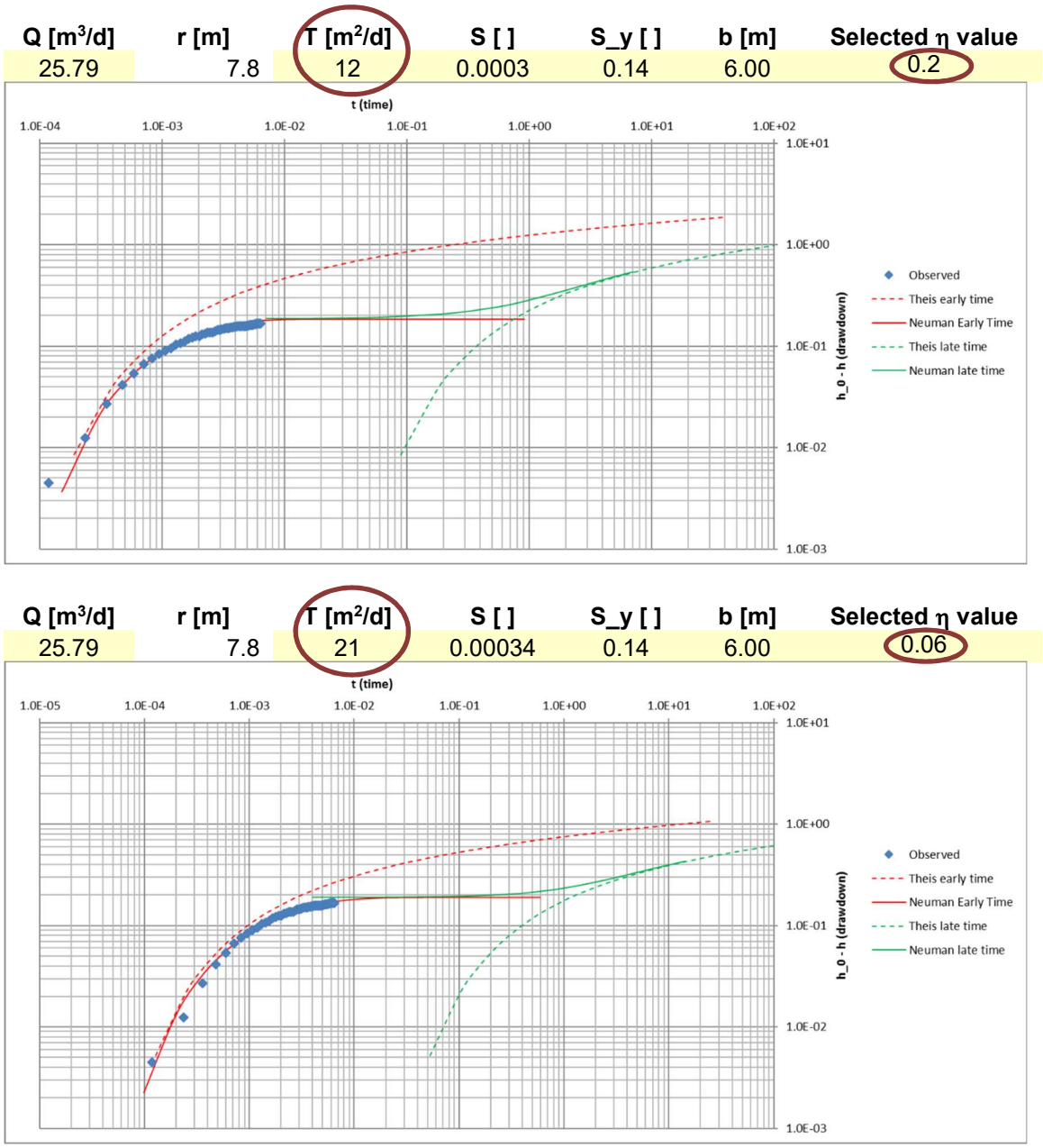

Figure 6.15. The effect of the choice of the background curve.

After choosing the background curve, the fit itself needs to be done. The shape of the curve does not always follow perfectly the background curve. Especially, the first measurement points can be separated from the line. When the distance between the test well and the monitoring well increases, the response is delayed and decreased. In the pumping test the drawdown during the first minute should be steep. This effect does not always occur clearly in the far away wells. To be able to plot the values correctly the plotting needs to be started with values that are sometimes even few minutes after the start of the pumping test. The choice for the starting moment for the plotted data is also judgmental, especially, when the drawdown stays at low rate for a long period of time. When doing the fitting, the beginning or the end of the test can be given a greater value. In this analysis the weight was on the first ten measurement points, sometimes neglecting the first three if they were completely out of line. A different weighting leads to different results.

6.6 Reliability of results

The values obtained with this method represents the K and S values between the test well and the monitoring well. The soil is known to be heterogenous and anisotropic due to the different layers revealed by the ground investigations. The goal of the injection is to increase this anisotropy in the injection line. When the monitoring well is situated on the other side of the injection line, the zone of reduced permeability was included in the values. Based on the first pilot and the laboratory tests, the hydraulic conductivity of the injection line was expected to be reduced almost 40- times. The reduced permeability barrier was expected to be 1 m thick. However, since the value analyzed with the Neuman method represents all the soil in the aquifer situated between the monitoring well and the test well, the total reduction will be significantly less. The anisotropy created by the wall is illustrated in figure 6.16.

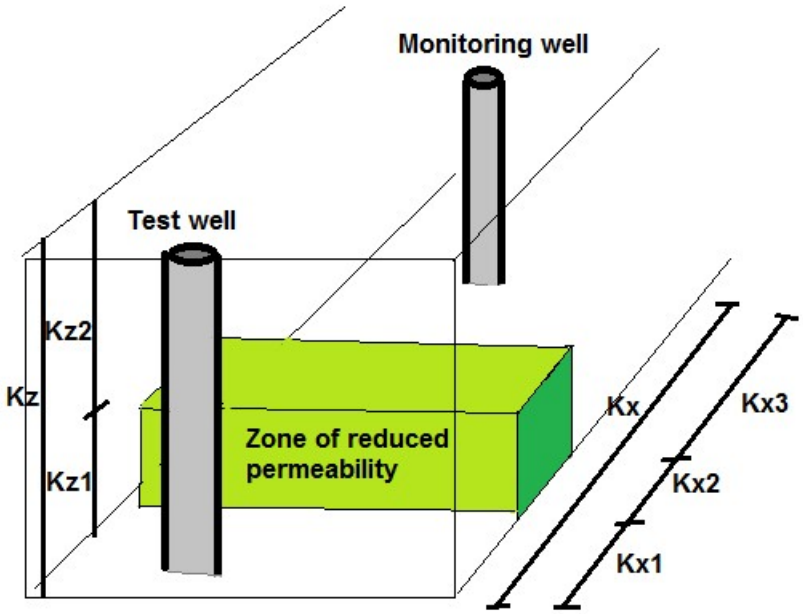

Figure 6.16. The hydraulic conductivity in the injection line changes in vertical and horizontal direction.

The changing hydraulic conductivity can be considered in the calculations. Leonards (1962) defined the vertical and hydraulic conductivity with the equation 23 and 24.

$$K_x = \frac{\sum_{i=1}^{M} b_i K_{xi}}{\sum_{i=1}^{M} b_1} \quad \text{(Eq. 23)}$$

Where K_{hi} is the equivalent hydraulic conductivity for layer i and b_i is its thickness.

$$K_z = \frac{\sum_{i=1}^{M} b_i}{\sum_{i=1}^{M} b_i / K_{zi}} \quad \text{(Eq. 24)}$$

Where K_{vi} is the vertical hydraulic conductivity of layer i.

The Eq. 22 shows the relationship between the vertical and radial hydraulic conductivity. The radial and horizontal K are supposed to be the same in this case. The curve-fitting provides the radial hydraulic conductivity and based on it, the vertical hydraulic conductivity can be calculated. However, to define the permeability of the injected line, the K_{hi} and K_{vi}

values of the wall should be calculated. The Neuman method does not permit dividing the soil into several layers, so the value obtained is just the average K_h and K_v between the monitoring well and the test well.

The Neuman method is composed of early time and late time curves. The pumping test conducted on-site mostly only reached the early time curve. According to literature especially the late time curve is suitable for estimating the transmissivity. The significance of the late time curve and long pumping test was realized only during the analysis of the data from the after the injection pumping tests.

The Neuman method was developed for homogenous anisotropic unconfined aquifers which are pumped at a constant rate. The aquifer in the water reservoir is unconfined, anisotropic and the pumping rate was kept constant or the measurements occurring after the change of rate were ignored. However, the aquifer of the is heterogenous. In the vertical direction, the aquifer is in two different soil layers, a medium/coarse sand layer and a fine sand layer (figure 4.4). The objective of the injection was to form a vertical barrier of reduced permeability. The heterogeneity is present, and it should not be neglected. However, the Neuman (1975) does not consider the heterogeneity. The Neuman method was chosen for the analysis for its simplicity but the simplifications might affect the results considerably. In the section 8, recommendation for methods better suitable for heterogenous aquifers are presented.

The hypothesis of the location and shape of the barrier based on the specific yields and the electrical conductivity, should be evaluated critically. The specific yield values obtained was based only on one pumping test conducted in zone C and the preliminary data for the specific yield. The increase in EC indicates only the migration of chloride ions. Since after the flocculation reaction the aluminum and chloride are not bound together anymore, it might be that they do not behave similarly. The chloride-ions move freely with water whereas the flocs are attached to the soil particles with a chemical bound and physical blocking. The chemical bound is formed between the organic matter that has a negative charge and iron that is present in the sand as an impurity. The importance of physical blocking in the pores becomes more important with the growing floc size. If the formation of floc has not started as expected, the probability of floc migration increases.

Overall, there is too little data and too many uncertainties to give reliable results. There has been a change in the groundwater flow after the injection. It is however hard to estimate with the current analysis, whether the change was due to the injection or just caused by the seasonal change. The measured change in aquifer parameters are all in the error range.

6.7 Comparison to literature values

The obtained hydraulic conductivity values were compered to values suggested by several sources. One table of typical hydraulic conductivity values for different soil types is the table 2.2. Bouwer (1978) suggested that fine sands has K-values from 1-5 m/d and medium sand from 5-20 m/d. Morris et al. (1967) suggested representative hydraulic conductivity for different soil materials determined in a laboratory with a repacked sample. The K-value suggested for fine sand is 2.5 m/d, for medium sand 12 m/d and for coarse sand 45 m/d. In the water reservoir, the different zones gave slightly different values of hydraulic conductivity. They are represented in the tables 6.2, 6.6 and 6.7. In average the values were

between 1.5 m/d and 3 m/d for all the zones, before and after injection. According to both Bouwer (1978) and Morris et al. (1967), the obtained values correspond to hydraulic conductivity of a fine sand. However, according the soil profiles (Appendix 1), the aquifer is composed mostly of medium coarse/ fine sands. The obtained values were lower than expected since the hydraulic conductivity should reflect the presence of coarser sand.

The storativity values obtained from the short pumping tests are only composed of specific storages. For unconfined aquifers the specific yield should be defined, too. The specific yield is a few orders of magnitude higher than the specific storage. Storativity is the sum of the specific storage and the specific yield, which means that the specific yield is dominant. The specific storage value depends on the density of sand. The aquifer is assumed to be dense sand. The specific storage value of dense sand ranges from $1.2 \cdot 10^{-4}$ and $2.1 \cdot 10^{-4}$ (Domenico et al. 1965). The Neuman method excel tool calculates the storativity, so for the comparison the specific storage values should be multiplied with the aquifer thickness (~5,5 m). This gives a range of storativity from $6.6 \cdot 10^{-4}$ to $1.2 \cdot 10^{-3}$. Loose sand has specific storage values one order of magnitude higher and rock one order of magnitude lower than the specific storage values for dense sand. The range of values obtained is presented in the tables 6.2, 6.6 and 6.7. The values from the analysis are not all in the range defined by Domenico et al. (1965), but the order of magnitude is correct in all most all the wells. The wells having unusually high storativity values were close the test well, which might have affected the results.

The values obtained for specific yield are significantly lower than values expected for medium coarse or fine sand. According to Bear (1979), the S_y of sand is 20-35 %. Values lower than 10 % are typical for clay. However, in the table 2.2 published by Johnson (1963) for United States Department of Interior Geological Survey, the S_y values vary in a larger range. The minimum S_y for sand is still 10 %, so above the measured values.

The low specific yield can indicate that the aquifer material would have changed to resemble a finer soil. The volume of the aquifer in zone C between the well C8 and the injection line is roughly 900 m^3. The amount of mixture injected in zone C was 40 m^3 which represents less than 5 % of the total aquifer volume. The porosity of soil is expected to be around 30 %, so 15 % of the pores can be filled with the injected mixture. Considering this, there is probably a smaller area where the flocs are gathered and it affects all the water flow passing through it.

Even though the drawdown curve looked like it would start to follow the S-shape and enter the late time curve, the length of the pumping test was not long enough to confirm the entrering to the late phase. According to Beretta et al. (2018), the pumping test needs to be at least from 24 to 36 hour-long to define the specific yield with the Neuman method. The pumping test conducted in October was 6 hours. The slight increase of drawdown taking place after an hour of pumping can be due to the tide even though its effect was partly eliminated.

7 Conclusions

The aim was to prove that there has been a reduction in soil permeability of the dike. However, the analysis fails to show a clear quantitative reduction in the hydraulic conductivity values. The reduction was also smaller than expected from the first pilot and the laboratory results. The Neuman (1975) method showed on average a small reduction in the hydraulic conductivity values on the lower part of the dike but the reduction was so small that it can be in the error margin. The uncertainties came from the measurements, the assumption of the analysis method and from the analysis tool. The most important limitation of the analysis was the assumption of aquifer homogeneity. The injection itself created a zone of heterogeneity. The Neuman method provides aquifer parameters that are average values of the whole aquifer between the test well and the monitoring well. For that reason, the analysis failed to show the magnitude of the hydraulic conductivity reduction occurring due to the injection.

However, the injection has changed the flow path of the water in the aquifer. This can be observed from different comparison of data methods. The natural hydraulic gradient between the top part of the dike and low part of the dike has increased (figure 6.1). The drawdowns of the pumping tests conducted after the injection show an accelerated drawdown during the first minutes of the pumping test on the same side of the injection line as the test well. A delayed drawdown was observed on the other side of the injection line (figure 6.5). The delay can be an indication of resistance to flow so a lower permeability area.

The three zones had a slightly different organic matter concentrations and injections patterns. The results of the zones also differed but the variation is probably more due to the soil heterogeneity and presence of high permeability zones. The complete analysis was done for the zone C but it might not be the zone with the most efficient reduced permeability barrier. The measurements done few months after the injections showed that the zone A would be the most successful one. There was no pumping test data from zone A available after July so the estimation is based only on the change in hydraulic gradient (figure 6.2).

The comparison of data gives reason to suspect that the flocs have migrated from the injection line. The flocs have moved due to high permeability zones, pressure of the injections and the natural hydraulic gradient that is from the top of the dike toward the toe of the dike. Instead of the planned 1 m-thick barrier, the flocs are probably distributed to a larger area down the slope. The lower concentration of flocs reduces the effect of the low permeability barrier. One of the advantages of the SoSEAL method compared to jet grouting was that the flocs can spread to a wider area than just the injection point. However, since it seems that the flocs are more mobile than expected, the advantage may be a disadvantage. The behavior of the mixture under the injection pressure and a hydraulic gradient must be studied to ensure the longevity of the reduced permeability barrier.

Both comparison of data and the Neuman method shows that there has been a change in the behavior of drawdowns after the injection. However, the results are not straightforward, and the changes measured are so small that they might be in the error range. Due to all the uncertainties mainly linked to the soil heterogeneity the Neuman (1975) is not a suitable method for this this analysis. Instead of analyzing the change in hydraulic conductivity of

individual wells, it could be more interesting to compare the shape of the cone of depression (figure 6.1), since it is the result of pumping and the distribution of the permeability field.

8 Recommendations

Since the results of the analysis were indecisive and contained many uncertainties that decrease the reliability of the results. Recommendations are given for further tests, better analysis methods and tools. Finally, recommendation for the use of SoSEAL-method is given.

8.1 Further tests in De Gijster

The trend of higher transmissivities for longer pumping test was present in the pumping test from De Gijster. Long pumping test are considered to give better representative values, especially for the transmissivity. According to Moench (1994), the early time data cannot be used to estimate aquifer storativity with the Neuman (1975) method since the wellbore storage affects the values. However, if the goal is to measure change, the baseline measurements and the end measurements should be conducted the same way to be able to compare the results. In this test zone in De Gijster, the baseline measurements were done as short pumping test. If the values of long pumping test are used for the after-injection measurements, the values should be compensated.

The pumping tests and water level measurements from the end of July and beginning of October show some variation. To eliminate the effect of the weather and the moisture content of the soil, new test sets and taking soil samples are suggested. The presence of the flocs and their size can be measured from the soil samples. Samples should be taken from all the zones and from different distances regarding the injection line (figure 8.1). For the pumping tests, the time interval of the new tests could be from few months to a year. The results obtained at this first stage suggest that the flocs have moved towards the lower part of the dike. The soil samples should be taken from all the zones. New measurements together with soil samples could either confirm or discard this hypothesis.

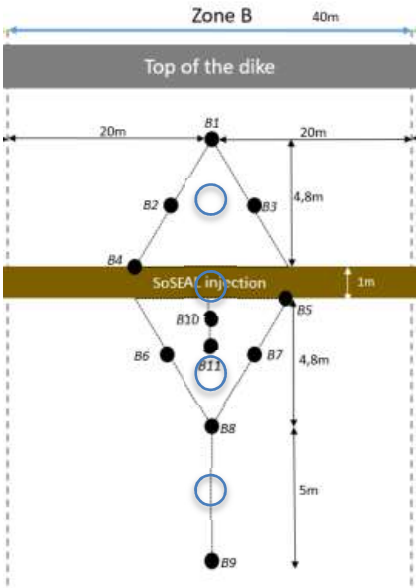

Figure 8.1 A proposition for soil sampling points in zone B

The filter of the current monitoring wells is only two meters long starting 0.5 m from the bottom of the well. For new test wells, a filter that covers the entire aquifer thickness is recommended. Especially in De Gijster, where the lowest two meter of the dike has a lower hydraulic conductivity, the short filter can affect the capacity of the monitoring well to represent the water flow around it.

The laboratory tests in 2016 were conducted without an additional hydraulic gradient. To better understand the behavior of the mixture, new tests with a flow corresponding to groundwater flows of aquifers in different soil types should be done. The results could help to understand the behavior of the mixture in De Gijster and give an indication, to what kind of conditions the SoSEAL method is suitable for.

To simplify the analysis process, only data from the zone C was analyzed with all the used methods. The injection of the zone C appeared to be the most successful one in the preliminary analysis that was conducted in all the zones. Also, the zone C was the only zone where none of the wells seemed to be clogged. Afterwards when the flocs clogging the wells had migrated further, it was noticed that the reduced permeability barrier of zone A seemed to be more successful. Especially the change in hydraulic gradient can be seen more clearly in zone A. The focus of the testing should be moved to zone A.

8.2 Different pumping test analysis methods

Mostly due to the heterogeneity of the of the aquifer, the Neuman (1975) method is not a suitable analysis method for the aquifer of the dike in De Gijster. Methods considering heterogeneity exist, but they are more complex. To apply them, uncertainties linked to the soil layers and the effect of the tide can be reduced. Neuman et al. (2007) concluded that the transmissivity values obtained from the graphical interpretation have a sizable error when the aquifer is randomly heterogeneous.

Butler (1988) conducted a pumping test analysis that considered the radial discontinuities by a straightforward Laplace-transform procedure. The type-curve methods offer a weighted average of the near-well and far-well parameters. It is not a representative for the aquifer. The reduced permeability barrier could be better detected as a radial discontinuity than just as a change in hydraulic conductivity in the whole aquifer, which is hard to detect due to its extent.

One alternative is to use a simpler pumping test analysis method and include more data. The method used can be the Theis method using drawdown corrected with equation 15. To estimate the effect of heterogeneity an assumption of homogeneity is done. With a complete analysis of all the measurements, the sources of the uncertainty can be then analyzed. The heterogeneity is one of the sources causing uncertainty and its effect could be this way estimated and eliminated.

8.3 Better tools for analysis

An automated feature using the nonlinear least square method could be added to the Excel to minimize the difference between the type curve and the measurement data. This would

reduce the role of the expert judgment in the curve fitting. Heidari et al. (1997) suggested a nonlinear least square analysis that can be added to the evaluation of unconfined aquifer parameters. In their study, the values obtained with the nonlinear least square method were close to the visual hand-fitting method.

To increase the reliability and efficiency of aquifer parameter analysis, the ANN (Artificial Neural Network) method was used as an alternative approach to curve matching method. With ANN input and output results can be better matched and even complicated relationships between them can be considered. The solution was tested by Balkhair (2002) for a large diameter well. The analysis method used was the Papadopulos and Cooper (1967) and the results were in good agreement with the previously published results from the same test data. (Balkhair, 2002).

8.4 Suitability of SoSEAL in soil permeability reduction

The implementation site for the SoSEAL injection should be chosen carefully. The length of the injection line can affect the results. At the beginning the reduced permeability barrier slows down the water flow but since the water always flows the path with least resistance, it will contour the reduced permeability zone. To improve the reliability of the results, the zone injection line should be longer. In an ideal test site, the injection line would go from one no-flow boundary to another or form a circle. In that case, the water could not contour the barrier and its full potential would be used.

So far, the SoSEAL method has been used only in porous media. The efficiency of the injection is based on clogging the voids. If the fraction of voids is smaller, the reduction potential decreases. The porosity and permeability of clay are already so low that often there is no need to reduce it. However, sometimes a leakage can occur in the clay layer and SoSEAL could be used to clog the leakage with flocs. The injection method needs to be redesigned if the soil type is changed. If SoSEAL would be used for soil containing organic matter, the amount of organic matter could be reduced.

References

Balkhair K. 2002. Aquifer parameters determination for large diameter wells using neural network approach. Journal of Hydrology. 265 (1-4). ISSN: 0022-1694. pp. 118-128.

Bear, J. 1979. Hydraulics of Groundwater. McGraw-Hill Inc. p.567. ISBN 0-07-004170-9

Bell, F. G. 1996. Lime stabilization of clay minerals and soils. Engineering Geology, ISSN: 0013-7952, Vol: 42, Issue: 4, Page: 223-0237. DOI:10.1016/0013-7952(96)00028-02

Beretta, G. P., Stevenazzi, S. 2018. Specific yield of aquifer evaluation by means of a new experimental algorithm and its applications. Acque Sotterranee-Italian Journal of Groundwater, 7(1). DOI: 10.7343/as-2018-325.

Bonfiglio, C. 2016. Hydraulic conductivity reduction induced by precipitation of aluminium-organic matter flocs in porous media. Master Thesis. Politecnico de Milano in co-operation with TU Delft

Bouwer, H. 1978. Groundwater Hydrology. McGraw Hill Book Company. New York. ISBN: 978-0070067158

Butler, J. J. and Healey, J. M. 1998, Relationship Between Pumping-Test and Slug-Test Parameters: Scale Effect or Artifact?. Groundwater. 36: 305-0312. DOI:10.1111/j.1745-6584.1998.tb01096.x

Butler Jr, J. J. 1988. Pumping tests in nonuniform aquifers—The radially symmetric case. Journal of Hydrology, 101(1-4), 15-30. ISSN: 0022-1694.

Calvache, M.L., Sánchez-Úbeda, J.P., Duque, C. et al. 2016. Evaluation of Analytical Methods to Study Aquifer Properties with Pumping Tests in Coastal Aquifers with Numerical Modelling (Motril-Salobreña Aquifer). Water Resources Management. 30: 559. DOI:10.1007/s11269-015-1177-6

Cooper, H., Bredehoeft, J. and Papadopulos, I. 1967. Response of a finite diameter well to an instantaneous charge of water. Water Resources Research, 3, 263–269. DOI: 10.1029/WR003i001p00263

Csubák, M. 2017. Characterization of humic acids of different main type of soils. Department of Soil Science. Faculty of Agriculture. University of Debrecen.

Deb, S., Shukla, M. 2011. A Review of Dissolved Organic Matter Transport Processes Affecting Soil and Environmental Quality. Journal of Environmental & Analytical Toxicology. DOI: 10.4172/2161-0525.1000106

Domenico, P.A., Mifflin, M.D., 1965. Water from low-permeability sediments and land subsidence. Water Resources Research. vol. 1. no. 4. pp. 563-576. DOI:10.1029/WR001i004p00563

Fang, H. Y., Varrin R. D. 1968. Groundwater and Seepage: Model Analysis of Hydraulic Conductivity of an Aquifer. Fritz engineering laboratory Report No. 341.2. Leigh university institute of research

F.A.S.T.WellTest- website. Visited 27.9.2018. http://fekete.com/SAN/TheoryAndEquations/WellTestTheoryEquations/Dimensionless_Wellbore_Storage_Constant.htm

Greenland, D. 1971. Interaction between humic and fulvic acids and clay. Soil Science. Vol: 111. p.34-41. DOI: 10.1016/0016-7061(76)90078-1

Fitts, C. 2012. Groundwater science. p.692 ISBN: 9780123847065

Hayes, M., Mylotte, R. and Swift, R. 2017. Chapter Two - Humin: Its Composition and Importance in Soil Organic Matter. Advances in Agronomy, ISSN: 0065-02113, Vol: 143, p 47-138

Heidari, M., Wench, A. 1997. Evaluation of unconfined-aquifer parameters from pumping test data by nonlinear least squares. Journal of Hydrology, 192(1-4), 300-313. DOI: 10.1016/S0022-1694(96)03101-0

Heimovaara, T. and Jansen, B. 2014. Water 2014. Technical report. ISSN: 0022-1694

Hiscock, Kevin M. Bense, Victor F.2014. Hydrogeology - Principles and Practice (2nd Edition). John Wiley & Sons. Retrieved from https://app.knovel.com/hotlink/toc/id:kpHPPE0033/hydrogeology-principles/hydrogeology-principles

Johnson, A. I. 1967. Specific yield: compilation of specific yields for various materials. United States Department of Interior Geological Survey. Open File Report. 63-59. DOI: 10.3133/wsp1662D

Jones, M. N. and Bryan, N. D. 1998. Colloidal properties of humic substances. Advances in Colloid and Interface Science. 78(1):1–48. 13. DOI: 10.1016/S0001-8686(98)00058-X

Kansas Geological Survey, Geology. 1965. Retrieved from the website. Placed on web Nov. 1998. originally published Dec. 1965. Visited 26.9.2018. http://www.kgs.ku.edu/General/Geology/Sedgwick/gw01.html

Laumann S., Zhou, J. and Heimovaara, T. 2017. Presentation: Baseline session SoSEAL pilot De Gijster (31.3.2017)

Laumann S., Bonfiglio, C., Zhou J. and Heimovaara T. 2018. Poster: Laboratory Investigations on the Interaction between Aluminum and Organic Matter and its Impact on Soil Permeability. EGU April 2018.

Leonards, G. 1962. Foundation engineering. McGraw Hill. New York. ISBN: 978-0070371989

Lietaert, B. Maucotel, F. 2012. Summary of the short courses of the IS-GI 2012 latest advances in Marine grouting. In *Proc. Of the Intern. Symposium on Ground Improvement IS-GI.-Brussels*. p.3-72.

Lunardi, P. 1997. Ground Improvement by Means of Jet-Grouting. Ground improvement. vol. I. n. 2. DOI: 10.1680/gi.1997.010201

Moench, A. 1994. Specific yield as determined by type-curve analysis of aquifer-test data. Ground Water, 32 (6) (1994), pp. 949-957.
Moench, A. 1995. Combining the Neuman and Boulton Models for Flow to a Well in an Unconfined Aquifer. Groundwater. 33: 378-384. doi:10.1111/j.1745-6584.1995.tb00293.x.

Moench, A. 1997. Flow to a well of finite diameter in a homogeneous, anisotropic phreatic aquifer. Water Resour Res, 33 (6). pp. 1397-1407. doi: 10.1029/97WR00651.

Morris, D. A., Johnson A. I. 1967. Summary of hydrological and physical properties of rock and soil materials, as analyzed by the Hydrologic Laboratory of the U.S: geological Survey 1948-60. U.S Geological Survey Water- Supply Paper 1839-D. DOI: 10.3133/wsp1839D

Neuman, S. 1972. Theory of flow in unconfined aquifers considering delayed response of the water table, Water Resour. Res., 8(4). 1031. DOI: 10.1029/WR008i004p01031

Neuman, S. 1973. Supplementary comments on 'Theory of flow in unconfined aquifers considering delayed response of the water table,'.Water Resour. Res., 9(4), 1102. DOI: 10.1029/WR009i004p01102

Neuman, S. 1974. Effect of partial penetration on flow in unconfined aquifers considering delayed gravity response, Water Resour. Res..10(2), 303.DOI: 10.1029/WR010i002p00303

Neuman, S. 1975. Analysis of Pumping Test Data From Anisotropic Unconfined Aquifers Considering Delayed Gravity Response. Water Resour. Res., 11(2), 329–342, DOI: 10.1029/WR011i002p00329.

Neuman, S., Blattstein, A.,Riva, M.,Tartakovsky, D.,Guadagnini, A. and Ptak, T. 2007, Type curve interpretation of late-time pumping test data in randomly heterogeneous aquifers, Water Resour. Res., 43, W10421, DOI:10.1029/2007WR005871.

NPTEL. 2018. Lecture 1: Introduction to ground water hydrology. National Program on Technology Enhanced Learning. Government of India. Visited 18.10.2018 https://nptel.ac.in/courses/105103026/module1/lec1/4.html

Otwell, B. 2016. Groundwater- Invisible but precious. FLOW-website. Visited 18.10.2018. http://flowforwater.org/groundwater-invisible-precious/

Papadopulos, S. and Cooper H. Jr. 1967. Drawdown in a well of large diameter. Water Resources Research. 3(1). p.241–244. DOI: 10.1029/WR003i001p00241.

Renard, P., Glenz, D., Mejias, M. 2009. Hydrogeology Journal. Volume 17. Issue 3. p 589-600. DOI: 10.1007/s10040-008-0392-0

Renard, P.2017. Hytool: an open source Matlab toolbox for the interpretation of hydraulic tests using analytical solutions. Journal of Open Source Software. 2(19). p. 441. DOI:10.21105/joss.00441

Richard S, Chesnaux, R., Rouleau, A., Coupe, R. 2016. Estimating the reliability of aquifer transmissivity values obtained from specific capacity tests: examples from the Saguenay-Lac-Saint-Jean aquifers, Canada, Hydrological Sciences Journal, 61:1, 173-185, DOI: 10.1080/02626667.2014.966720

Schwartz, F. W. and Zhang H. 2003. Fundamentals of Groundwater. USA. ISBN: 0471137855

Tang, Y. Zhou, J., Yang, P. Groundwater Engineering. 2016. Springer-Verlag Berlin Heidelberg and Tongji University Press. DOI 10.1007/978-03-662-048581-1_2

Tartakovsky, G., Neuman, S. 2007. Three-dimensional saturated-unsaturated flow with axial symmetry to a partially penetrating well in a compressible unconfined aquifer. Water Resour. Res., 43, W01410. DOI: 10.1029/2006WR005153.

TestWells Ltd, 2018, London, UK, visited 17.9.2018
https://www.testwells.com/the-skin-factor/

Theis, C. V. 1935. The relation between the lowering of the Piezometric surface and the rate and duration of discharge of a well using ground-water storage, Eos Trans. AGU, 16(2), 519–524, DOI: 10.1029/TR016i002p00519.

Thiem, G. 1906. Hydrologische methoden. Leipzig, J.M. Gebhardt's Verlag.

Todd, D. 1959. Groundwater Hydrology. John Wiley and Sons, Inc. p. 535. ISBN 0-0471-87616-X

Townsend, F. C. and Anderson, J. B. 2004. A Compendium of Ground
Modification Techniques Submitted by Florida Department of Transportation. Technical report. Report number: 4910-04504-887

Van Koningsveld, M., Mulder, J., Stive, M., Van Der Valk, L. and Van Der Weck, A. 2008. Living with Sea-Level Rise and Climate Change: A Case Study of the Netherlands. Journal of Coastal Research: Volume 24,. Issue 2: pp. 367 – 379. DOI: 10.2112/07A-0010.1.

Van Passen, L. 2009. Biogrout- Ground Improvement by Microbially Induced Carbonate Precipitation. Phd Thesis. TU Delft

Van Zomeren, A. 2008. On the nature of organic matter from natural and contaminated materials. PhD Thesis. ISBN 9789085049937

Van Essen Instruments. 2018. Photo of the diver. Visited 21.9.2018.

https://www.vanessen.com/images/tiles/tile-ctd-diver.png

Van Essen Instruments. 2018. The product manual from the diver manufacturer. Visited 24.9.2018. https://www.vanessen.com/images/PDFs/Diver-ProductManual-en.pdf

Xu, Z. 2013. General report Geotechnical problems of dikes (TC 201)
and dams (TC 210). Rapport général. CIMSG 2013. (Tc 201):3281–3287

Zhou J., Laumann S., Zhao H. and Heimovaara T. 2017. Presentation: SoSEAL pilot De Gijster Permeability reduction vie direct injection of Al-OM flocs. 2.11.2017

List of Appendices

Appendix 1: The soil profiles of the monitoring wells

Boring: A3

Date: 05-04-2018

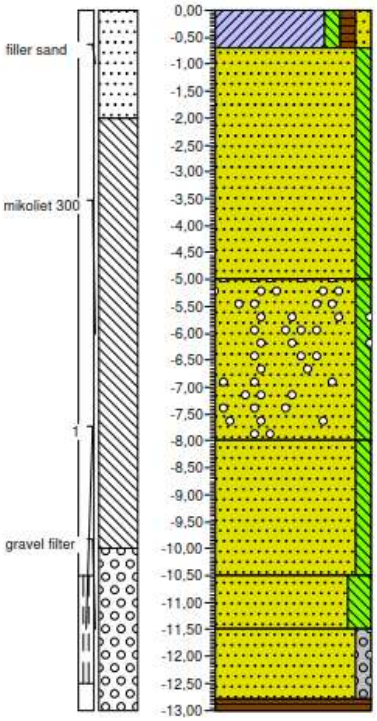

0,00 grass

clay, slightly silty, slighly humus

-0,70 slightly sandy, brown

sand, medium fine, slightly silty,

lumps of clay, greybeige

-5,00

sand, medium fine, slightly silty,

slightly gravely, greybeige

-8,00

sand, medium fine, slightly

silty, grey

-10,50

sand, very fine, medium silty, clay

layers, grey

-11,50

sand, medium coarse, slightly

gravely, grey

-12,80

-13,00 peat, brown

Boring: A9

Date: 03-04-2018

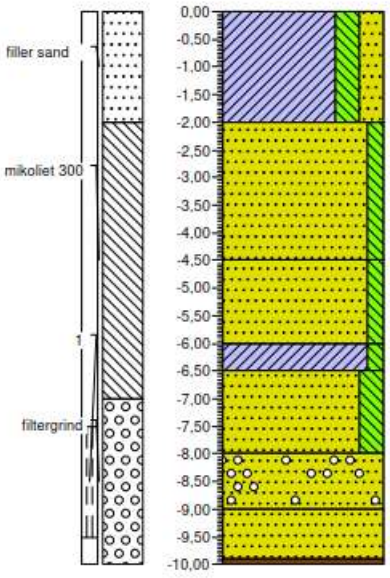

0,00 grass

clay, medium silty, medium

sandy, greybrown

-2,00

sand, medium fine, slightly

silty, greybeige

-4,50

sand, medium fine, slightly

silty, lumps of clay, grey

-6,00

-6,50 clay, slightly silty, grey

sand, very fine, medium silty, clay

layers, dark grey

-8,00

sand, very coarse, very

gravely, dark grey

-9,00

sand, medium coarse, dark

grey

-10,00 peat, brown

Drawn according to NEN 5104

Boring: B1

Date: 09-04-2018

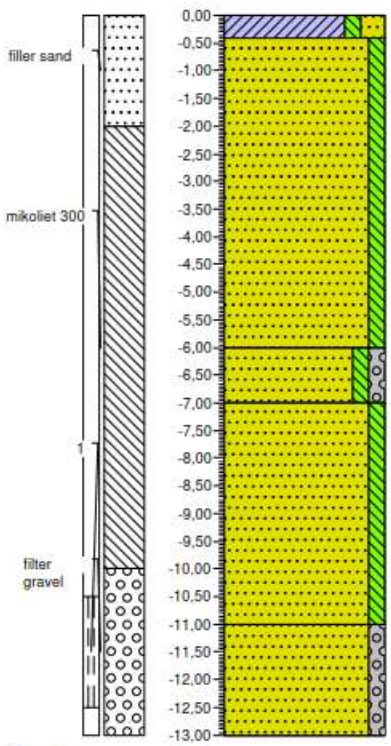

0,00 grass

-0,40 Clay, slightly silty, medium sandy, greybrown

Sand, medium fine, slightly silty, greybeige

-6,00

Sand, medium fine, slightly silty, slightly gravely, greybeige

-7,00

Sand, medium fine, slightly silty, clay residues, grey

-11,00

Sand, medium coarse, slightly gravely, grey

-13,00

Boring: B6

Date: 10-04-2018

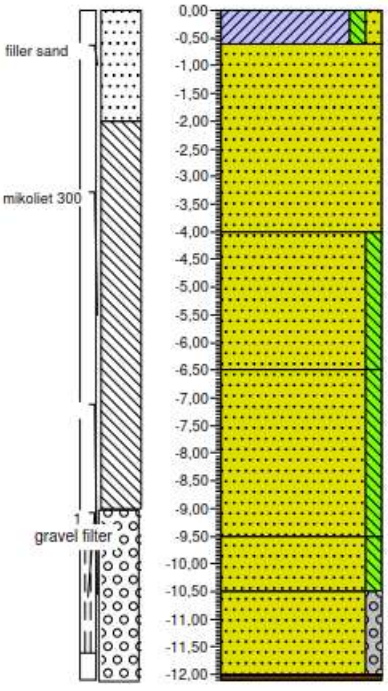

0,00 grass

-0,60 clay, slightly silty, slightly sandy, greybrown

sand, medium coarse, greybeige

-4,00

sand, medium fine, slightly silty, clay residues, greybeige

-6,50

sand, medium fine, slightly silty, clay residues, grey

-9,50

sand, very fine, slightly silty, clay layers, grey

-10,50

sand, medium coarse, slighlty gravely, grey

-12,10

peat, brown

Drawn according to NEN 5104

Boring: C4

Date: 12-04-2018

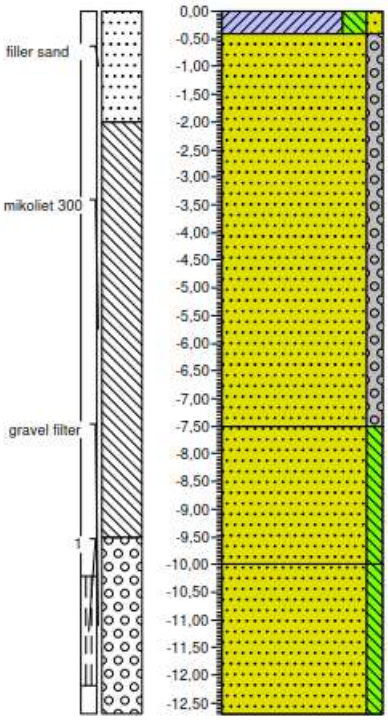

0,00 grass

-0,40 clay, mediumsilty, slightly sandy brown

sand, medium coarse, slightly gravely, clay residues, light beigebrown

-7,50

sand, medium fine, slightly silty, grey

-10,00

sand, medium fine, slightly silty, clay layers, grey

-12,70

Boring: C8

Date: 12-04-2018

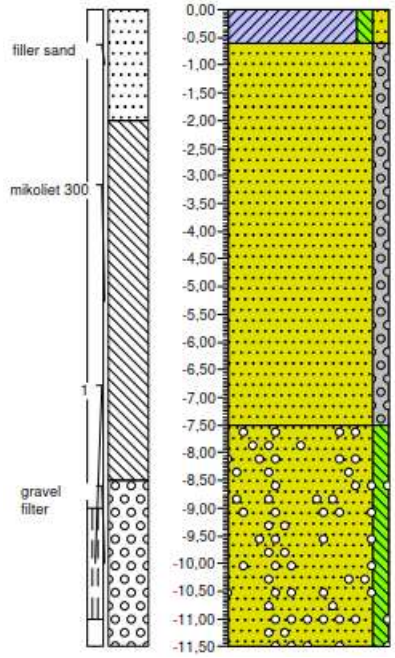

0,00 grass

clay, slightly silty, slightly sandy, brown

-0,60

sand, medium coarse, slightly gravely, clay residues, light beigebrown

-7,50

sand, medium fine, slightly silty, clay layers, gravel layers

-11,50

Drawn according to NEN 5104

Appendix 2: The water level variation in De Gijster and in Amer

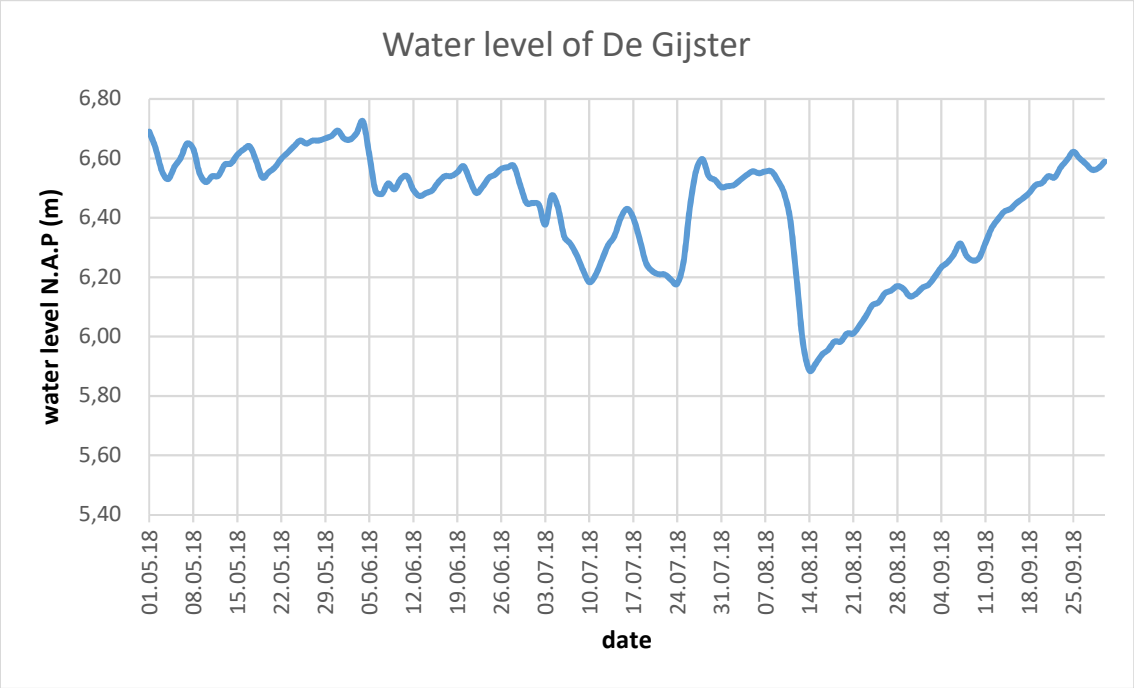

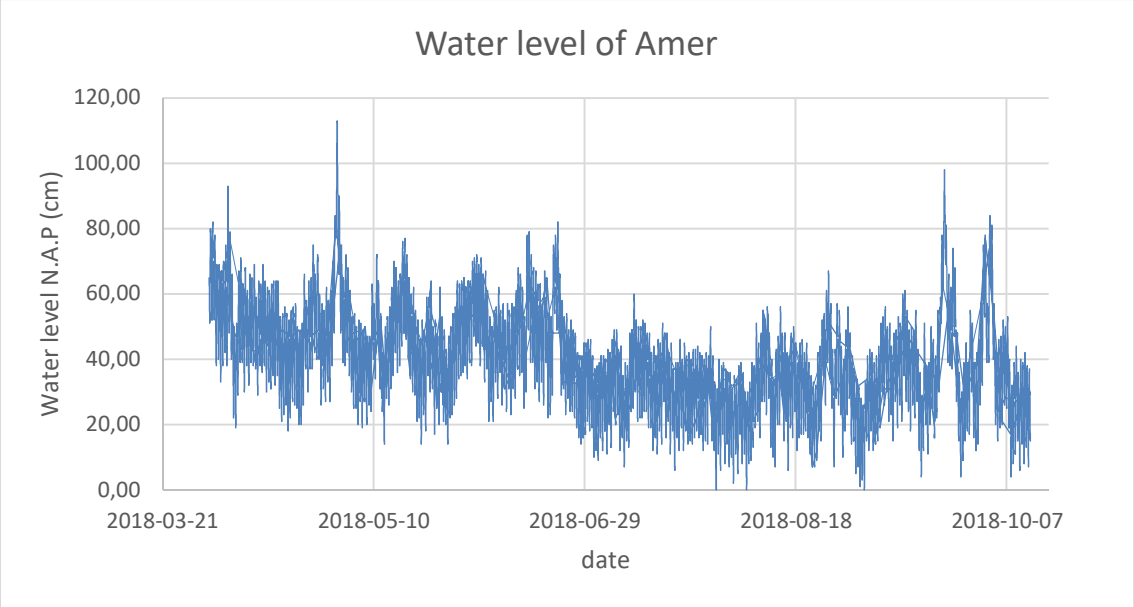

Appendix 3: The pumping test conducted in De Gijster 2.5-2.10.2018

*Pumping refers to water being pumped from the well and infiltration to water being pumped out of the well.

ZONE A			**BEFORE**	**AFTER**
Monitoring well	**Date**	**Test** *	**Flow rate (m^3/d)**	**Flow rate (m^3/d)**
A1	16.5.2018	infiltration	19.68	0.00
A2			0.00	0.00
A3	16.5.2018 (18.07.2018)	infiltration	21.63	30.86
			30.86	
	19.7.2018	pumping		28.35
A4	2.5.2018	infiltration	19.14	0.00
	29.5.2018	infiltration	18.76	0.00
A5	2.5.2018	infiltration	21.66	0.00
	29.5.2018	infiltration	37.40	0.00
A6	2.5.2018	pumping	13.64	0.00
	29.5.2018	infiltration	28.12	0.00
A8	2.5.2018	pumping	16.62	0.00
	29.5.2018	pumping	14.64	0.00
A9	2.5.2018(18.07.2018)	pumping	30.76	36.00
A10	3.5.2018	pumping	0.00	0.00
	16.5.2018	infiltration	23.96	0.00
	29.5.2018 (18.07.2018)	infiltration	31.29	27.50
ZONE B				
Monitoring well	**Date**	**Test**	**Flow rate (m^3/d)**	**Flow rate (m^3/d)**
B1	7.5.2018	infiltration	26.76	0.00
B2	9.5.2018 (19.07.2018)	infiltration	22.98	27.03
B3	7.5.2018 (19.07.2018)	infiltration	21.31	26.71
B4	1.5.2018	infiltration	21.41	0.00
	7.5.2018	infiltration	29.74	0.00
	15.5.2017	infiltration	21.07	0.00
B5	9.5.2018	infiltration	32.79	0.00
	15.5.2018	infiltration	25.99	0.00
B6	9.5.2018	pumping	17.86	0.00
B7	9.5.2018	infiltration	21.70	0.00
	15.5.2018	infiltration	24.26	0.00
	16.5.2018	infiltration	24.58	0.00
B8	1.5.2018	pumping	21.73	0.00
	7.5.2018	infiltration	23.13	0.00
	15.5.2018	pumping	22.71	0.00
B9	1.5.2018 (19.07.2018)	pumping	31.33	32.56
	1.5.2018	pumping	31.13	0.00
B10	1.5.2018	infiltration	22.92	0.00
	15.5.2018 (20.07.2018)	infiltration	20.85	25.88

B11	7.8.2018	pumping	5.95	0.00
	9.5.2018	infiltration	19.18	0.00
	9.5.2018	pumping	6.11	0.00
ZONE C				
Monitoring well	**Date**	**Test**	**Flow rate (m^3/d)**	**Flow rate (m^3/d)**
C1	4.5.2018	infiltration	24.09	0.00
C2	4.5.2018 (27.7.2018)	infiltration	25.79	26.35
	1.10.2018	infiltration		26.18
	1.10.2018	infiltration		32.00
C3			0.00	0.00
C4	4.5.2018	infiltration	22.64	0.00
C5	3.5.2018	infiltration	21.08	0.00
C6	3.5.2018 (27.7.2018)	infiltration	0.00	23.57
	29.5.2018	pumping	19.54	0.00
C7	3.5.2018	pumping	11.39	0.00
C8	3.5.2018	pumping	12.59	0.00
	29.5.2018	pumping	14.17	0.00
C9	3.5.2018 (20.07.2018)	pumping	22.98	24.77
	4.5.2018	infiltration	26.70	0.00
	1.10.2018	pumping		27.00
	2.10.2018	pumping		32.00

Appendix 4: The pumping test used for the Neuman (1975) method analysis and the well distances

date	starting time	test well	flow rate (m3/d)
16.5.	12:40	A3	21.63
19.7.	8:40	A3	28.35

date	starting time	test well	flow rate (m3/d)
15.5.	13:46	B10	20.85
20.7.	8:45	B10	25.88

Location and distance from the test well A3

Well ID	x	y	distance in m
A1	116693.83	415484.56	2.49
A2	116695.312	415482.45	2.50
A4	116696.993	415480.27	4.53
A5	116699.863	415484.79	3.55
A6	116700.113	415480.16	5.96
A7	116701.357	415482.7	5.45
A8	116702.698	415480.74	7.54
A9	116707.022	415478.8	12.25
A10	116699.216	415482.12	3.92

Location and distance from the test well B10

Well ID	x	y	distance in m
B1	116705.803	415512.5	4.19
B2	116704.011	415514.3	6.23
B3	116706.521	415514.9	4.19
B4	116707.676	415510.6	3.03
B5	116709.769	415515.3	2.83
B6	116711.082	415510.9	1.99
B7	116711.813	415513.5	2.08
B8	116713.303	415511.6	3.42
B9	116718.032	415510.4	8.31
B11	116710.933	415512.3	0.97

Location and distance from the test well C2

date	starting time	test well	flowrate (m3/d)
4.5.	10:55	C2	25.79
27.7.	9:31	C2	23.57

Well ID	x	y	distance in m
C1	116711.884	415549.74	2.39
C3	116714.164	415550.94	2.49
C4	116716.164	415546.8	2.80
C5	116718.084	415552.04	5.50
C6	116719.386	415547.79	5.52
C7	116719.796	415550.44	6.22
C8	116721.686	415549.01	7.80
C9	116726.17	415548.5	12.27

Appendix 5: The comparison of the drawdowns before and after injection during the first 10 minutes of pumping